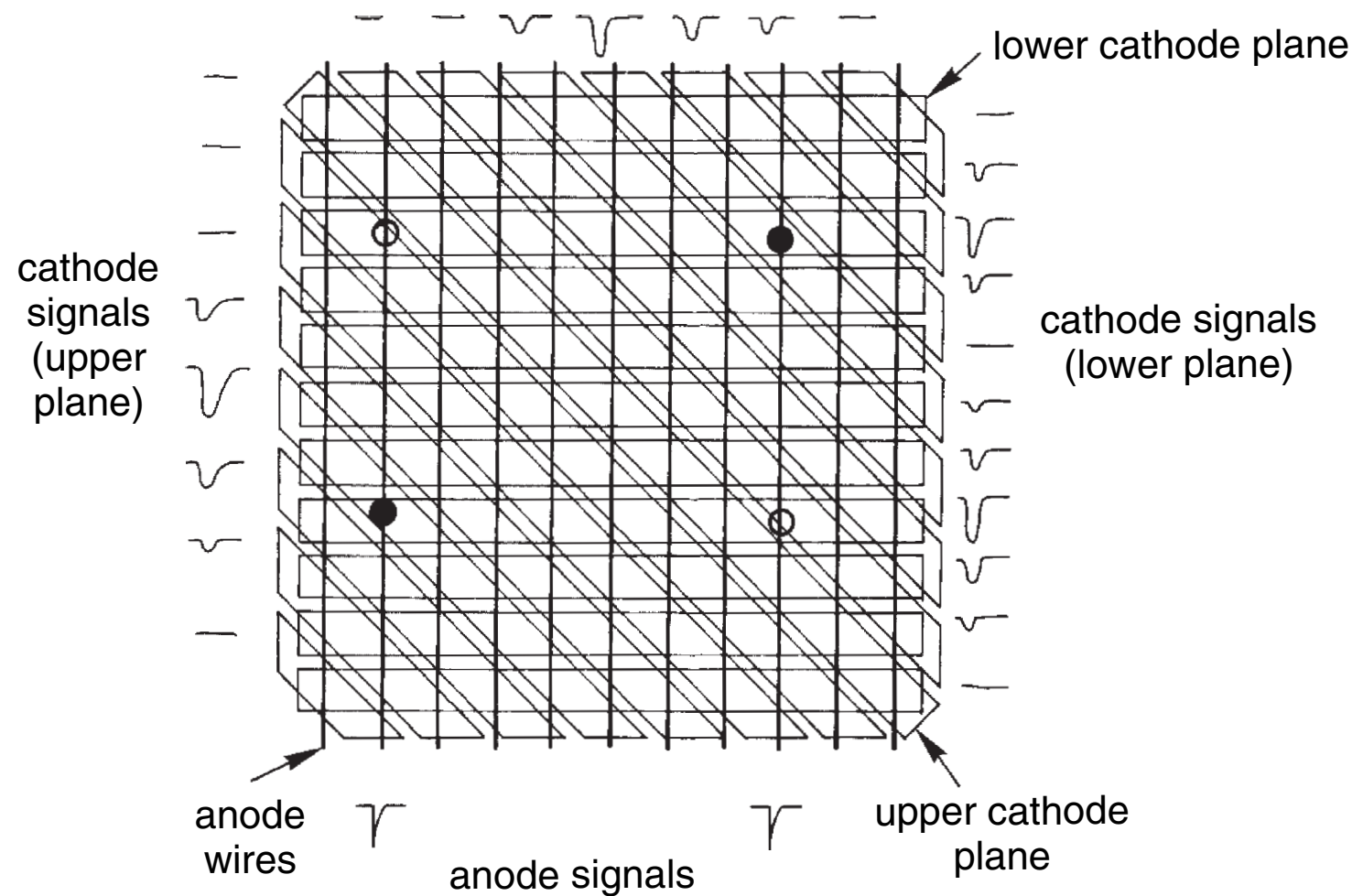


Multi-Wire Proportional Chamber (MWPC)

MWPC ...

substantial functionality improvement
due to cathode strips/pads ...



Cathode readout yields:

- 2-dim. information
true 2d: use pads ...
- high spatial resolution
due to center of gravity reconstruction
- resolving ambiguities
using second strip pattern or pads

Can wires be avoided?

Micro-strip Gas Chambers (MSGC)

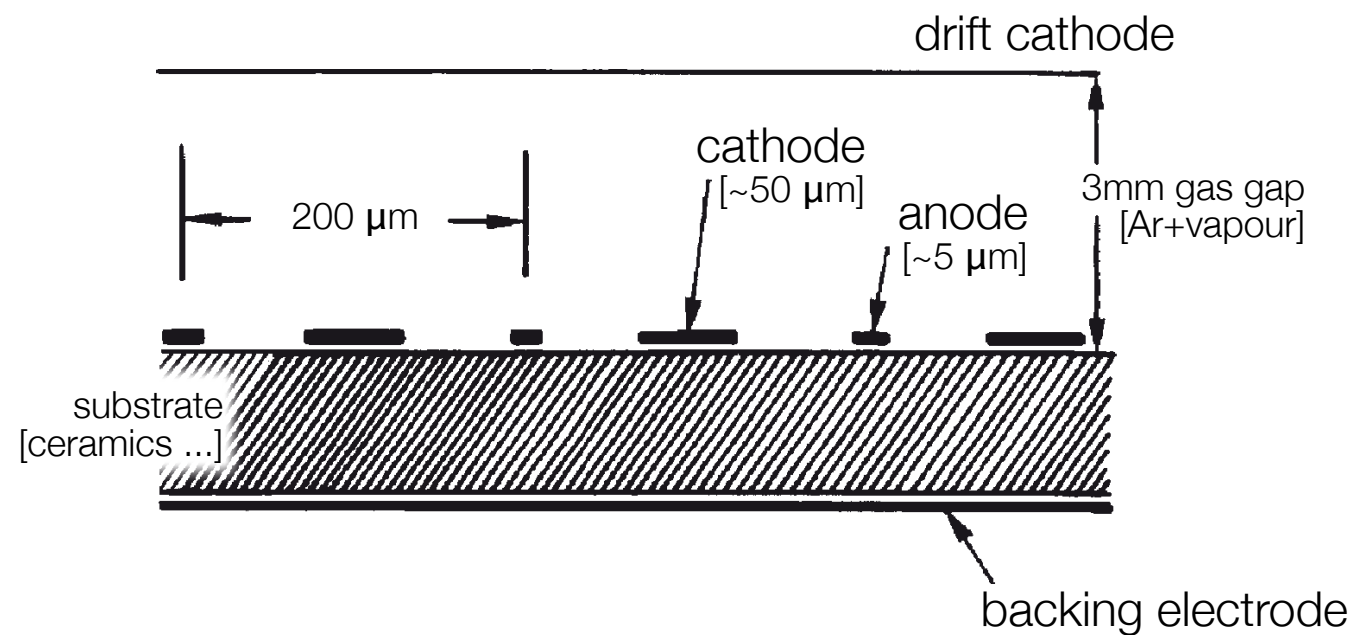
Can one avoid wires?

Anode realized via microstructures
on dielectrics ...

Simple construction (today)
Enhanced stability & flexibility
Improved rate capabilities

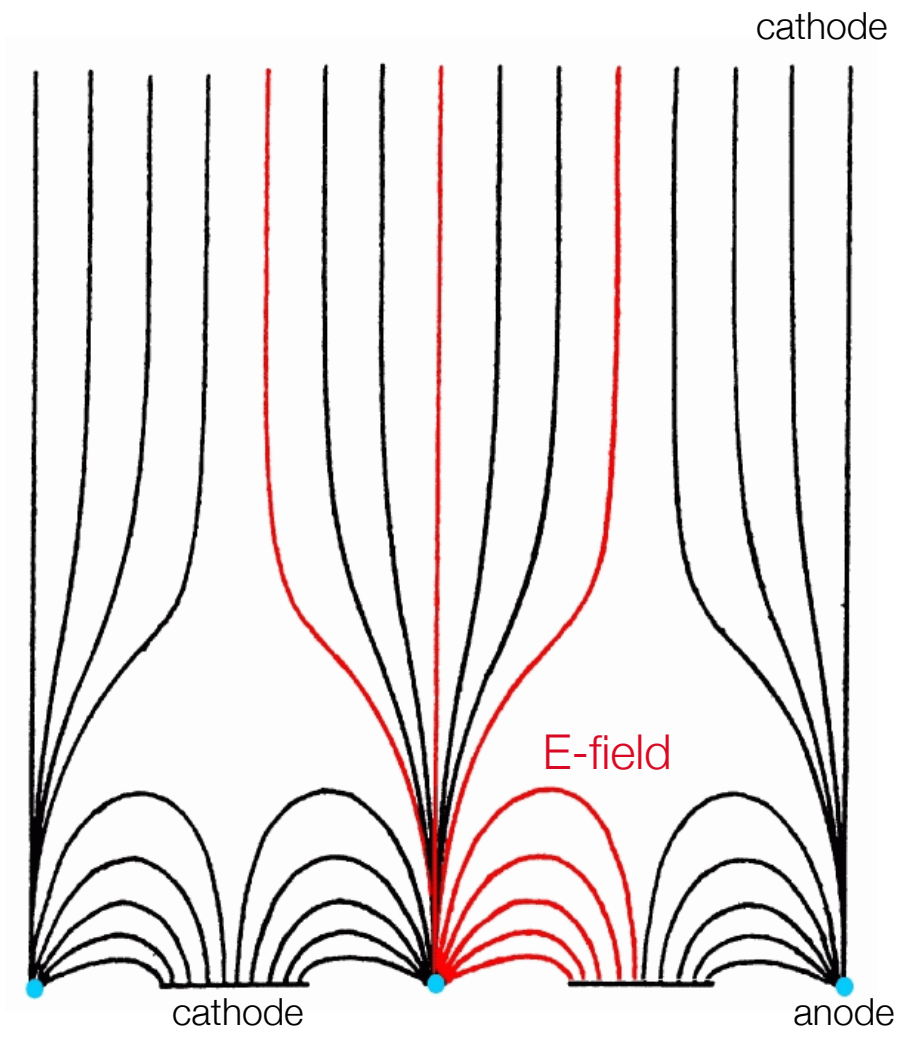
First MSGCs developed in 1990ies ...

Problems: charging of isolation structure
[→ time-dependent gain; sparks, anode destruction]



Schematics of MSGC
field lines

high field directly above anode
ions drift only 100 μm; yields low dead time ...



Micro-strip Gas Chambers (MSGC)

MGSCs prone to aging problems ...

Solution: intermediate grid ...

e.g.: Micromegas
GEM detectors [Sauli, 1997]

Micromegas:

Fine cathode mesh collects ions
still fast; no wires ...

GEM (Gas Electron Multiplier):

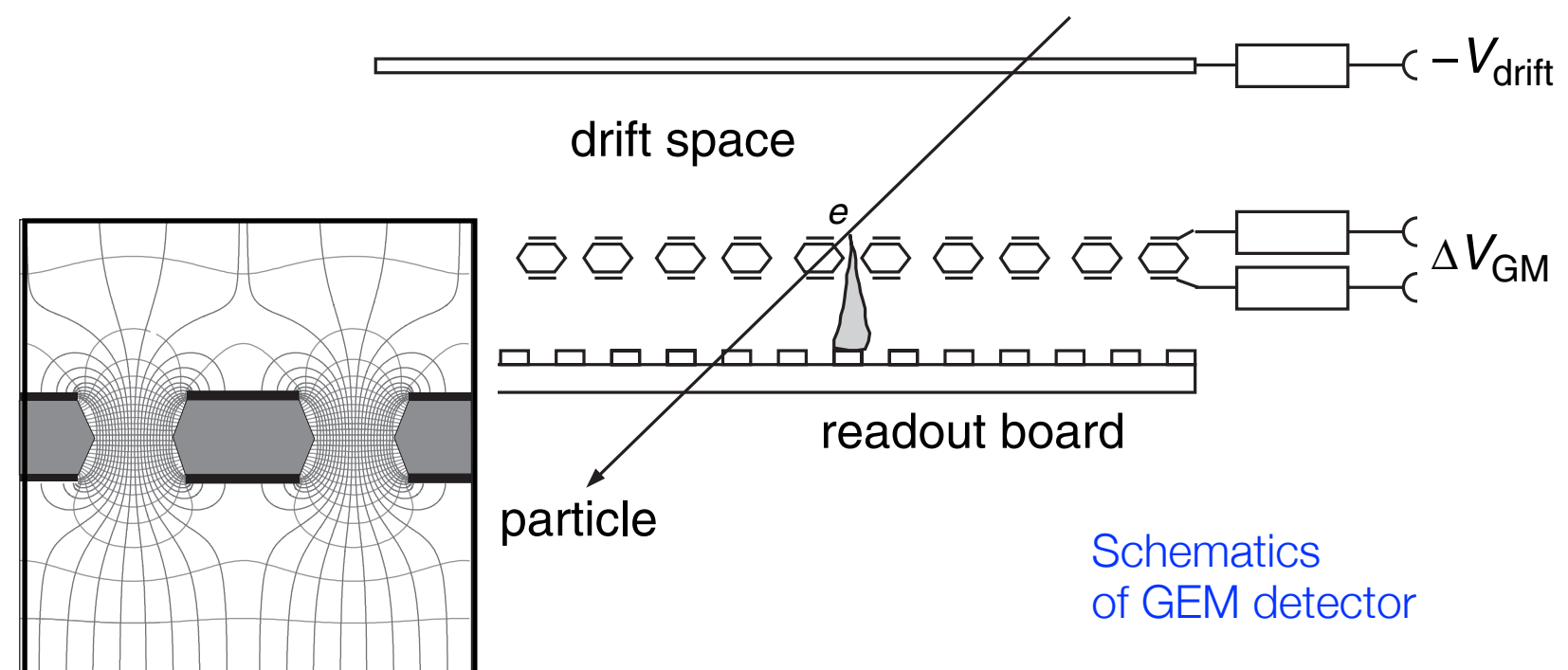
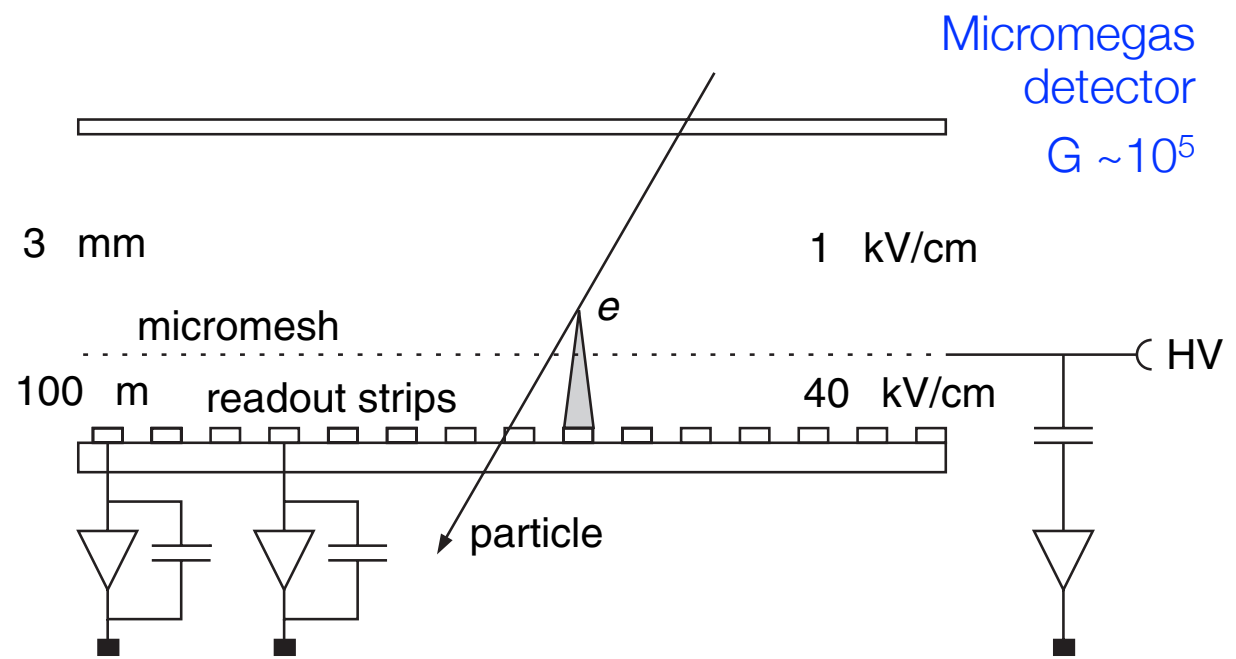
Thin insulating kapton foil
coated with metal film ...

Contains chemically produced
holes [100-200 μm]

Electrons are guided by high
electric drift field of GEMs ...

Avalanche production ...

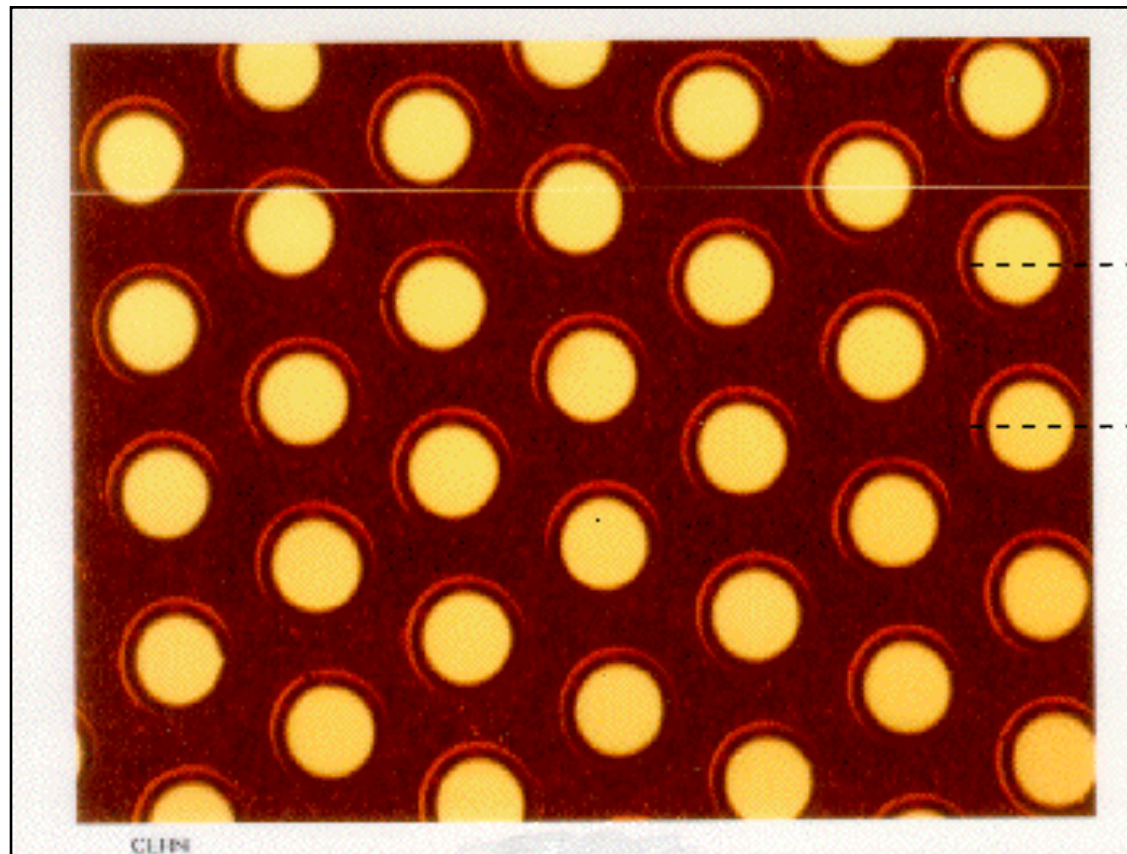
Electrons drift to anode
GEM collects ions



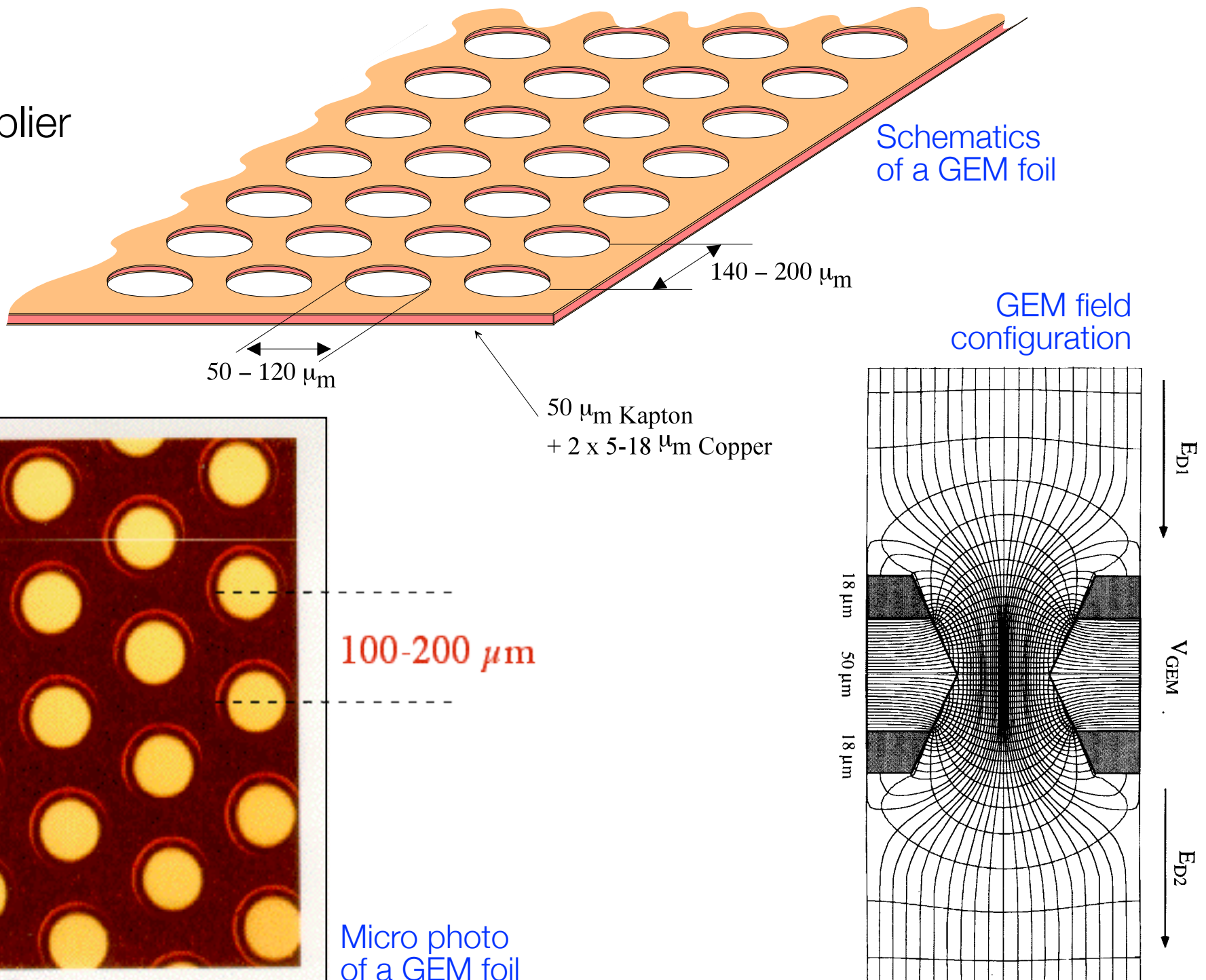
Schematics
of GEM detector

Micro-strip Gas Chambers (MSGC)

GEM
Gas Electron Multiplier



Micro photo
of a GEM foil



Schematics
of a GEM foil

GEM field
configuration

Ionization Chambers – Signal Shape

Pulse mode operation

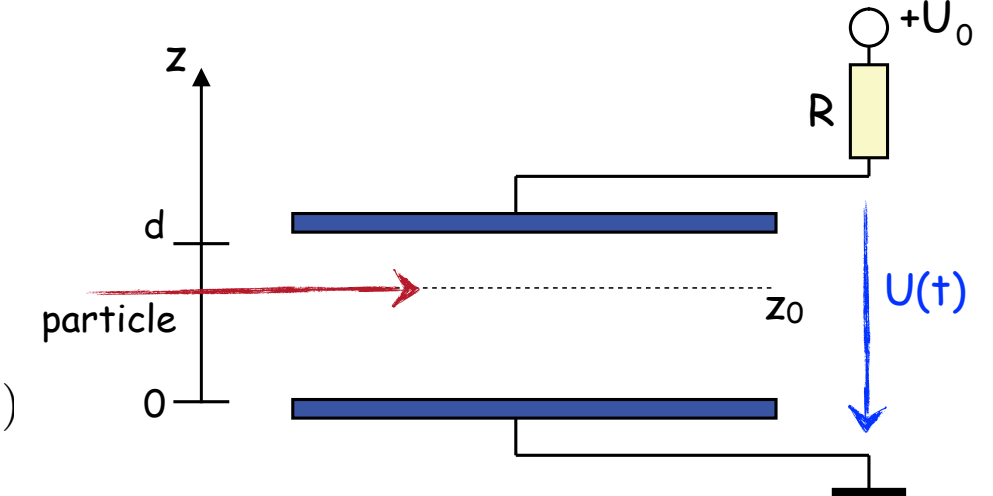
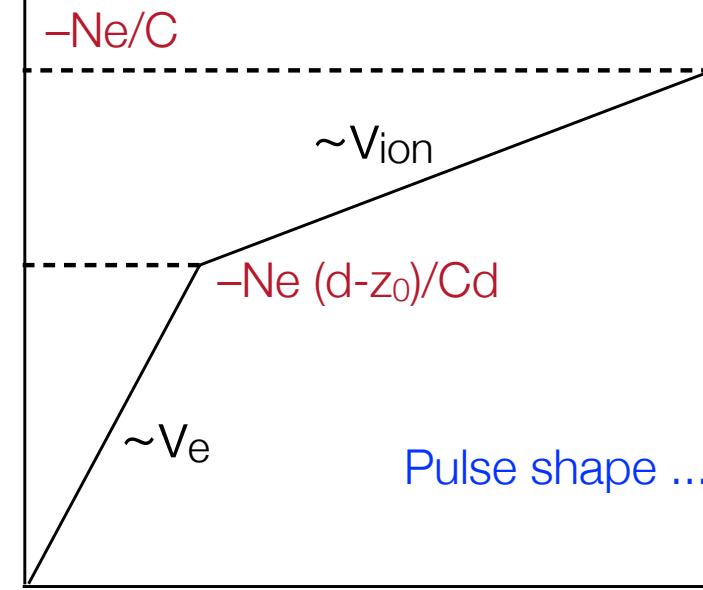
derive signal for single ionizing particle [$R = \infty$]

$$\begin{aligned} W &= \frac{1}{2} CU^2 = \frac{1}{2} CU_0^2 - N \int_{z_0}^{z_f} qE_z dz \\ &= \frac{1}{2} CU_0^2 - N_+ q_+ \frac{U_0}{d} (z_+ - z_0) + N_- q_- \frac{U_0}{d} (z_- - z_0) \end{aligned}$$

$$U = U_0 + \Delta U \quad U^2 = U_0^2 + 2\Delta U U_0 + \Delta U^2$$

$$\Delta U = -\frac{N_+ q_+}{Cd} (d - z_0) + \frac{N_- q_-}{Cd} (0 - z_0) = \Delta U_- + \Delta U_+$$

$$-\Delta U = -\frac{N}{Cd} [e(d - z_0) - e(0 - z_0)] = -\frac{Ne}{C}$$



Schematic view
of an ionization chamber

Final signal independent of ionization position and of detector dimension ...
[see also Geiger counter]

Time evolution of pulse height:

$$\begin{aligned} z(t) &= v_D \cdot t \\ \Delta U &= -\frac{Ne}{Cd} (v_D^e + v_D^{\text{ion}}) t \end{aligned}$$

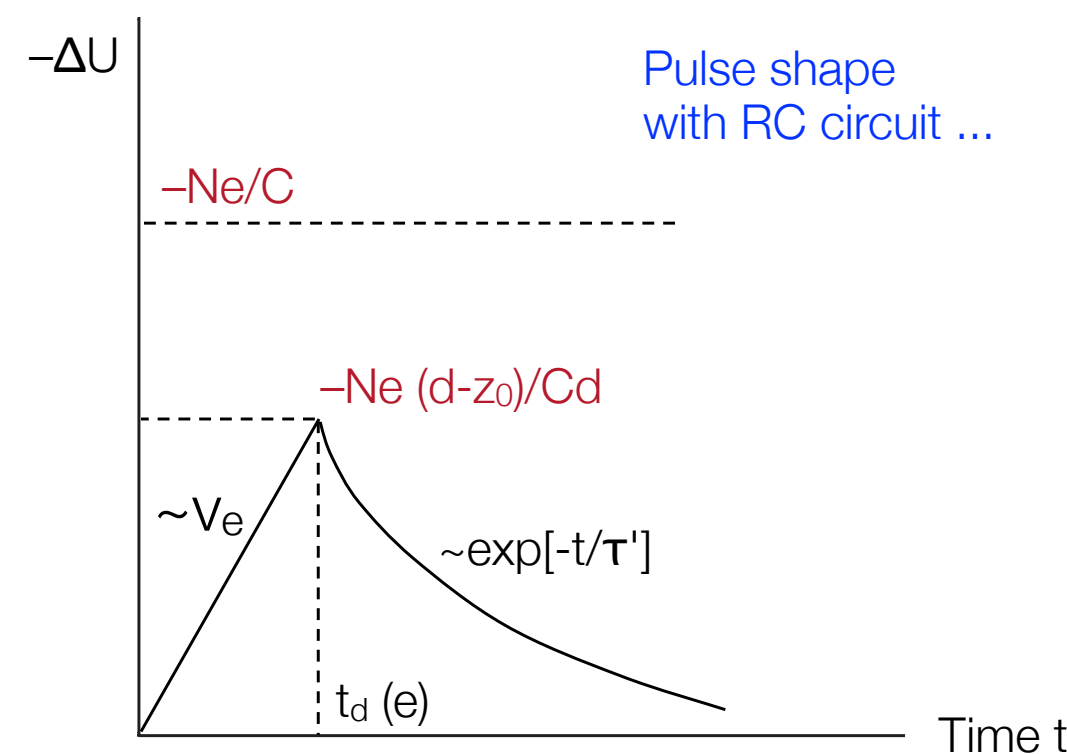
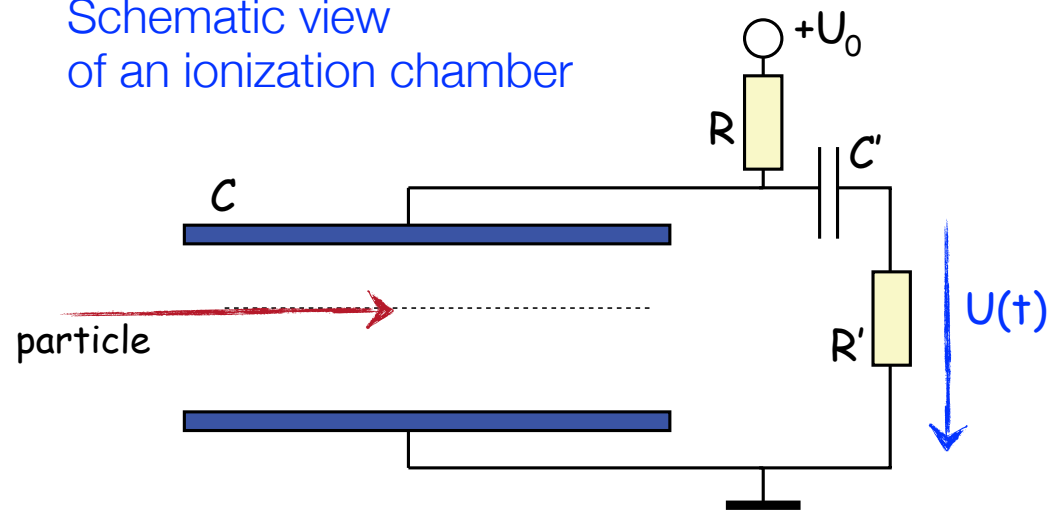
with:
 $v_D^e \approx 1000 \cdot v_D^{\text{ion}}$

Typical:

$$\begin{aligned} v_{d,e} &= 4 \text{ cm}/\mu\text{s} \\ v_{d,\text{ion}} &= 4 \text{ cm}/\text{ms} \end{aligned}$$

Ionization Chambers – Signal Shape

Schematic view
of an ionization chamber



Pulse mode operation
[Use RC circuit; R finite]

Response time of chamber: $\tau = RC$

Must be sufficiently large with respect to t_{signal}

Example: 2 x 2 x 10 cm³ chamber

Electron drift time: $t_{\text{max}}^- = d/v_{d,e} = 2\text{cm}/4\text{cm}/\mu\text{s} = 500\text{ ns}$

Ion drift time: $t_{\text{max}}^+ = d/v_{d,\text{ion}} = 500\text{ }\mu\text{s}$

Suppress ion signal by $C'R'$ high pass filter
with time constant $\tau' = R'C'$

Chose: $t_{\text{max}}^- < \tau' < t_{\text{max}}^+$

$$\begin{aligned} \text{Ex.: } \tau' &= 1\mu\text{s} \\ C &= 1\text{pF}, R &= 10\text{M}\Omega \\ C' &= 1\text{pF}, C_{\text{tot}} = CC'/(C+C') = 0.5\text{ pF} \\ R' &= \tau/C = 1\text{ }\mu\text{s}/0.5\text{ pF} = 2\text{ M}\Omega \end{aligned}$$

Features:

linear rise; exponential fall

dead time $T_{\text{dead}} \approx \tau'$

position dependent pulse height

position dependent resolution

Ionization Chambers – Frisch Grid

Removal of
position dependent signal ...
[O. Frisch, 1944]

Principle:

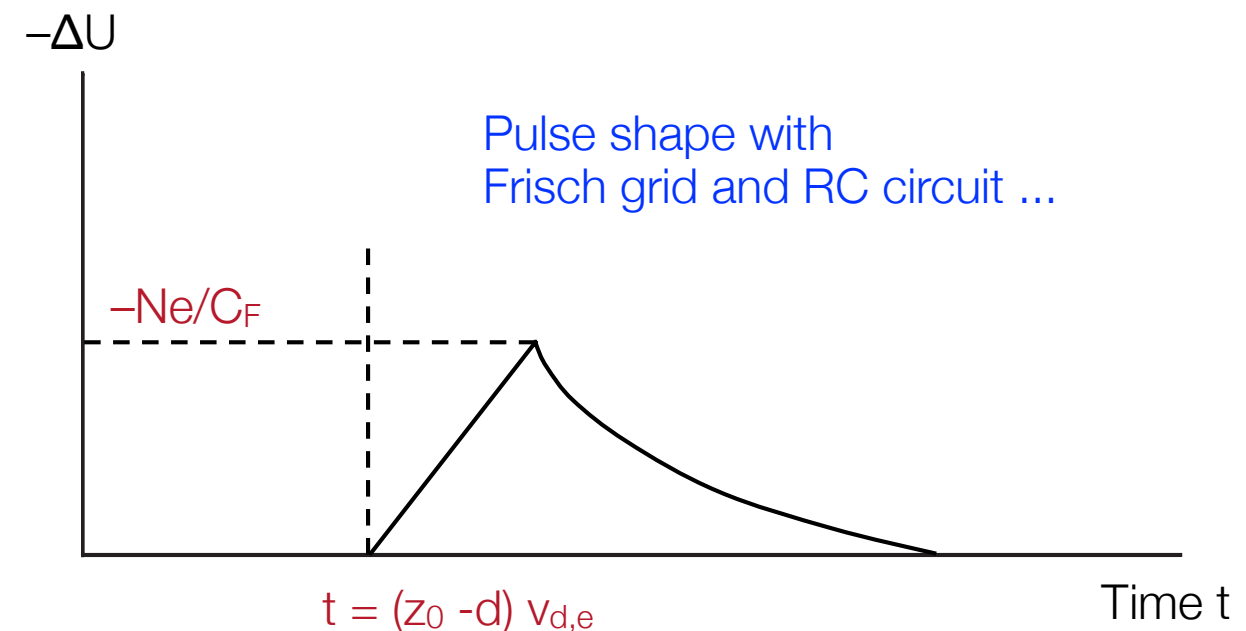
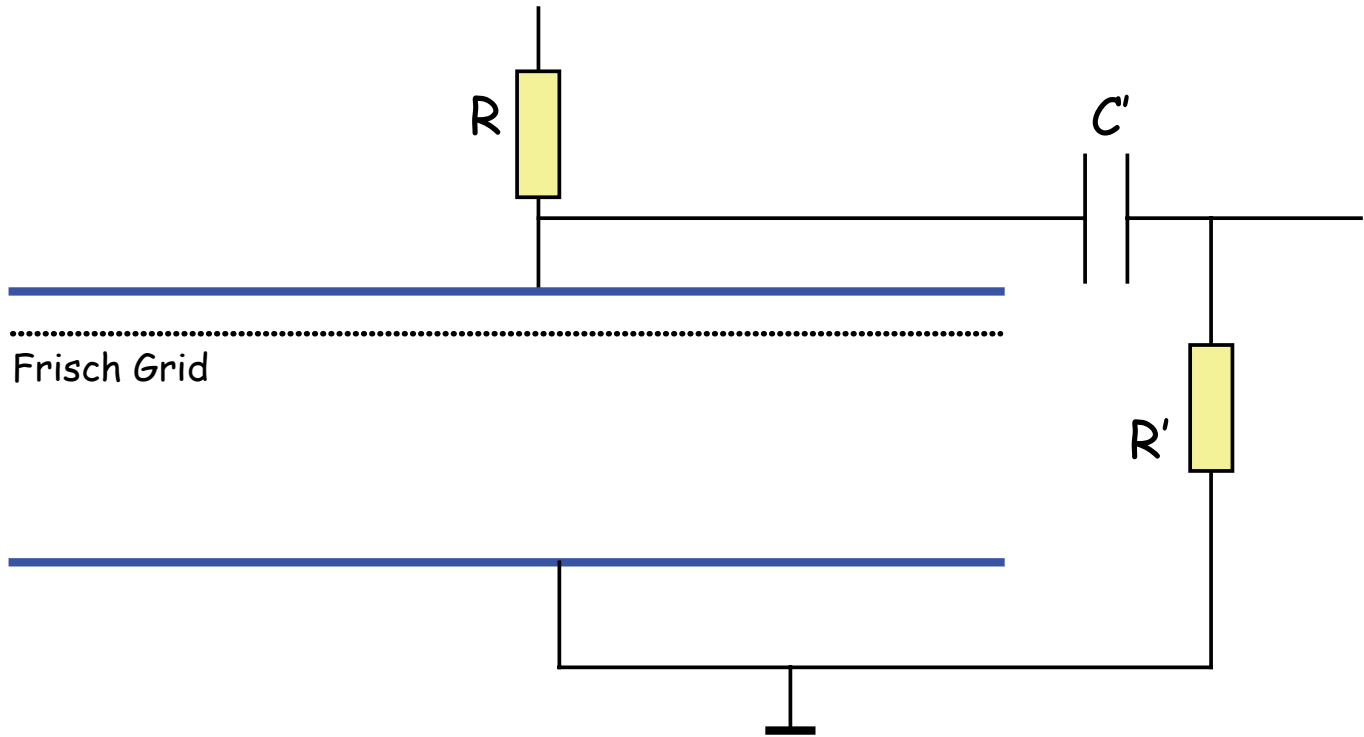
Introduce wire plane
at intermediate potential ...

Shielding of induced charges
Wire plane transparent to electrons

Signal on anode only generated
by electrons that have passed the Frisch grid

All electrons appear at the same distance
thus: no position dependence ...

Difficulty: Small signals ...
Need sensitive, low-noise pre-amplifiers ...

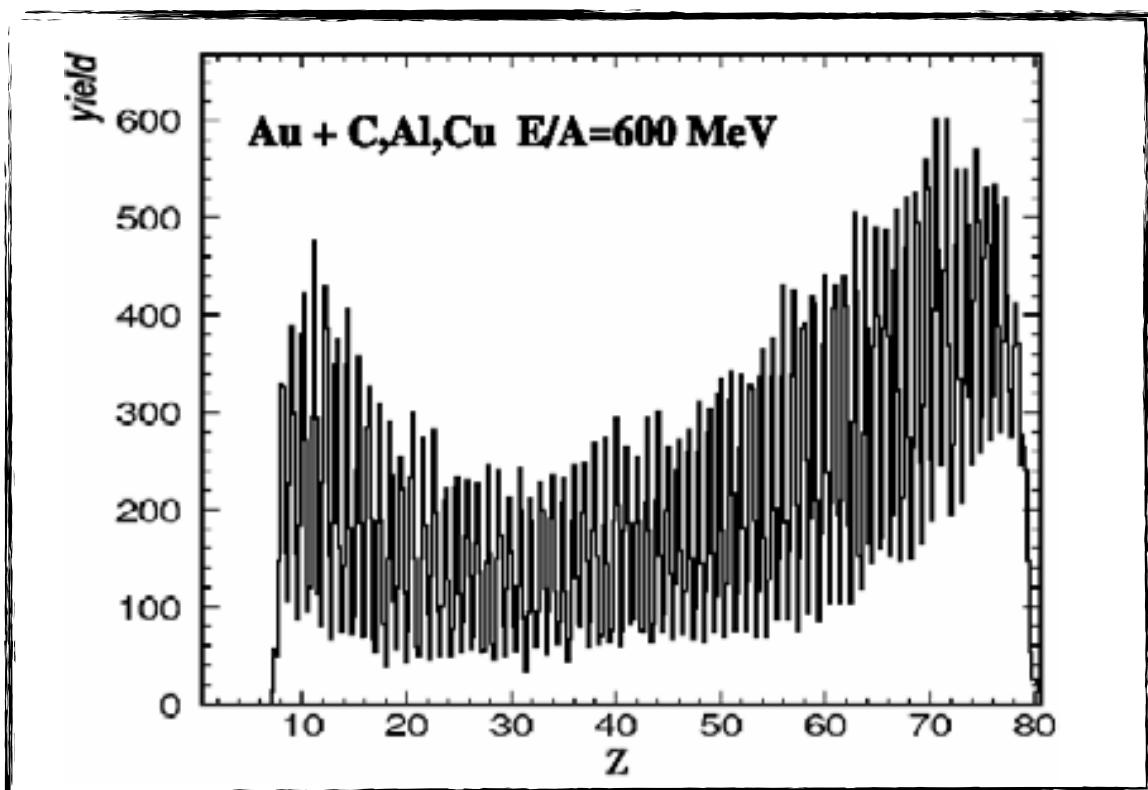


Ionization Chambers – Music II

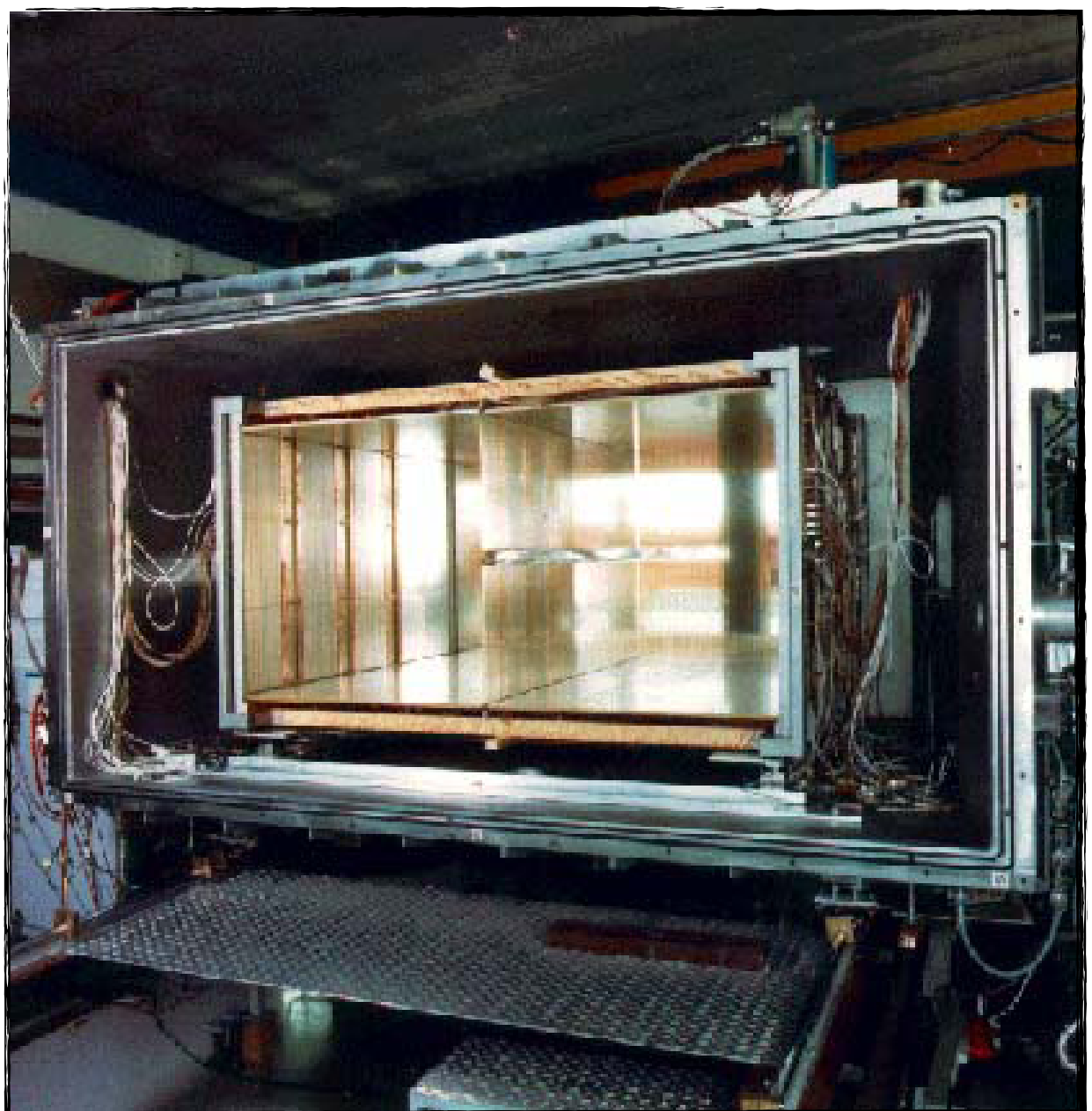
Parameters:

gas	P10 (Ar/Methan 90/10)
pressure	1 atm
active area	102 x 60 cm ²
depth	51 cm
electric field	150 V/cm
potential	9 kV
ionization	70 Z ² pairs/cm
drift velocity	5 cm/ μ sec

Fragment
charge spectrum



Multiple sampling
ionization chamber



Ionization Chambers – Na 48

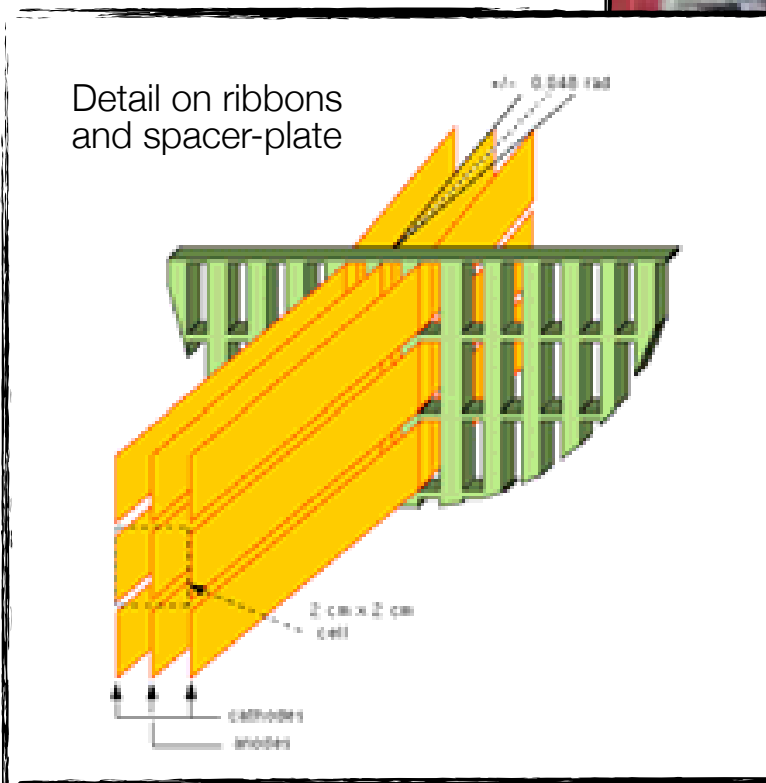
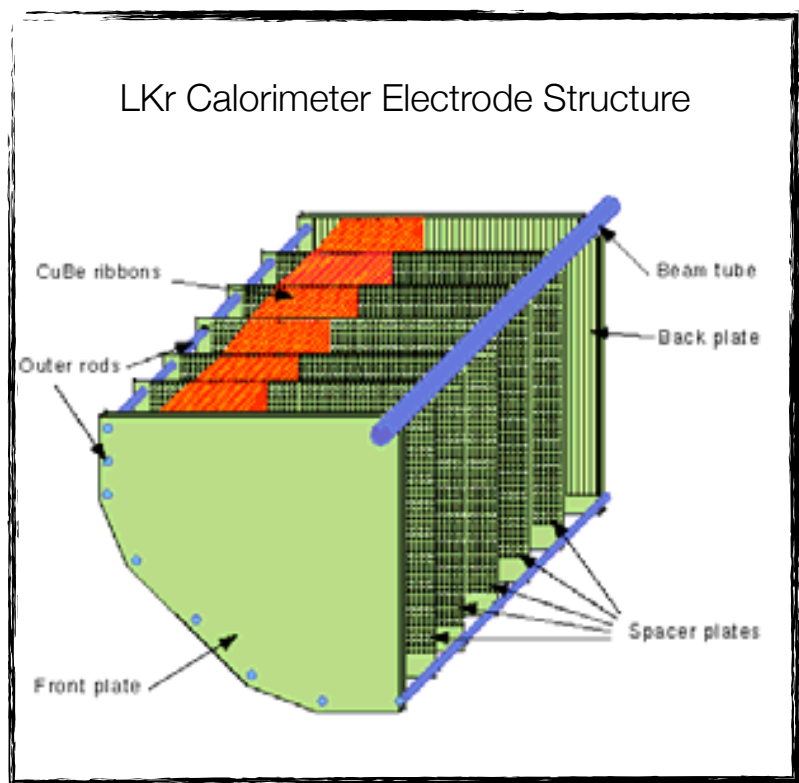
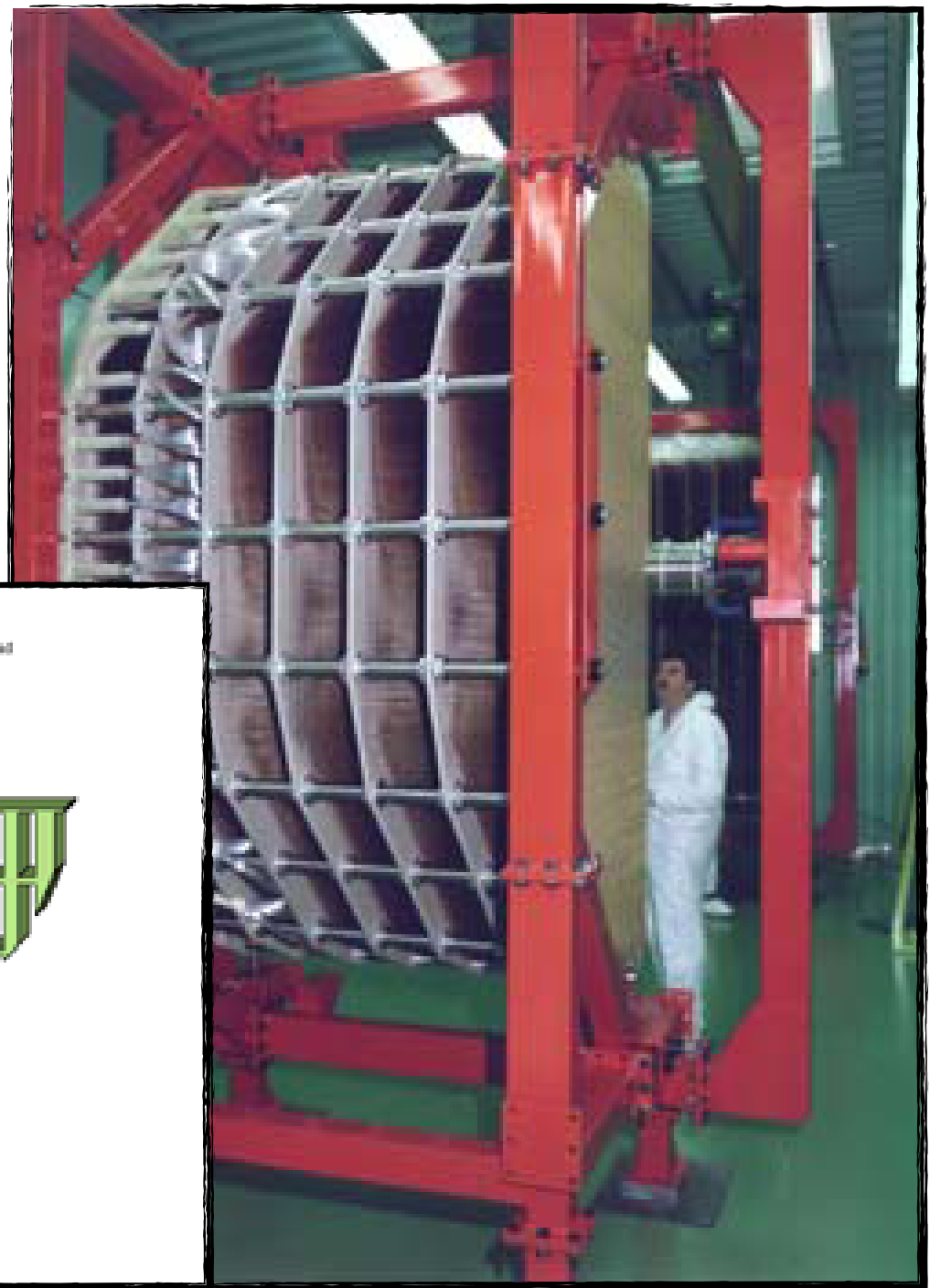
Liquid Krypton Ionization Chamber

Homogeneous LKr; gain = 1

184 cells formed by thin electrodes; cell size: $2 \times 2 \text{ cm}^2$

Each cell formed by two drift gaps sharing readout electrode

Electrodes: CuBe ribbons



Drift Chambers – Principle

Measure drift time t_D
[need to know t_0 ; fast scintillator, beam timing]

Determine location of original ionization:

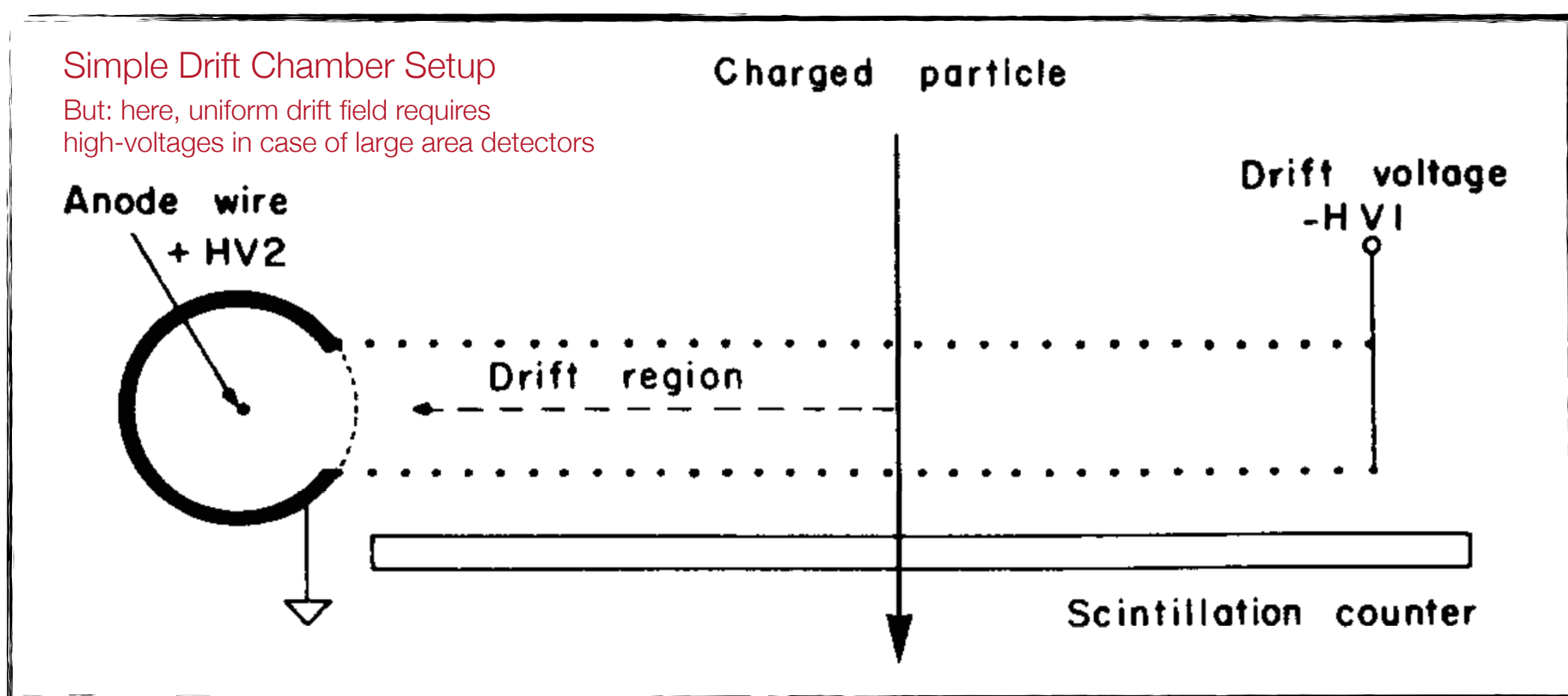
$$x = x_0 \pm v_D \cdot t_D$$

$$y = y_0 \pm v_D \cdot t_D$$

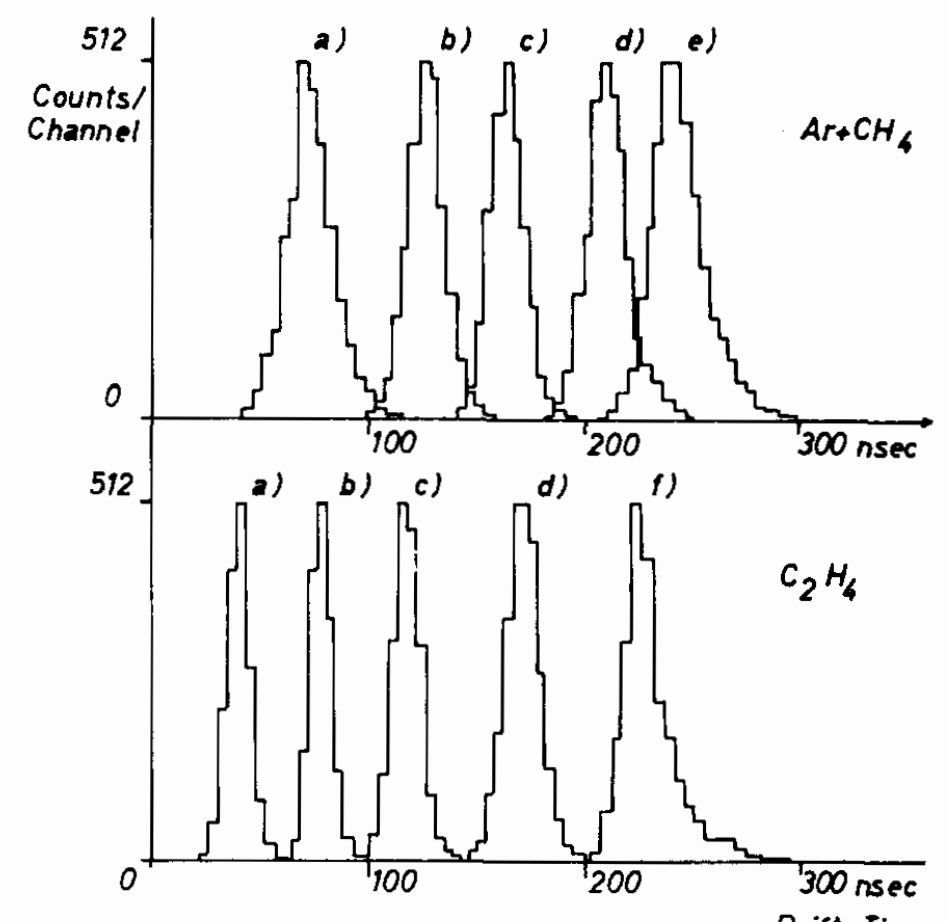
If drift velocity changes along path:

$$x = \int_0^{t_D} v_D \, dt$$

In any case:
Need well-defined drift field ...

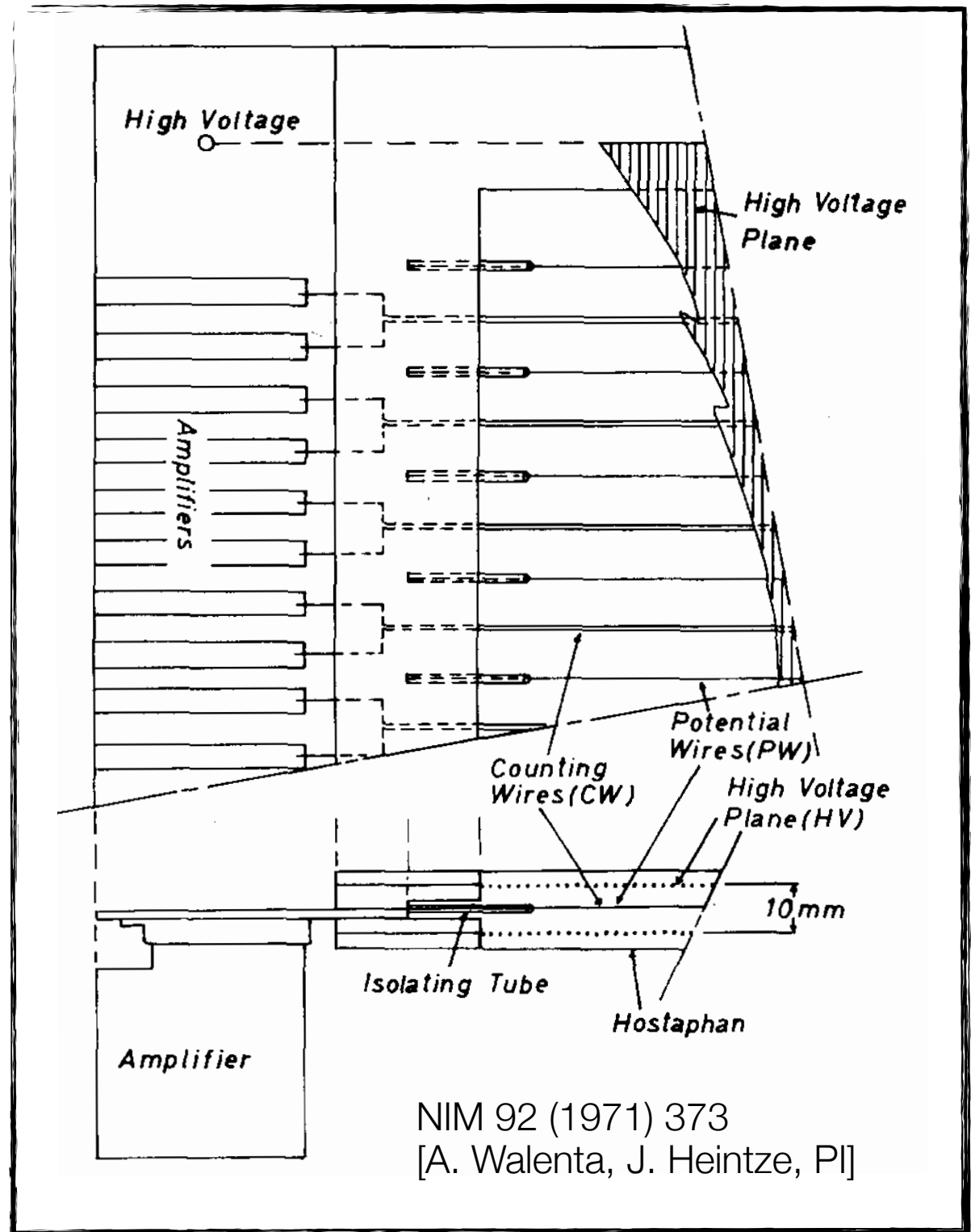


Drift Chambers – The First One



Distance from the Wire [mm] :
a) 1.8 c) 5.5 e) 8.5
b) 3.7 d) 7.4 f) 9.2

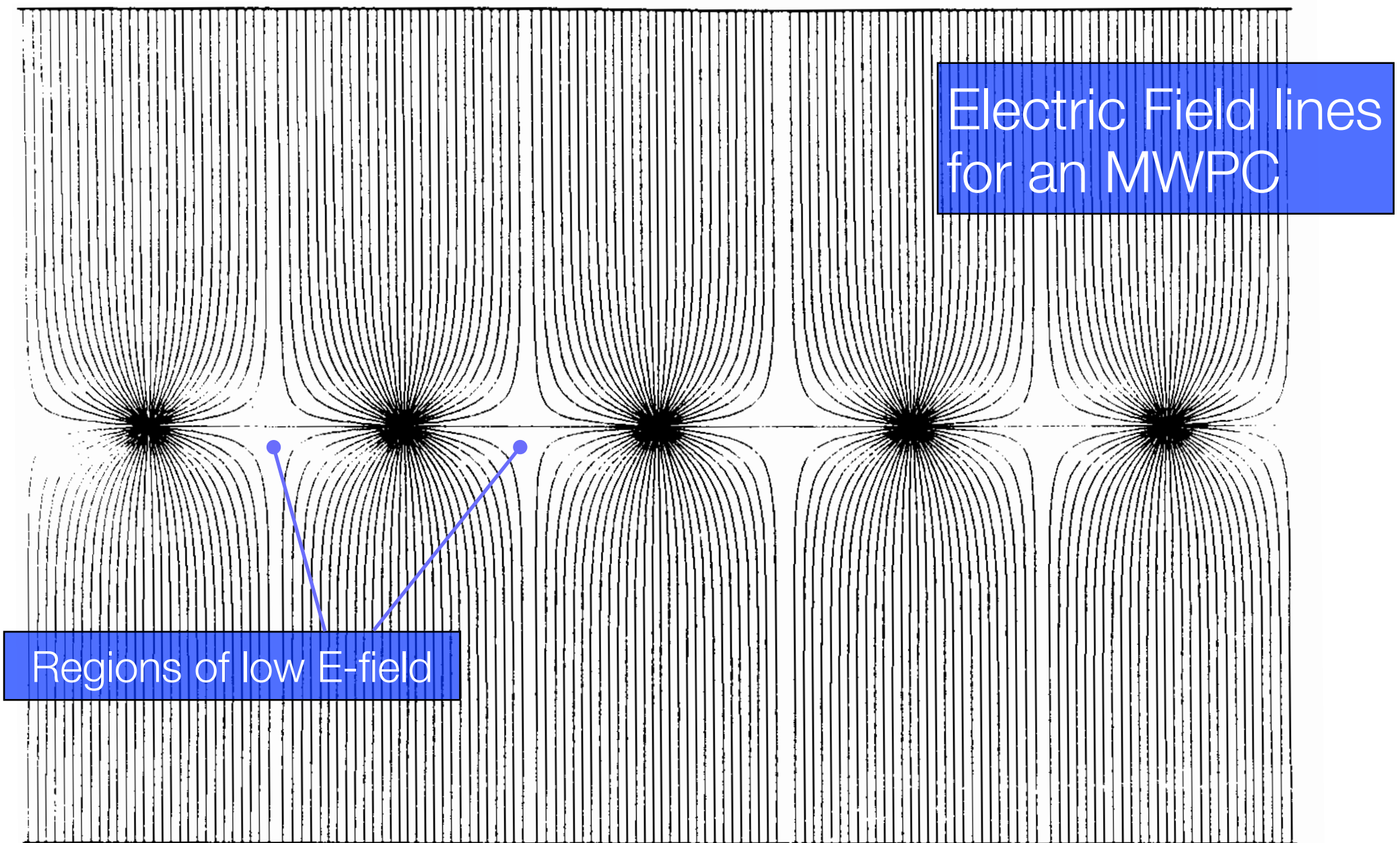
Drift Time Distribution
in $\text{Ar}+\text{CH}_4$ and C_2H_4



NIM 92 (1971) 373
[A. Walenta, J. Heintze, Pl]

J. Heintze

Drift Chambers – Field Formation



Drift Chambers – Field Formation

Modified MWPC ...

Introduce field wires to avoid low field regions, i.e. long drift-times

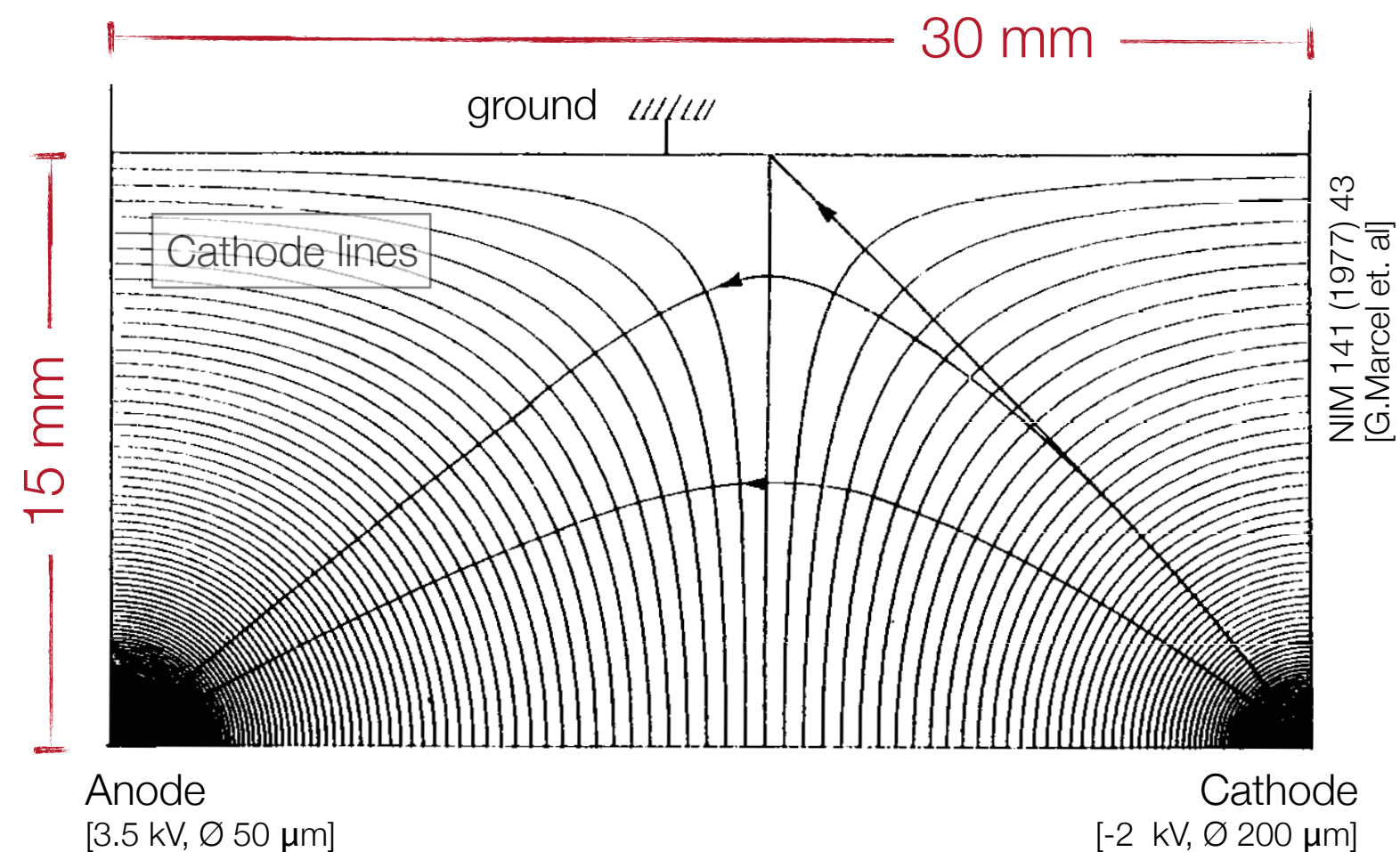
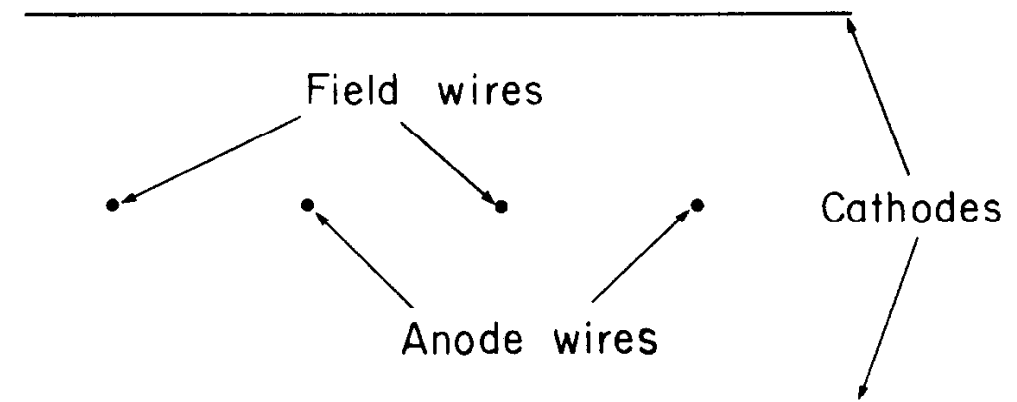
Field wires are at negative potential ...

Anode wires are at positive potential ...

Cathode planes are at zero potential ...

But:

Uniform drift field requires:
Gap length/wire spacing ≈ 1
i.e. for typical convenient wire spacing
one needs thick chambers ...



Drift Chambers – Field Formation

Principle of an
adjustable field multi-wire drift chamber

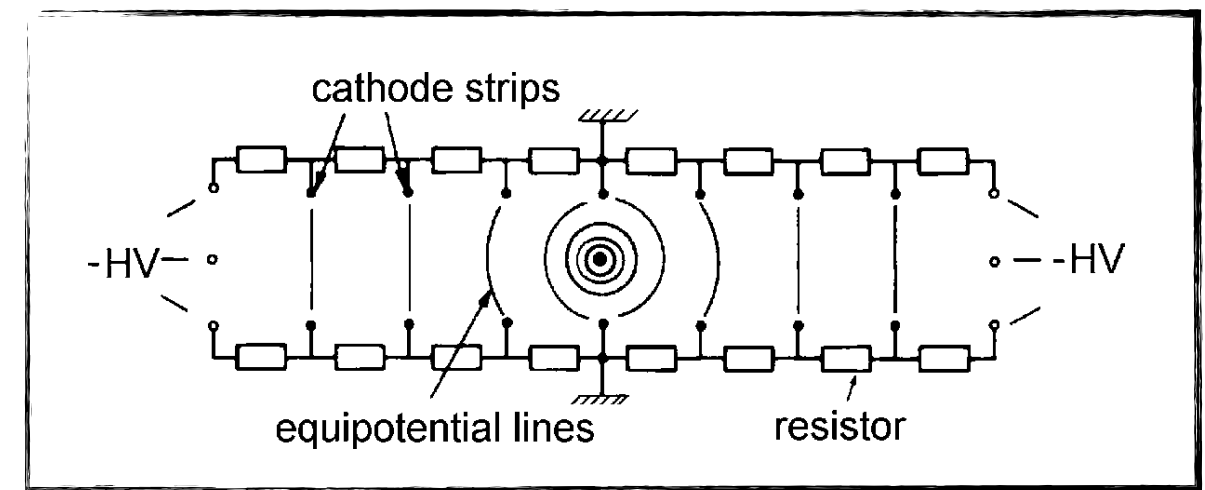
Introduction of voltage divider
via cathode wire planes ...

Features:

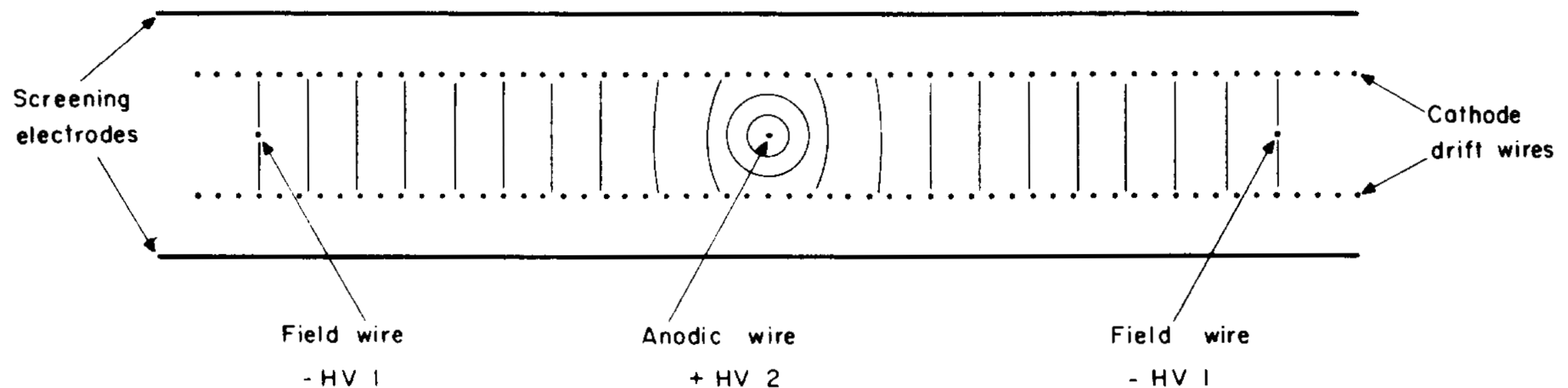
very few (or only one) anode wires

space point resolution limited by mechanical accuracy
[for large chambers: $\sigma \approx 200 \mu\text{m}$]

But: hit density needs to be low.

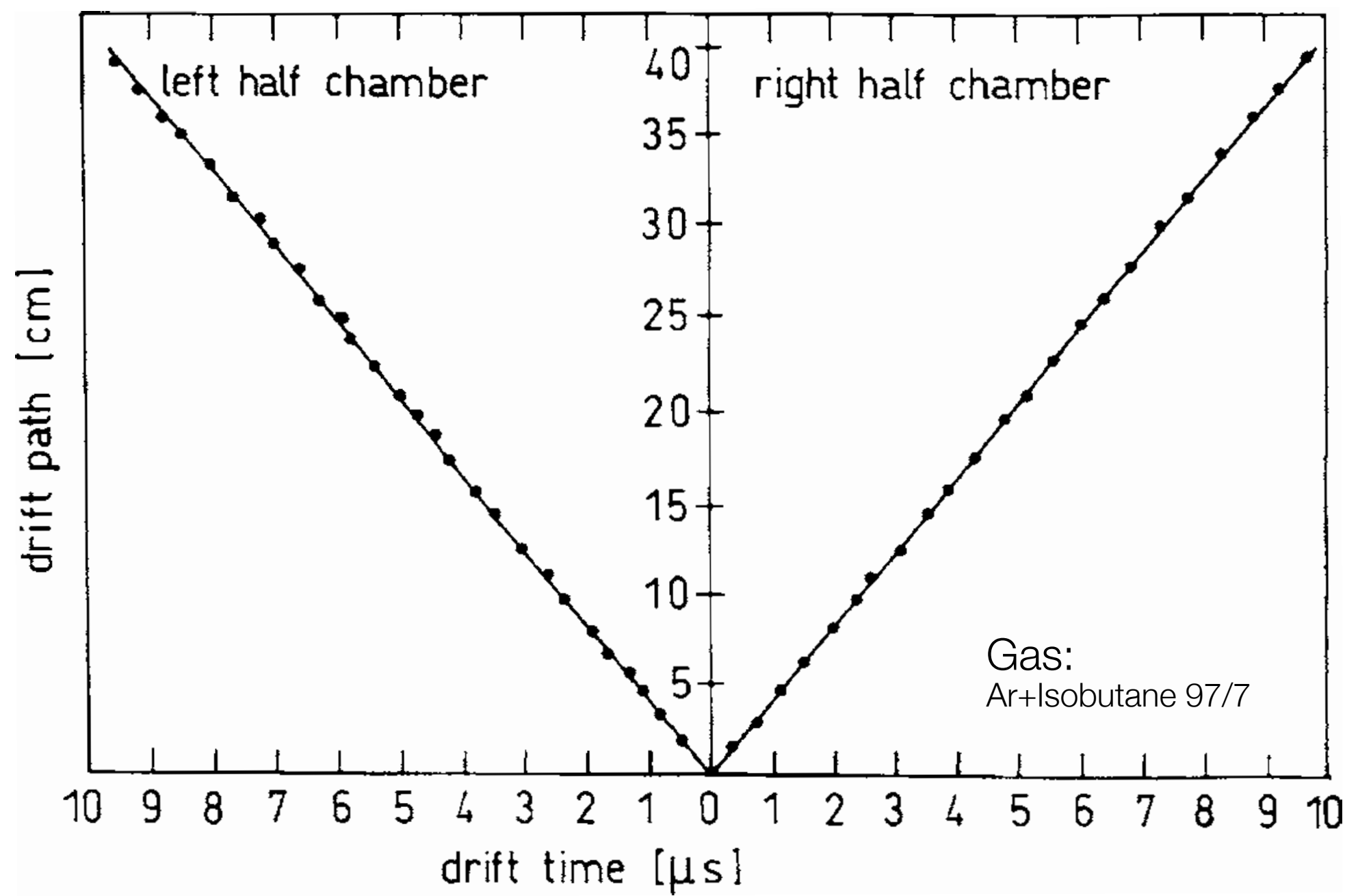


Schematics of voltage divider chain



Drift Chambers – Field Formation

Drift time space relation
for a large drift chamber ($80 \times 80 \text{ cm}^2$) with only one anode wire



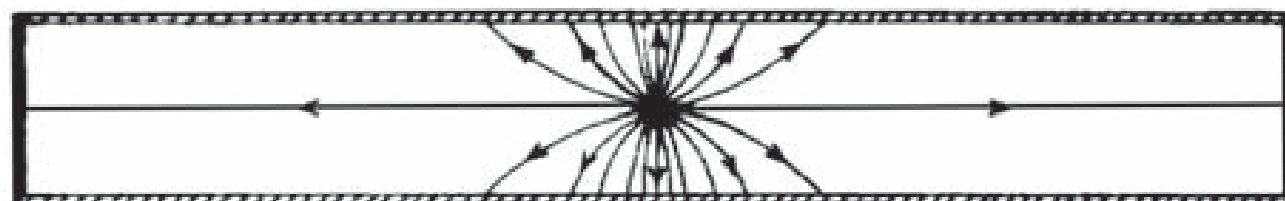
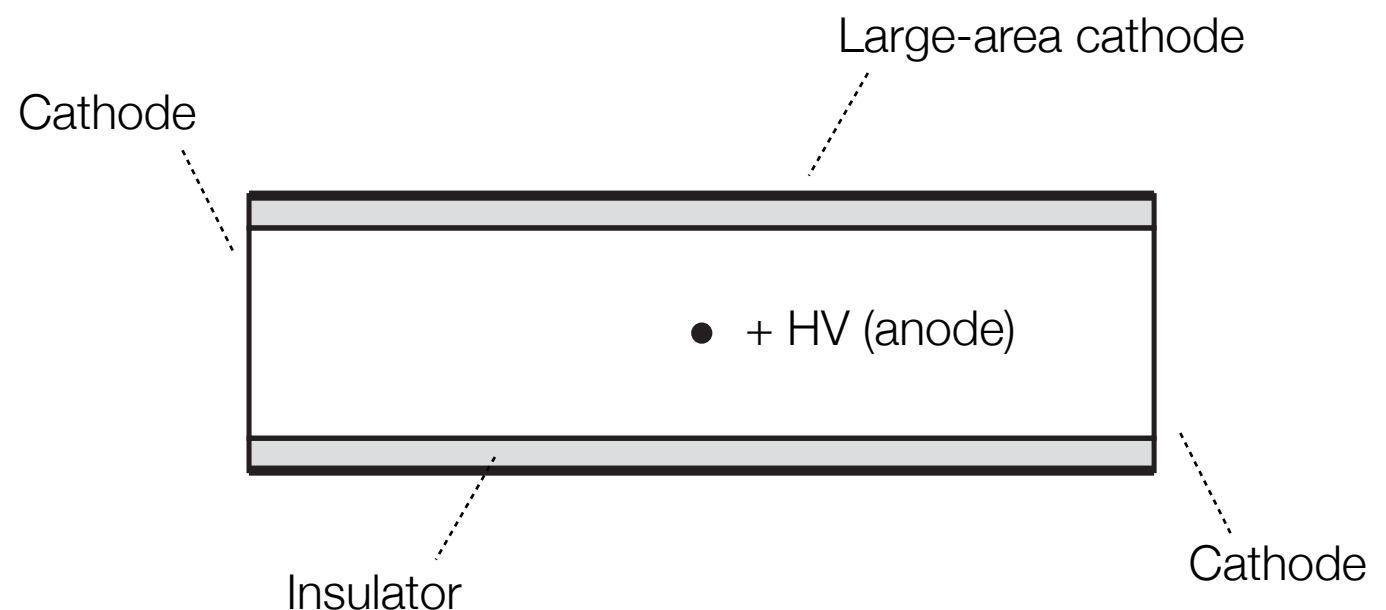
Drift Chambers – Field Formation

Alternative:

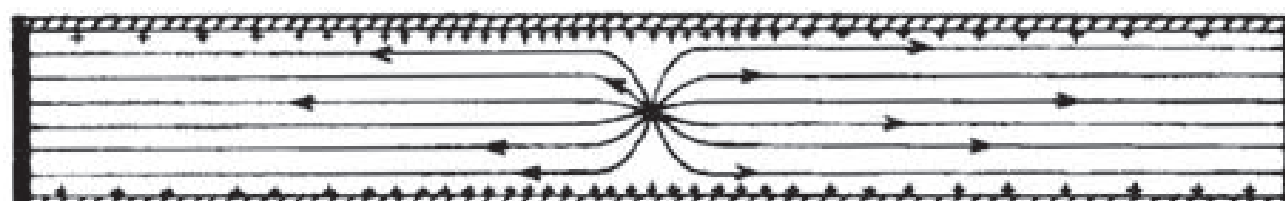
Field formation by charging
(insulated) chamber walls with ions ...

Electrodeless drift chamber
[Allison et al., 1982]

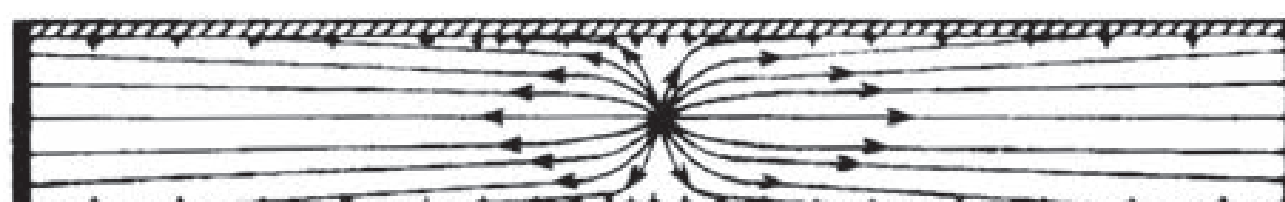
Requires some charging time ...



Before charging up:
field line end at cathode ...

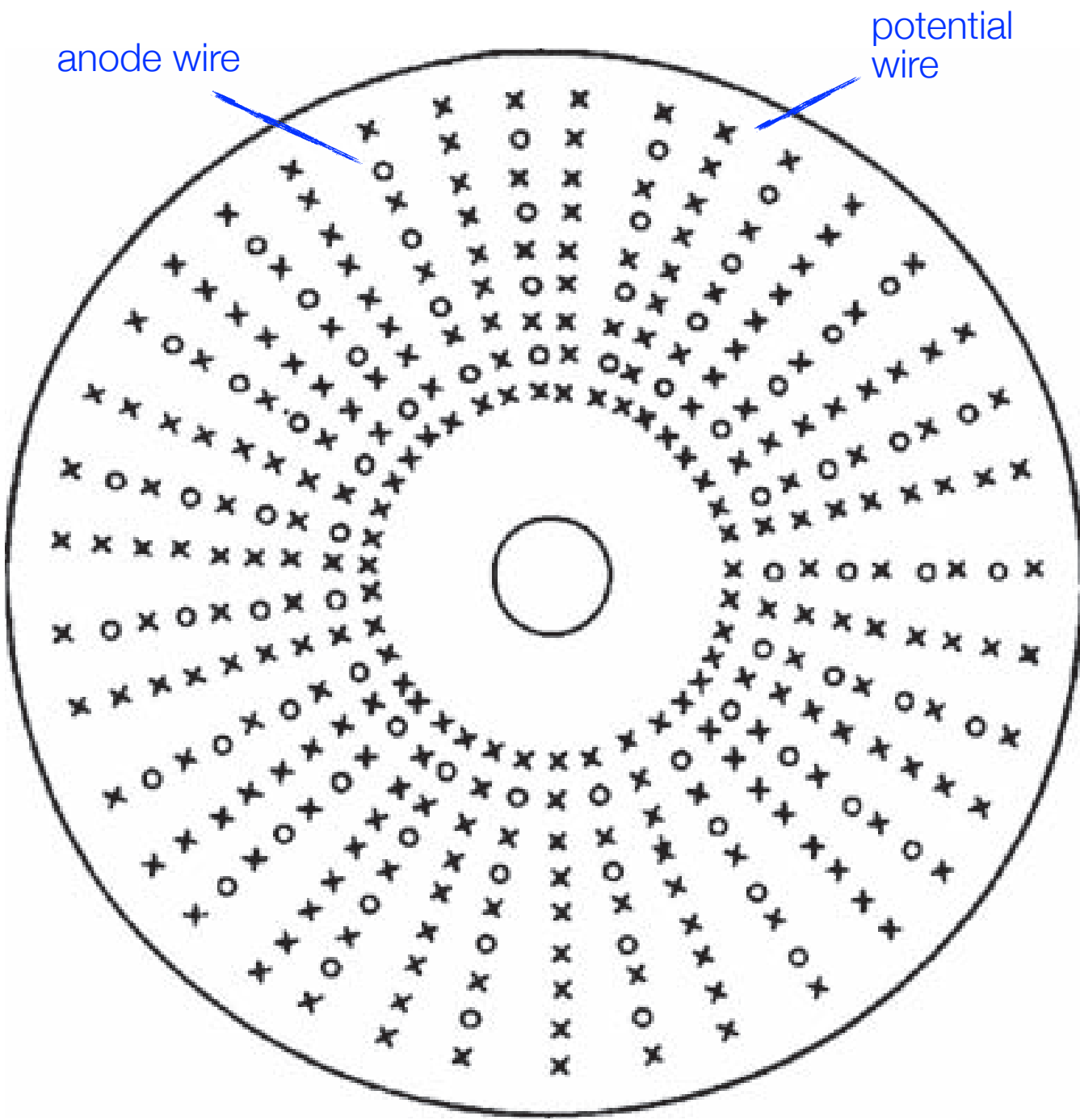


After charging time:
no field line end at cathode ...



To avoid overcharging:
Finite resistance of insulator
[i.e. some field lines end at cathode]

Cylindrical Drift Chambers



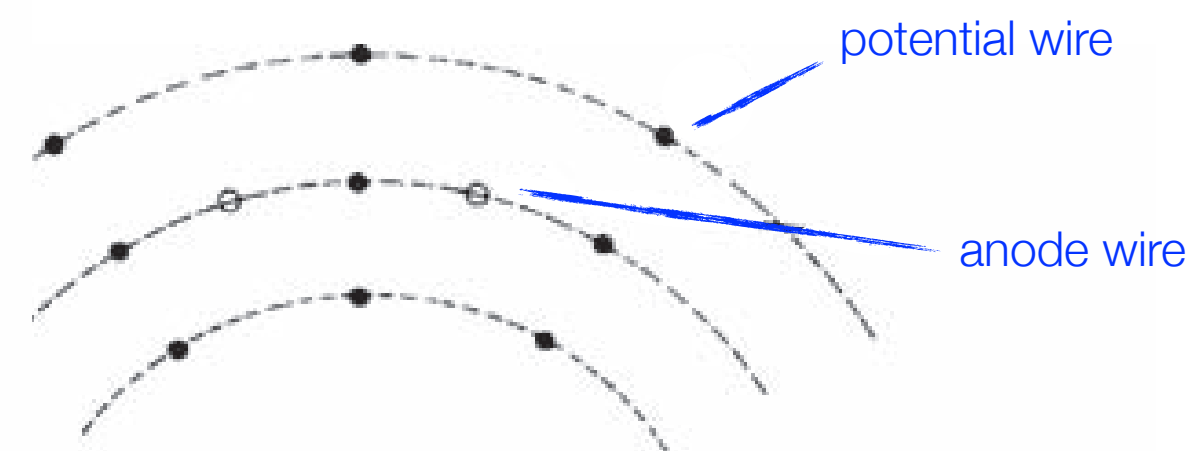
Application:

Collider experiments
[cylindrical wire arrangement needed]

Characteristica:

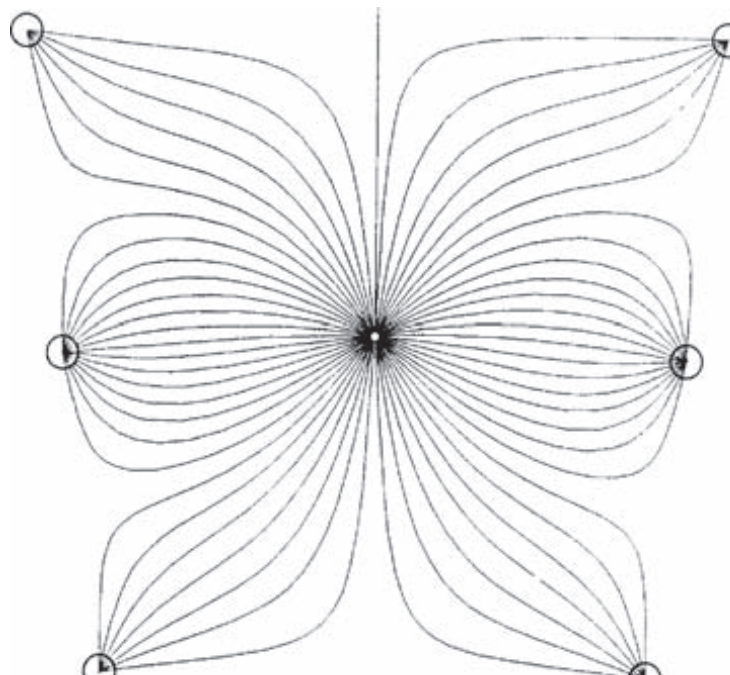
Cylindrical symmetry
Open drift cell geometry

Require: Simple space-time relation
given by E,B field and drift cell geometry



Cylindrical Drift Chambers

A Open drift-cells geometry

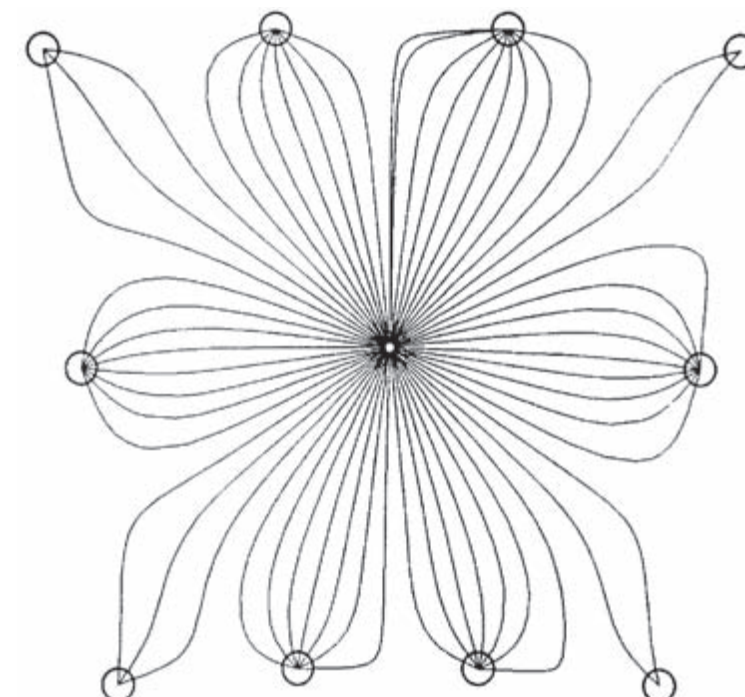


A

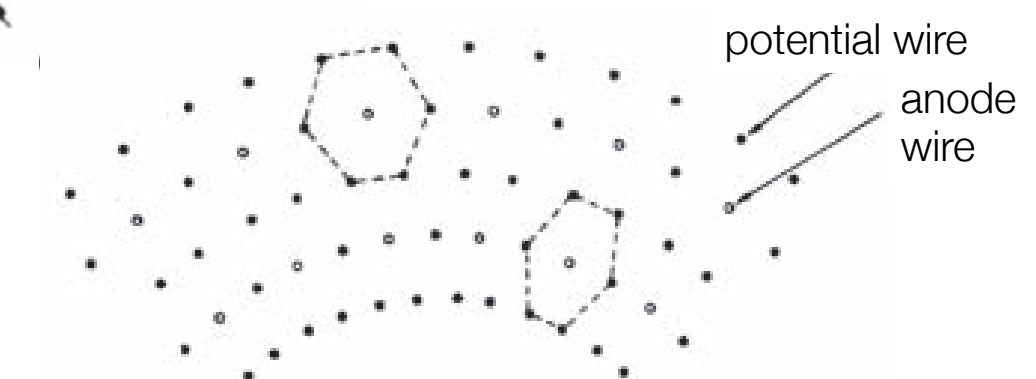
B



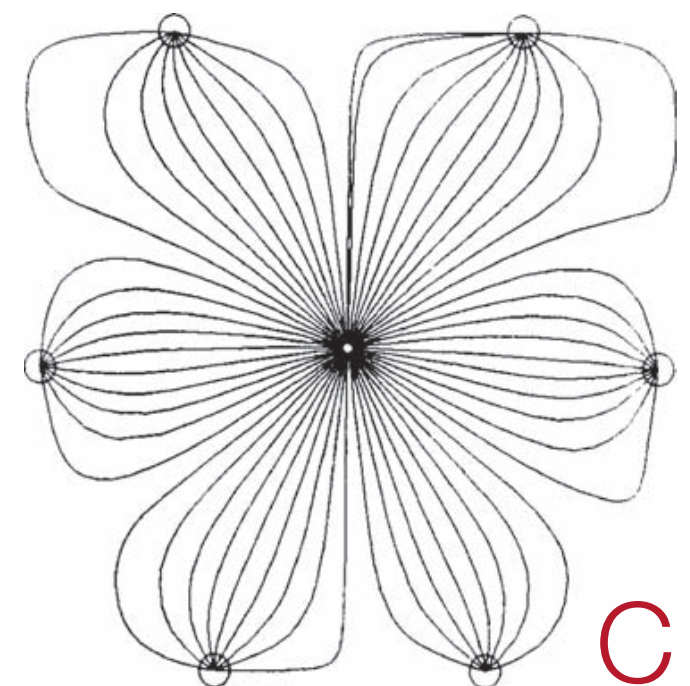
B Closed drift-cells geometry
[more wires]



C Hexagonal drift-cells geometry
[intermediate configuration]



C



Drift Chambers – Lorentz Angle

Require B field for momentum measurement ...

In general drift field $E \perp$ to B field ...

→ Lorentz angle: $\alpha_L = \alpha(\vec{v}_D, \vec{E})$...

Reminder:

$$\vec{v}_D = \frac{\mu |\vec{E}|}{1 + \omega^2 \tau^2} \left[\hat{\vec{E}} + \overbrace{\omega \tau \hat{\vec{E}} \times \hat{\vec{B}}}^{\text{Component } \perp \text{ to } E, B} + \overbrace{\omega^2 \tau^2 (\hat{\vec{E}} \cdot \hat{\vec{B}}) \hat{\vec{B}}}^{\text{Component in direction of } B} \right]$$

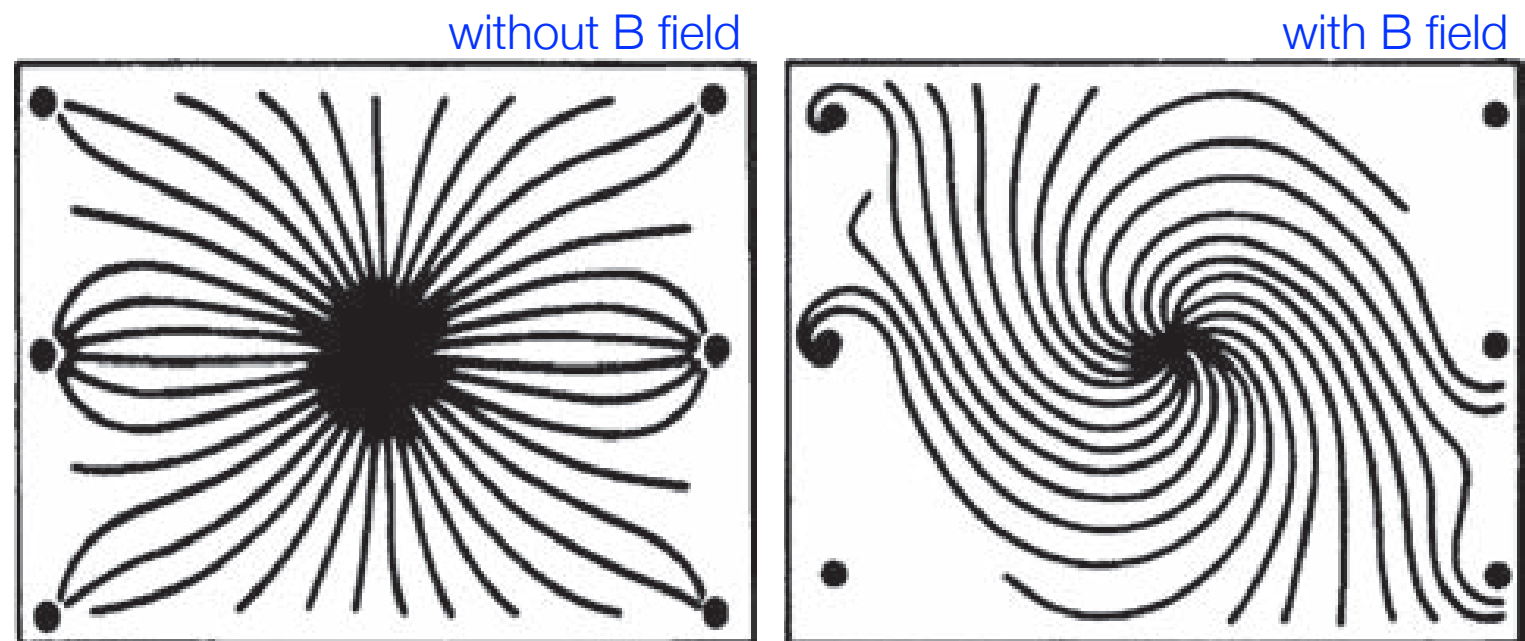
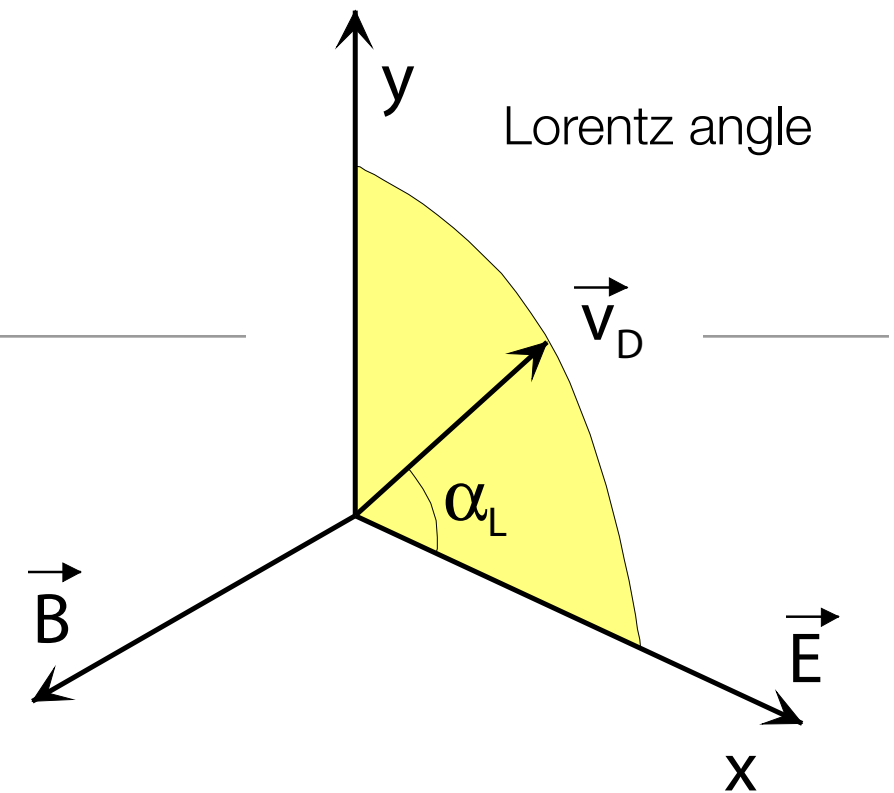
Using:

$$v_{D,x} = \frac{\mu E}{1 + \omega^2 \tau^2}$$

$$v_{D,y} = \frac{\mu E}{1 + \omega^2 \tau^2} \cdot \omega \tau$$

→ $\tan \alpha_L = \omega \tau$
 $= v_D \frac{B}{E}$

[with $\omega = \frac{eB}{m}$ and $\tau = \frac{mv_D}{eE}$]



Drift Chamber – Spatial Resolution

Resolution determined by
accuracy of drift time measurement ...

Influenced by:

Diffusion [$\sigma_{\text{Diff.}} \sim \sqrt{x}$]

see above: $\sigma^2 \sim 2Dt = 2Dx/v_D \sim x$...

δ -electrons [$\sigma_{\delta} = \text{const.}$]

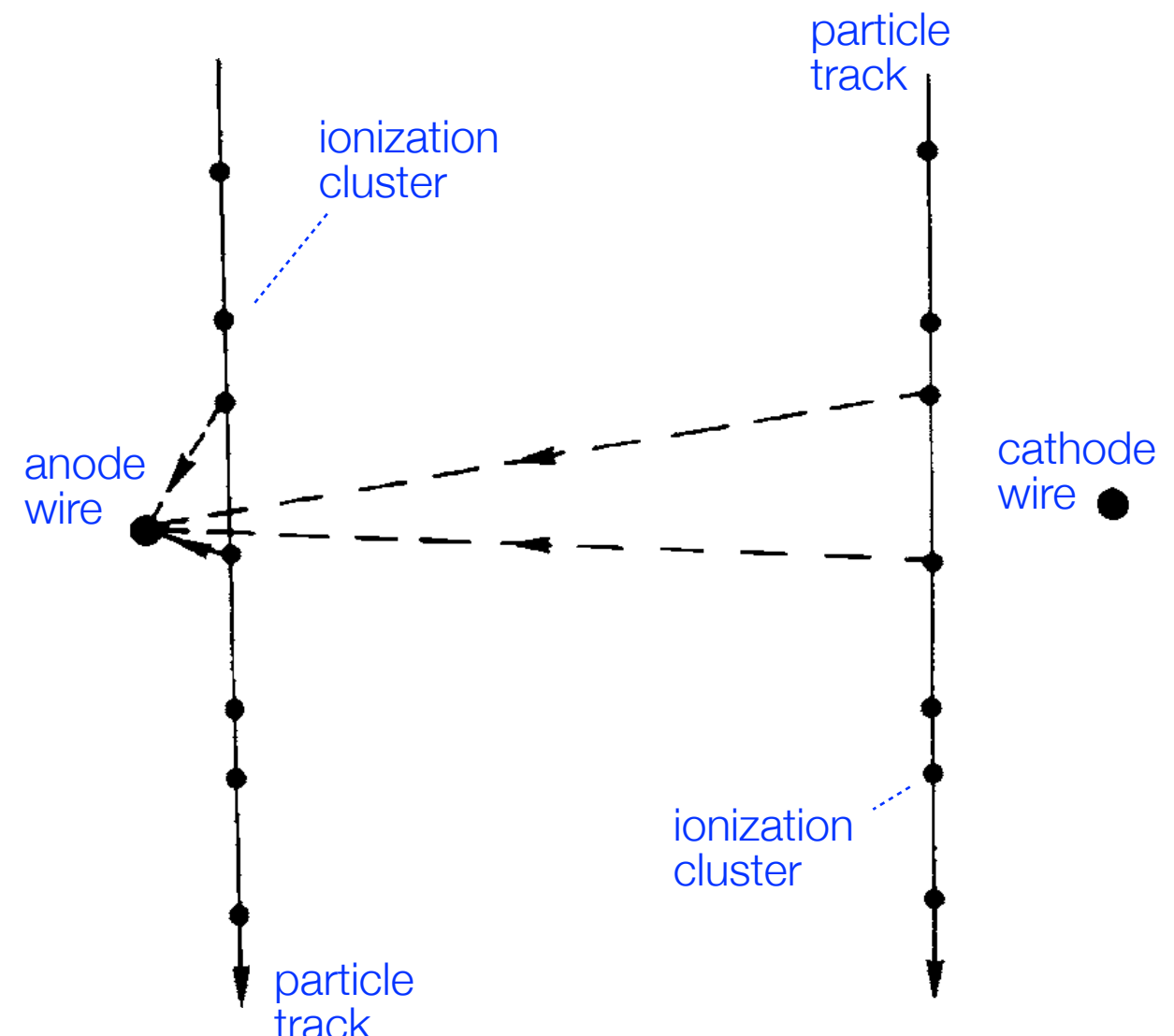
independent of drift length; yields constant
term in spatial resolution ...

Electronics [$\sigma_{\text{electronics}} = \text{const.}$]

contribution also independent of drift length ...

Primary ionization statistics [$\sigma_{\text{prim}} = 1/x$]

Spatial fluctuations of charge-carrier production result in
large drift-path differences for particle trajectories close to the anode ...
[minor influence for tracks far away from anode]



Drift Chamber – Spatial Resolution

Primary ionization statistics:

Step 1: Consider a track passing through an anode wire ...

Probability of no ionization within distance d :

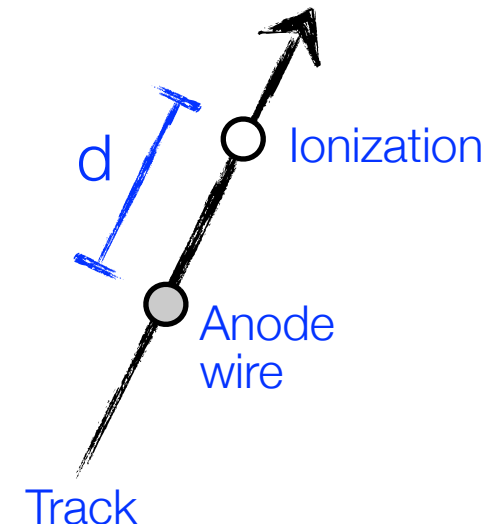
$$P_0(d) = e^{-2Nd}$$

with
N: number of ionizations per unit length

Average minimum distance of closest ionization cluster:

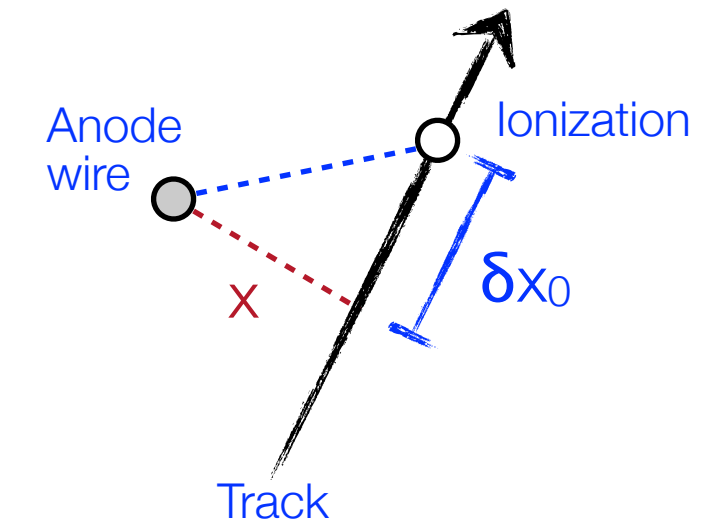
$$\delta x_0 = \langle d_{\min} \rangle = \int_0^\infty xe^{-2Nx} 2N dx = \frac{1}{2N}$$

$$\sigma_{\langle d_{\min} \rangle}^2 = \int_0^\infty (x - \frac{1}{2N})^2 e^{-2Nx} 2N dx = \frac{1}{4N^2}$$



Step 2: Track at distance x ...

$$\delta x = \sqrt{x^2 + (\delta x_0)^2} - x = x \left(\sqrt{1 + \left(\frac{\delta x_0}{x} \right)^2} - 1 \right) \approx \frac{x}{2} \left(\frac{\delta x_0}{x} \right)^2 \propto \frac{1}{x}$$



Drift Chamber – Spatial Resolution

$$\sigma_x^2 = \underbrace{\left(\frac{1}{64N^2} \right) \cdot \frac{1}{x^2}}_{\text{1st ionization statistics}} + \underbrace{\frac{2D}{v_d} \cdot x}_{\text{diffusion}} + \underbrace{\sigma_{\text{const}}^2}_{\text{electronics } \delta\text{-electrons}}$$

Possible improvements:

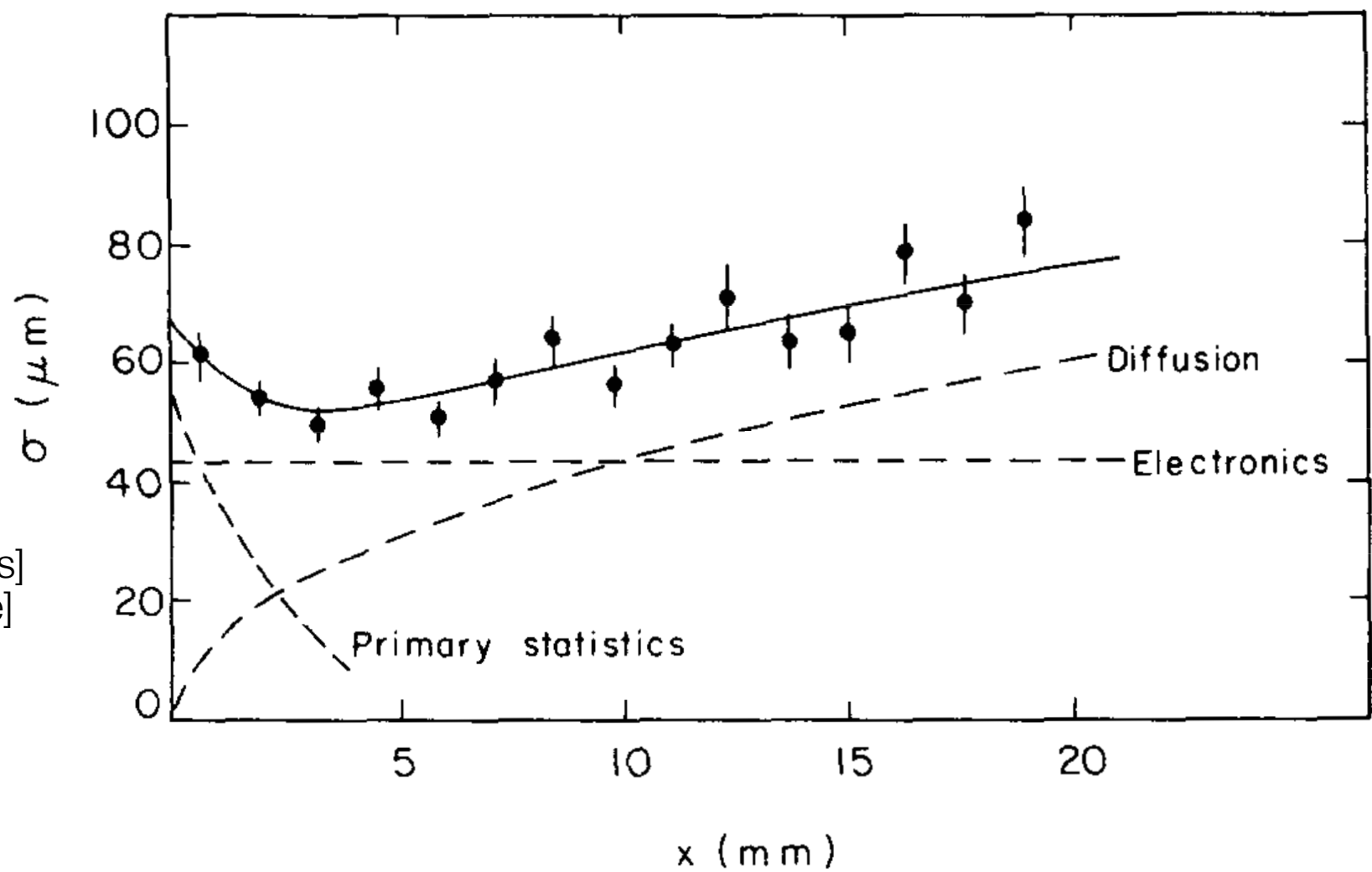
Increase N by increasing pressure ...

Decrease D by increasing pressure ...

$$D \sim \frac{\lambda_0^2}{\tau} \sim \frac{1/n^2}{1/n} \sim \frac{1}{n}$$

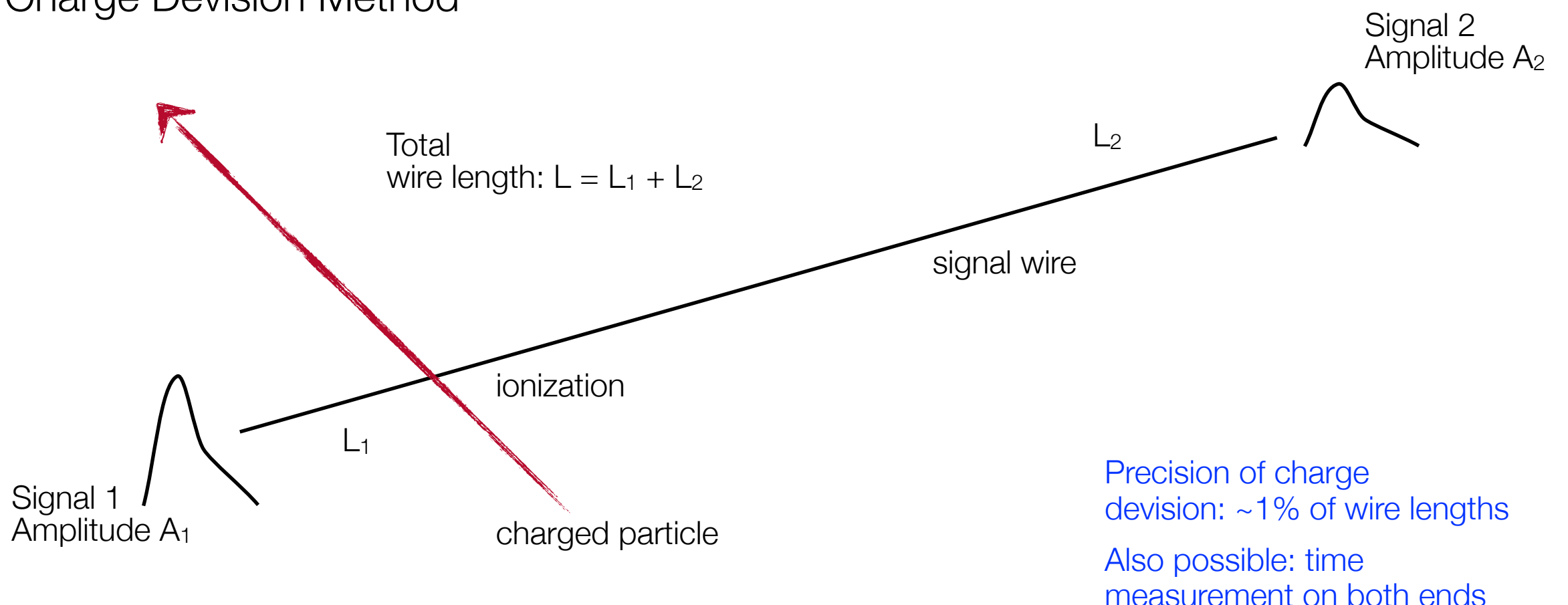
[n: particle density in gas]
[increases with pressure]

i.e.: increase pressure ...
[up to 4 atm possible]



Drift Chamber – Determination of z

Principle of
Charge Devision Method



Determination
of L₁, L₂:

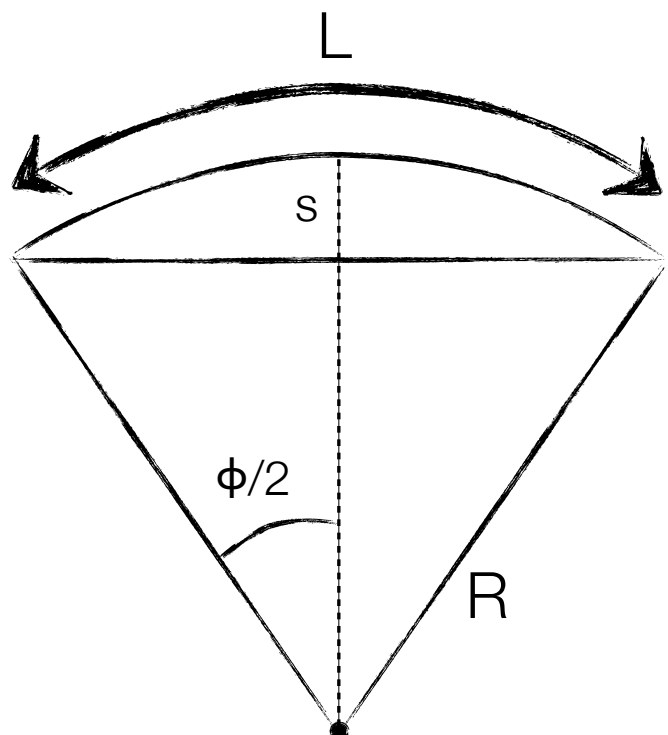
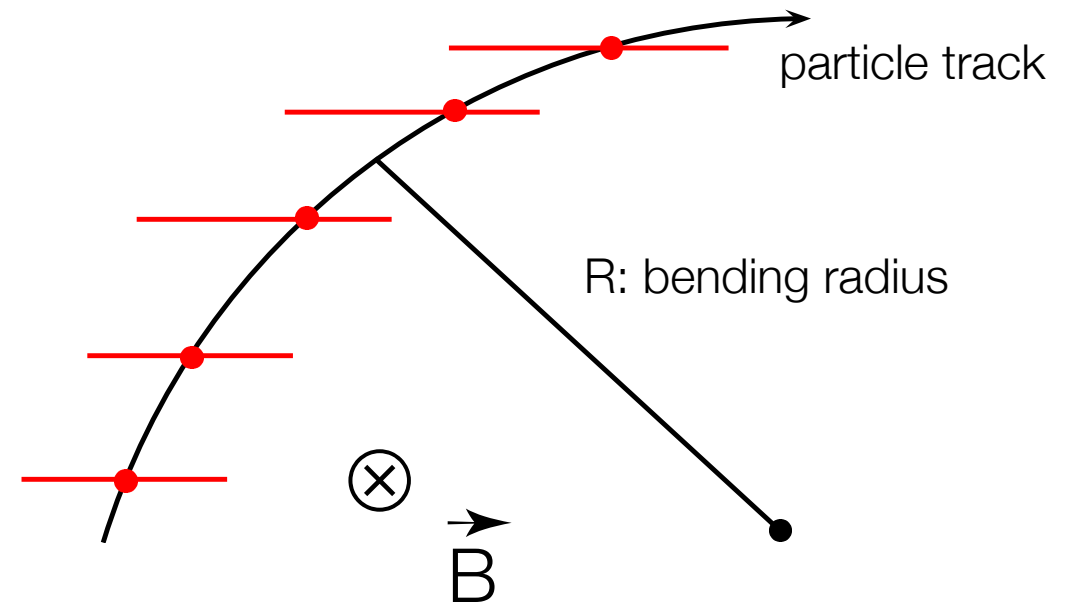
$$L_2 = \frac{A_1}{A_1 + A_2} \cdot L \quad L_1 = \frac{A_2}{A_1 + A_2} \cdot L$$

Magnetic Spectrometer Resolution

Momentum determination
in a cylindrical drift chamber ...

$$\frac{mv^2}{R} = evB \rightarrow p = eB \cdot R$$

$$p \left[\frac{\text{GeV}}{c} \right] = 0.3B [\text{m}] \cdot R [\text{T}]$$



For Sagitta s:

$$s = R - R \cos \frac{\phi}{2} \approx R \frac{\phi^2}{8}$$

$$s = R \frac{L^2}{8R^2} = \frac{L^2}{8R} \quad \text{and} \quad R = \frac{L^2}{8s}$$

$$\rightarrow \frac{\Delta p}{p} = \frac{\Delta R}{R} = \frac{L^2}{8Rs} \cdot \frac{\Delta s}{s}$$

$$\text{with } \phi = \frac{L}{R}$$

Magnetic Spectrometer Resolution

Momentum measurement

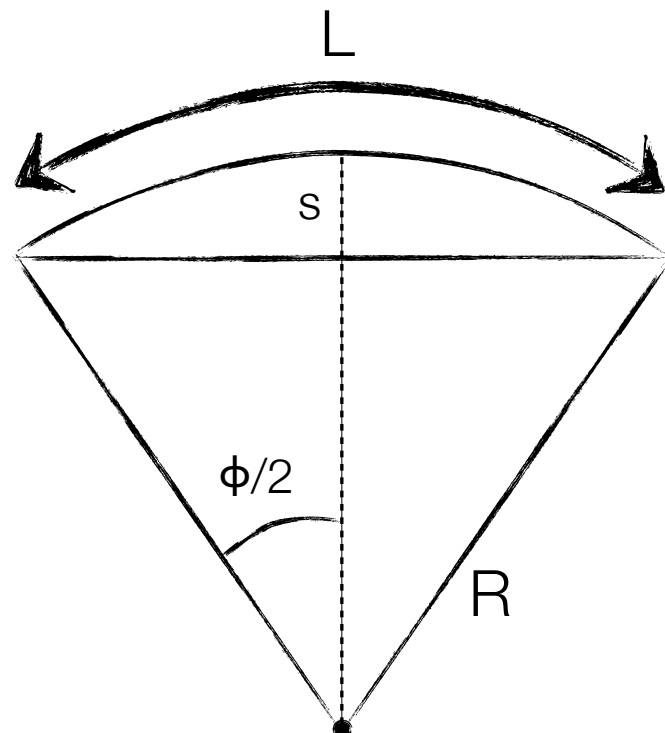
uncertainty:

$$\frac{\sigma_p}{p} = \frac{L^2}{8Rs} \cdot \frac{\sigma_s}{s} = \frac{L^2}{8R} \cdot \frac{\sigma_s}{L^4/64R^2} = \frac{\sigma_s}{L^2} \cdot 8R = \frac{\sigma_s}{L^2} \cdot \frac{8p}{eB} \sim p \cdot \frac{\sigma_s}{BL^2}$$

Uncertainty σ_s depends on number and spacing of track point measurements; for equal spacing and large N:

$$\sigma_s = \frac{\sigma_{r\phi}}{8} \sqrt{\frac{720}{N+5}}$$

see: Glückstern, NIM 24 (1963) 381 or
Blum & Rolandi, Particle Detection ...



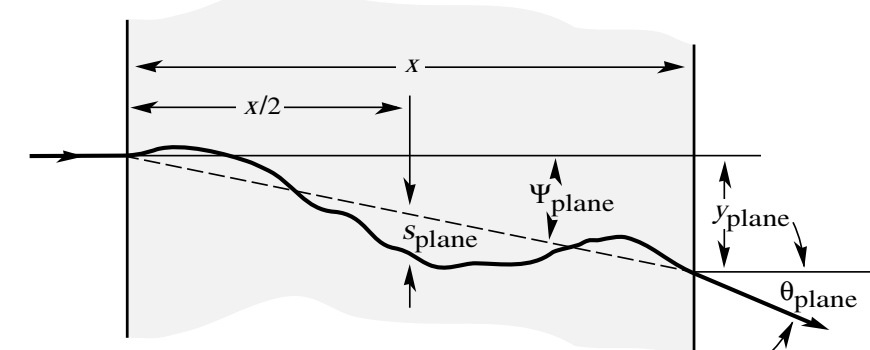
Multiple scattering contribution:

Reminder:

$$\sigma_\phi = \frac{13.6 \text{ MeV}}{\beta cp} z \sqrt{x/X_0} [1 + 0.038 \ln(x/X_0)]$$

$$\sigma_\phi \approx \frac{14 \text{ MeV}/c}{p} \sqrt{\frac{L}{X_0}} \quad \text{and} \quad \frac{\sigma_p}{p} = \frac{\sigma_R}{R} = \frac{\sigma_\phi}{\phi}$$

$$\text{as } R = \frac{L}{\phi}$$



Good momentum resolution:

- large path length L
- large magnetic field B
- good Sagitta measurement

Magnetic Spectrometer Resolution

Multiple scattering contribution:
[cont'd]

$$\frac{\sigma_p}{p} = \frac{\sigma_\phi}{\phi} = \frac{14 \text{ MeV}/c}{p} \sqrt{\frac{L}{X_0}} \cdot \frac{R}{L} = \frac{14 \text{ MeV}/c}{p} \sqrt{\frac{1}{LX_0}} \cdot \frac{p}{eB} \sim \frac{1}{\sqrt{LX_0} B}$$

Generally p_t measured:

$$\left(\frac{\sigma_{p_t}}{p_t} \right)^2 = \text{const} \cdot \left(\frac{p_t}{BL^2} \right)^2 + \text{const} \cdot \left(\frac{1}{B\sqrt{LX_0}} \right)^2$$

For momentum p :

$$\left(\frac{\sigma_p}{p} \right)^2 = \left(\frac{\sigma_{p_t}}{p_t} \right)^2 + \left(\frac{\sigma_\theta}{\sin \theta} \right)^2$$

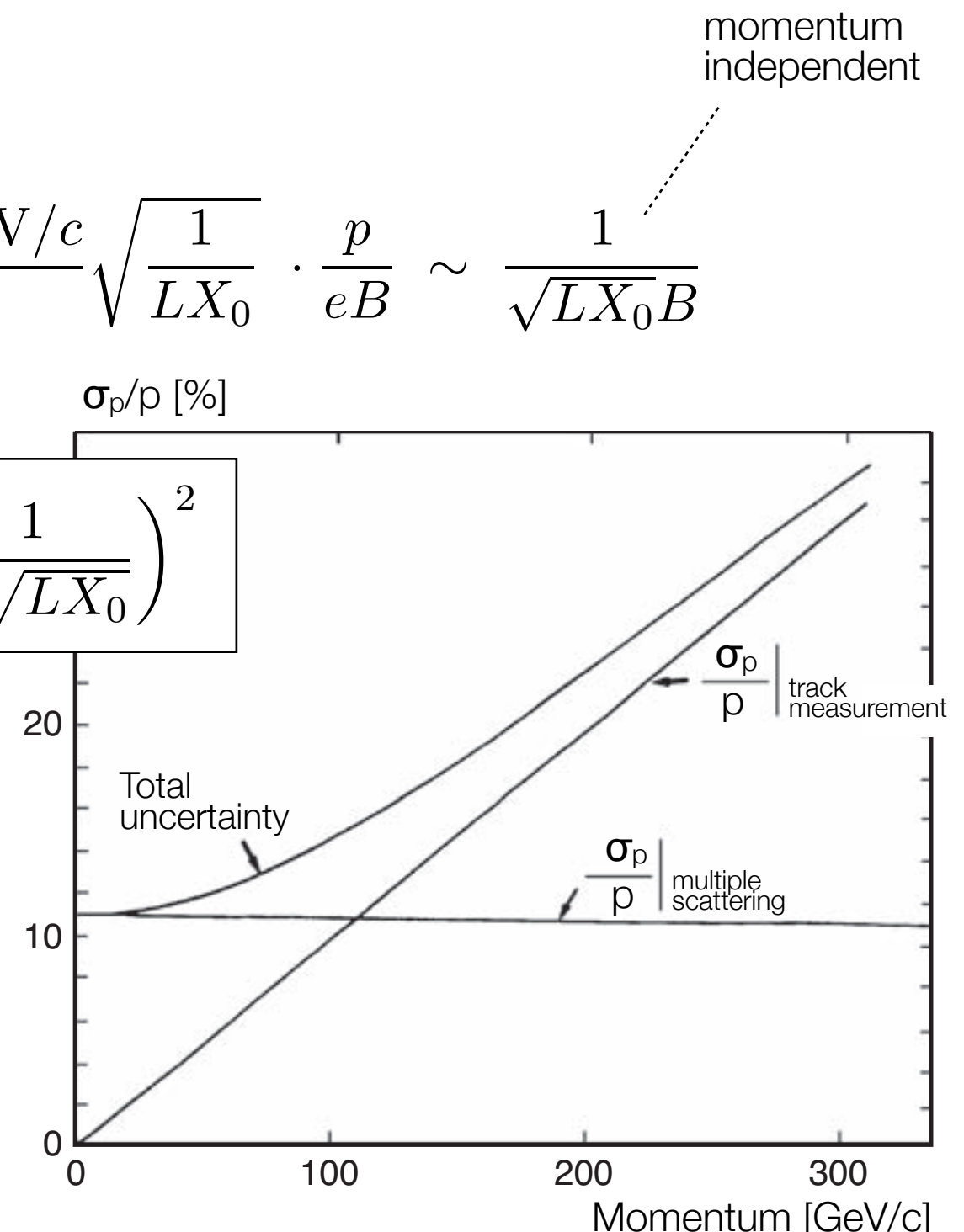
using $p = \frac{p_t}{\tan \theta}$

Examples:

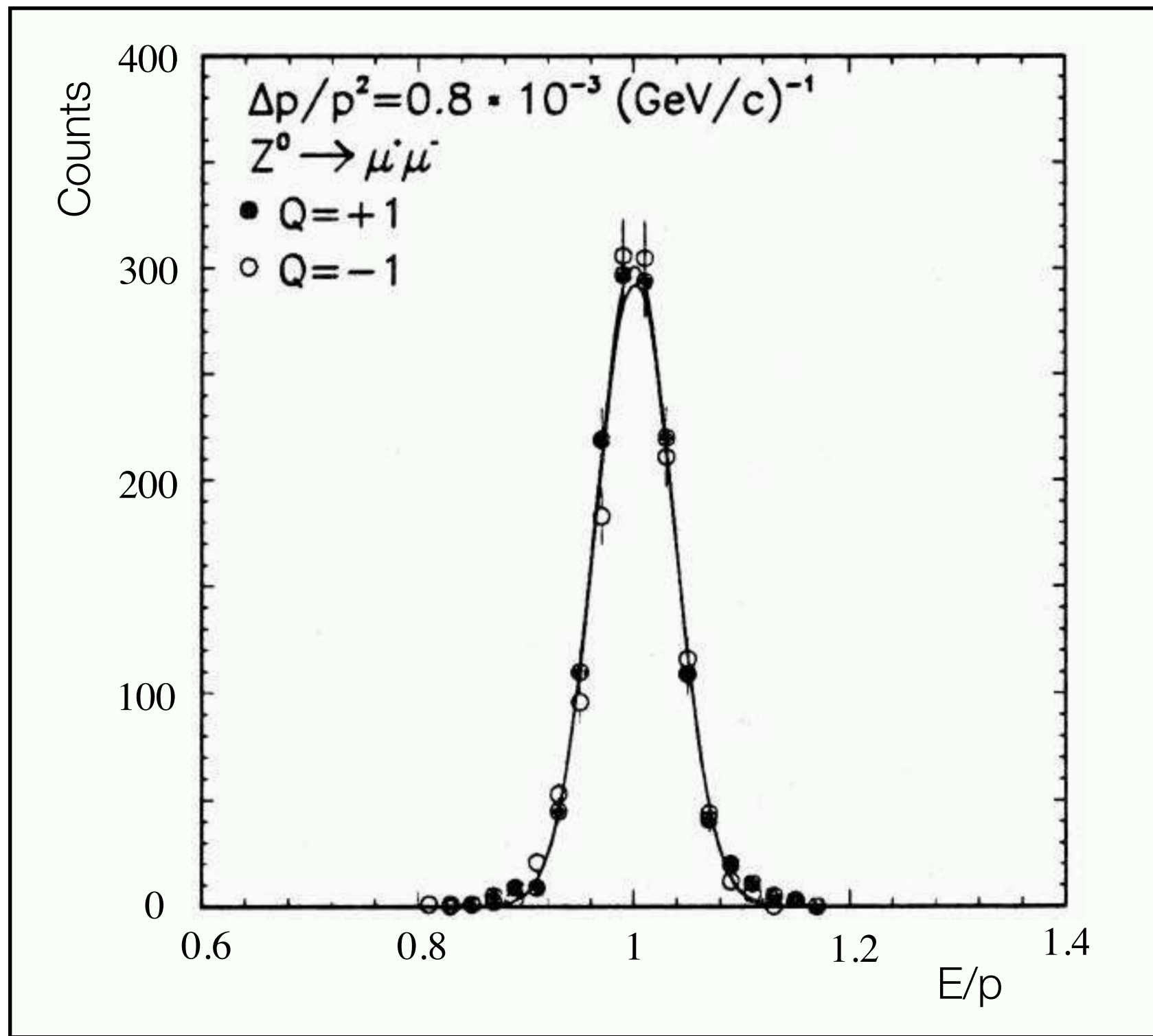
Argus: $\sigma_{p_t}/p_t = 0.009^2 + (0.009 p_t)^2$

ATLAS: $\sigma_{p_t}/p_t = 0.001^2 + (0.0005 p_t)^2$

[ATLAS nominal; TDR]



Magnetic Spectrometer Resolution

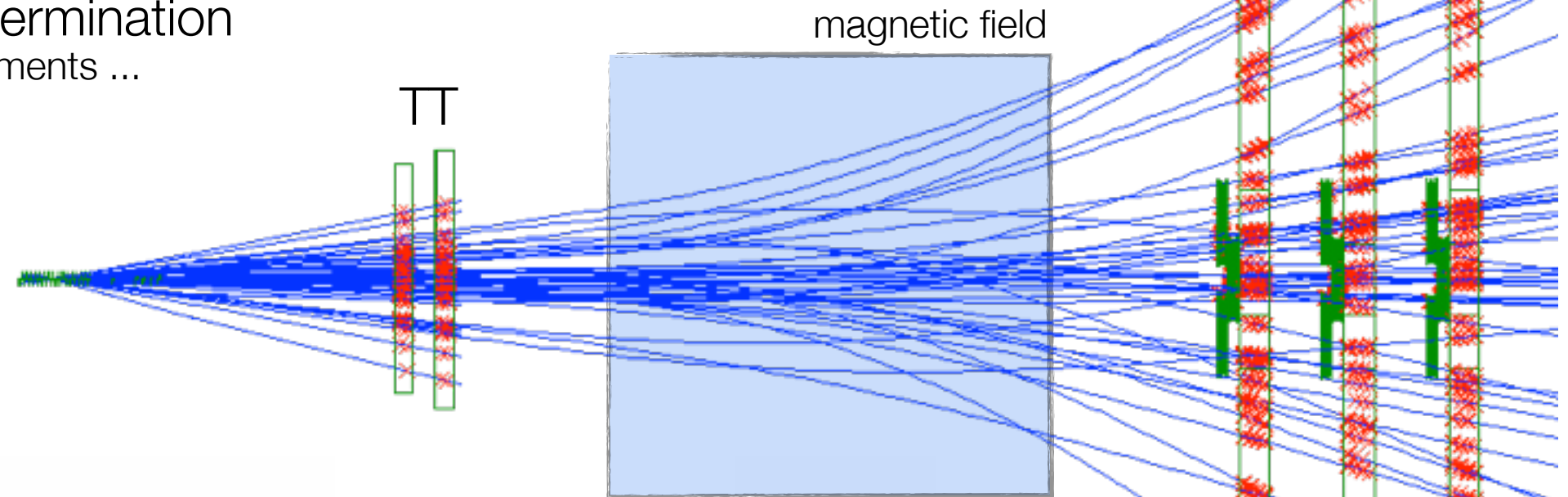


Momentum resolution
for muons in $Z \rightarrow \mu\mu$

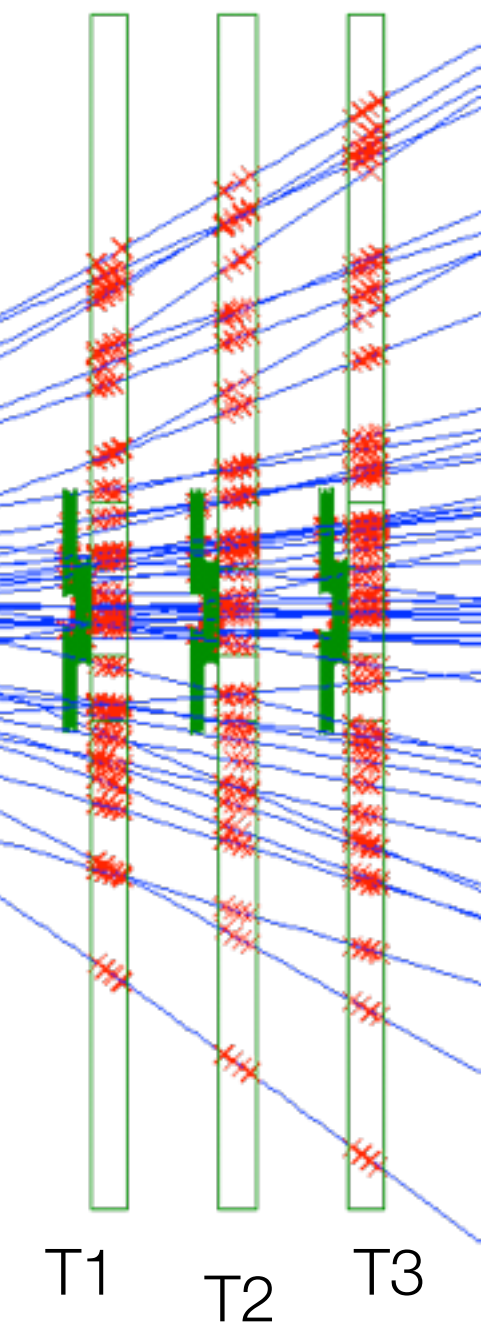
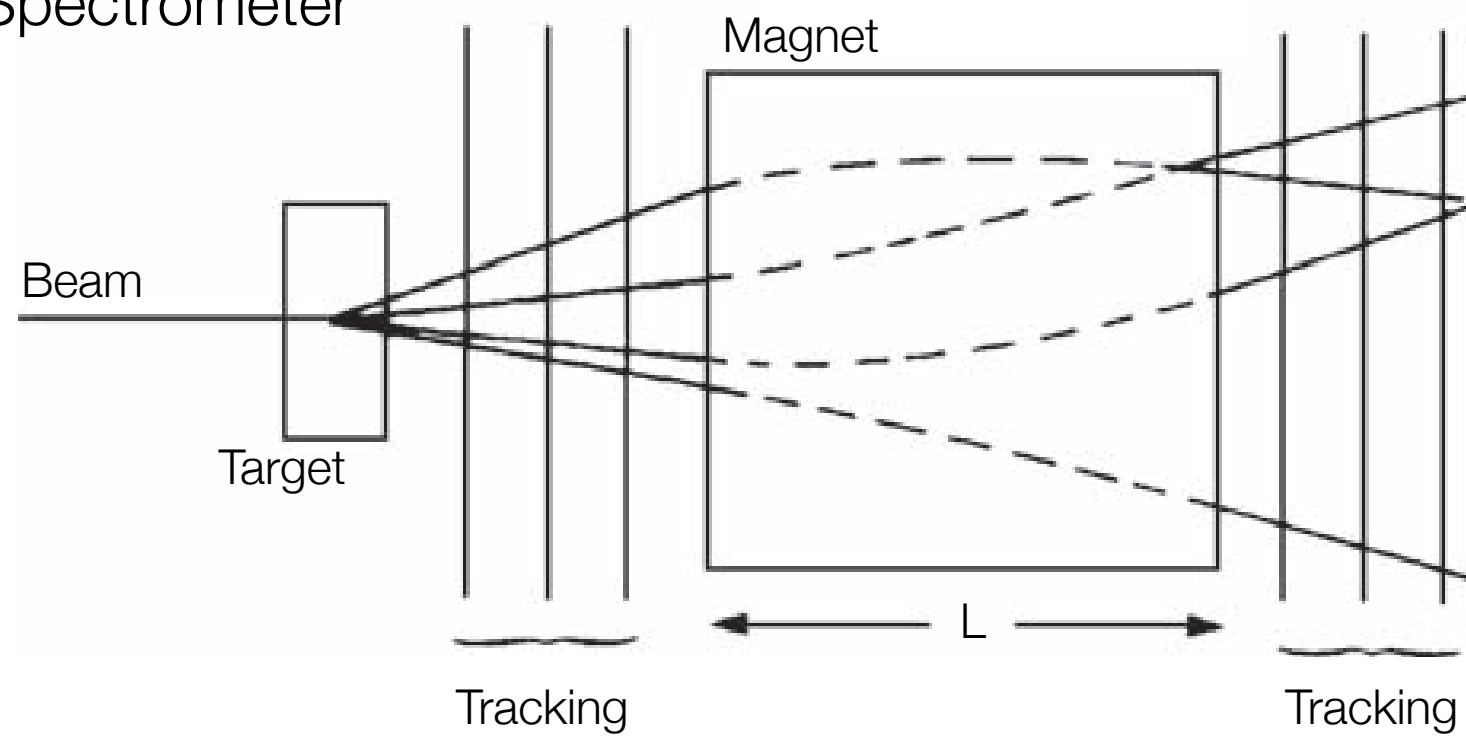
$s \sim 1/R \sim 1/p$ measured!
→ $1/p$ is Gaussian

Magnetic Spectrometer Resolution

Momentum determination
in fixed target experiments ...



Schematics of a
Spectrometer



Magnetic Spectrometer Resolution

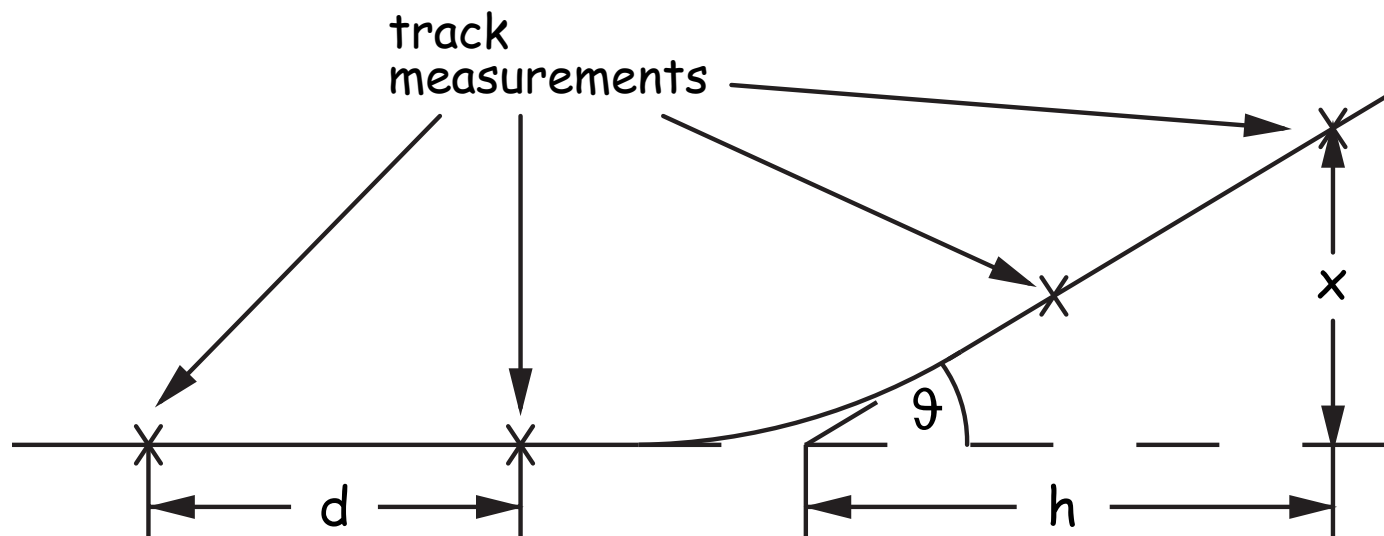
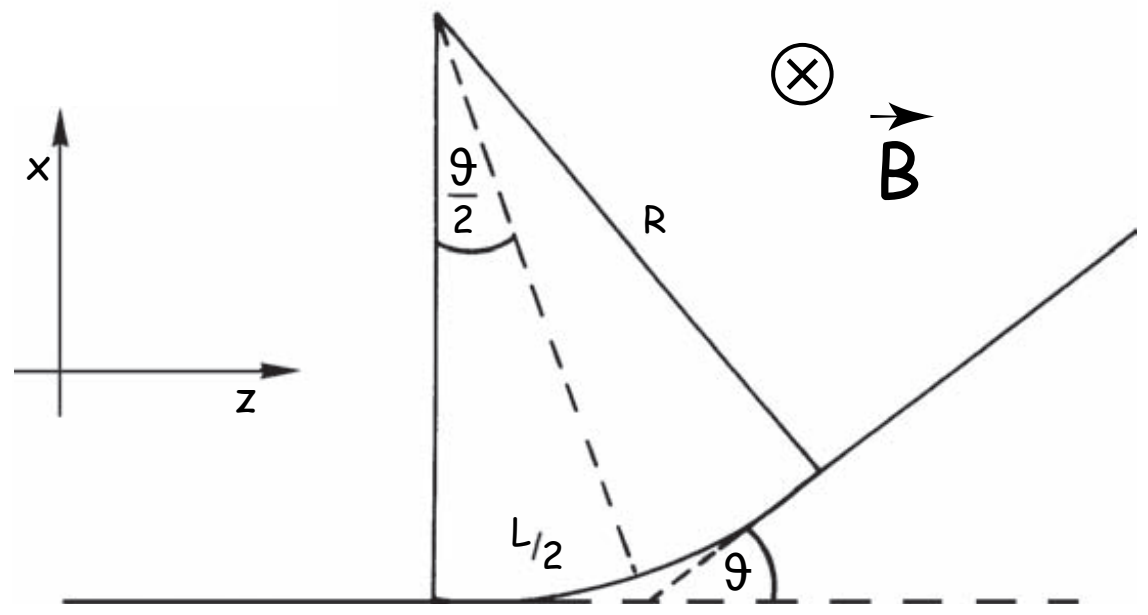
Momentum determination
in fixed target experiments ...

$$p = eRB \quad \vartheta = L/R \\ = L/p \cdot eB$$

$$p = eB \cdot L/\vartheta$$

Momentum resolution:

$$\rightarrow \frac{\sigma_p}{p} = \frac{\sigma_\vartheta}{\vartheta} \quad \text{with} \quad \sigma_\vartheta \sim \sigma_x$$



Determination
of σ_p/p :

$$\vartheta = \frac{x}{h} \quad \sigma_\vartheta = \frac{\sigma_x}{h}$$

$$\frac{\sigma_p}{p} = \frac{\sigma_\vartheta}{\vartheta} = \frac{\sigma_x}{h} \cdot \frac{p}{eBL}$$

Long lever arm improves
momentum resolution ...

Drift Chambers – Ambiguities

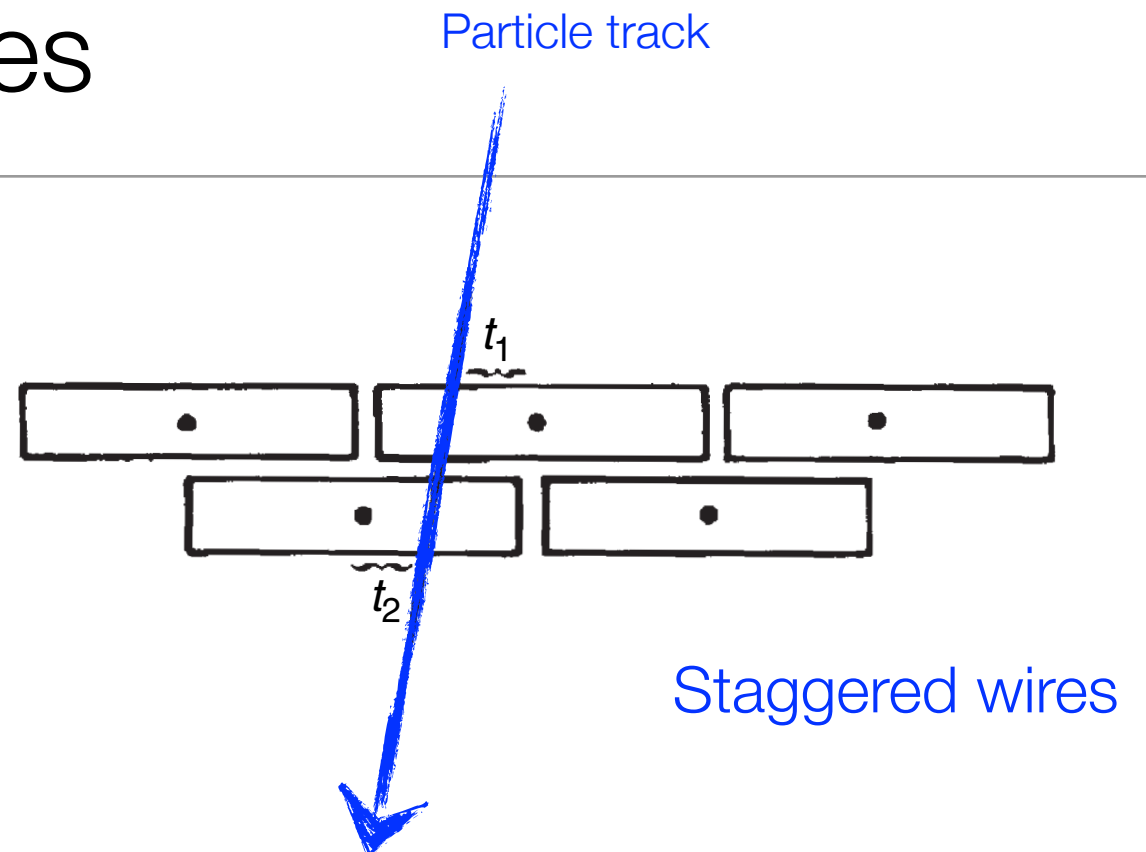
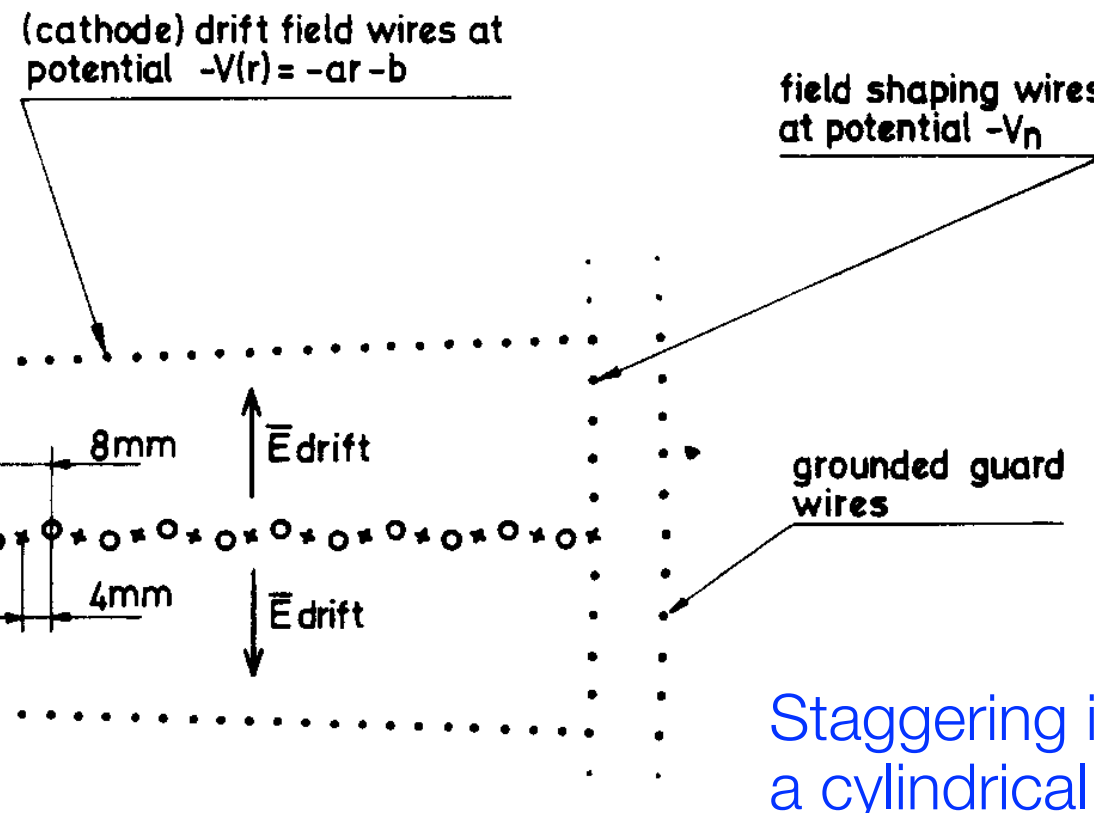
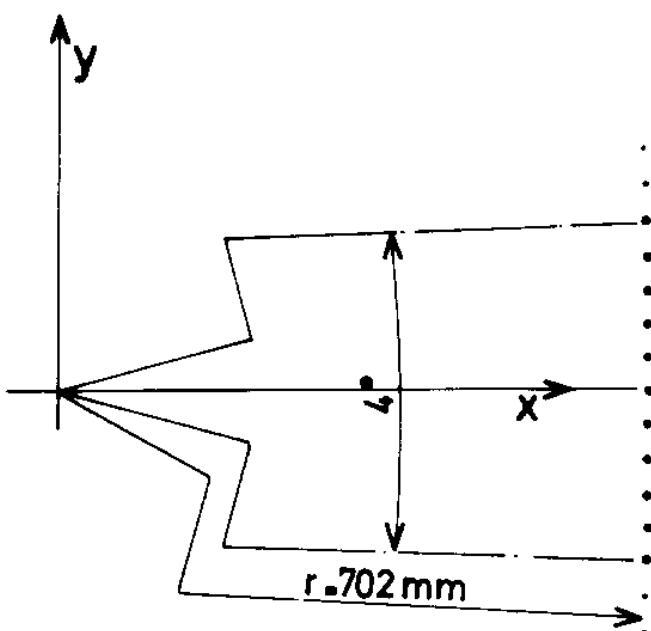
Difficulty:

Time measurement cannot distinguish whether particle has passed right or left from a wire ...

"Left-Right Ambiguity"

Solution: "Staggered wires"

Use multiple (two) layers displaced relative to each other ...

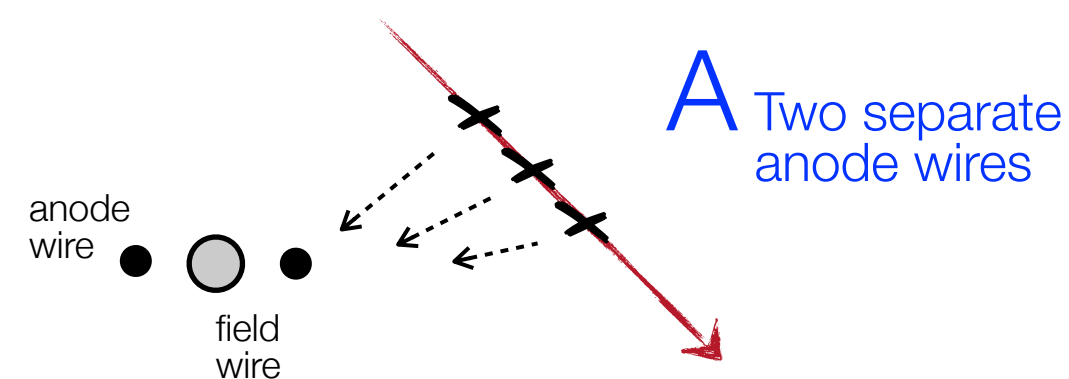
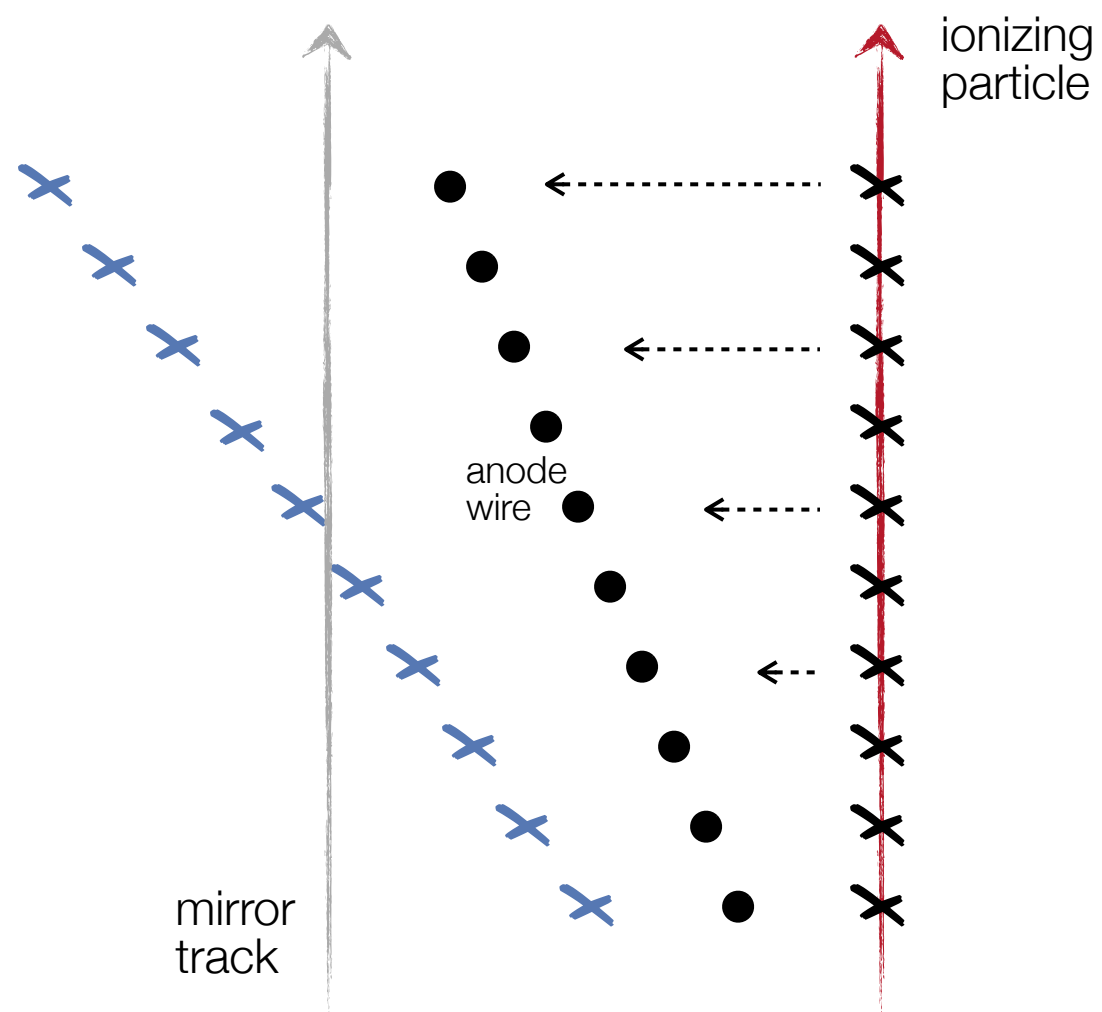


Staggering in
a cylindrical drift chamber [see later]

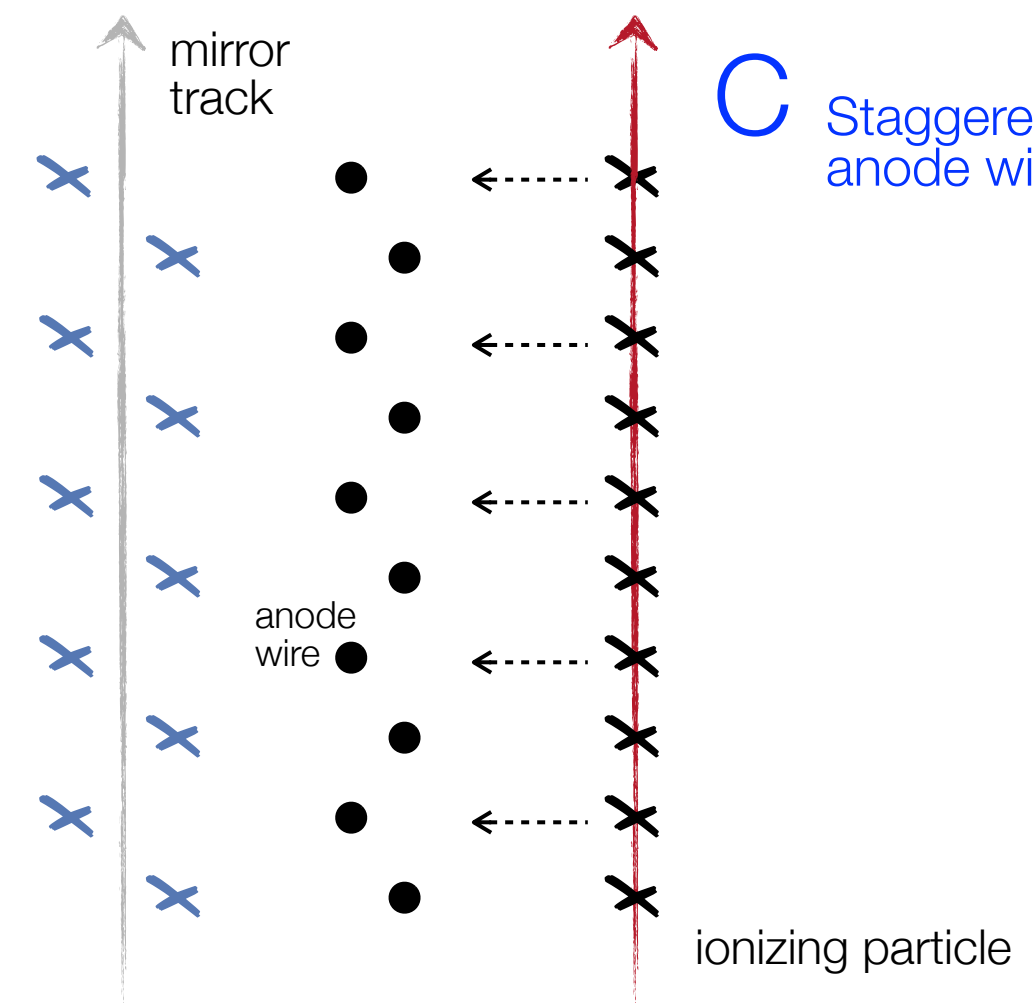
Drift Chambers – Ambiguities

Methods to resolve
left-right ambiguities ...

B Inclined
anode wires



C Staggered
anode wires



Aging in Wire Chambers

Avalanche formation can be considered as micro plasma discharge.

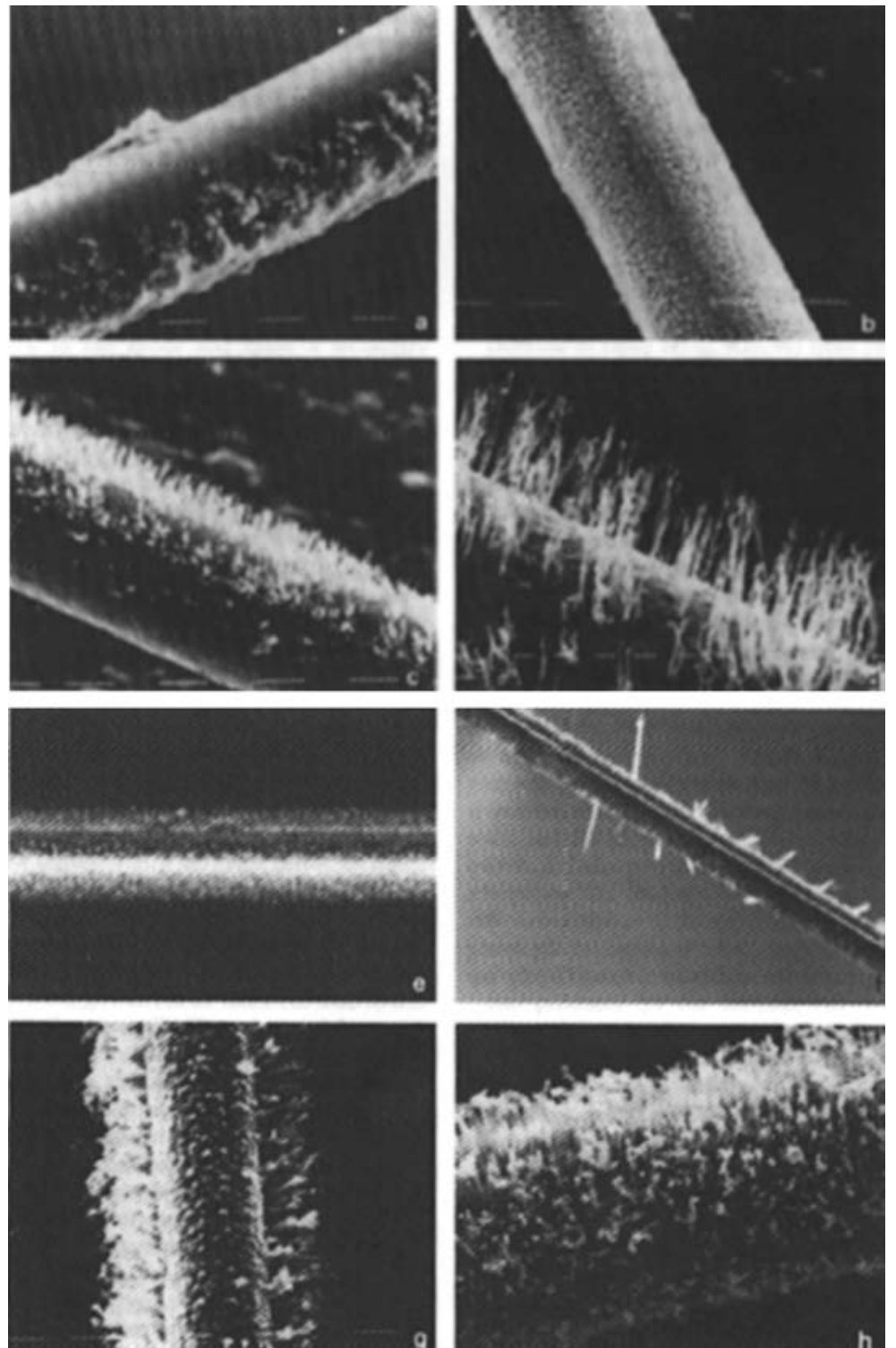
Consequences:

- Formation of radicals i.e. molecule fragments
- Polymerisation yields long chains of molecules
- Polymers may be attached to the electrodes
- Reduction of gas amplification

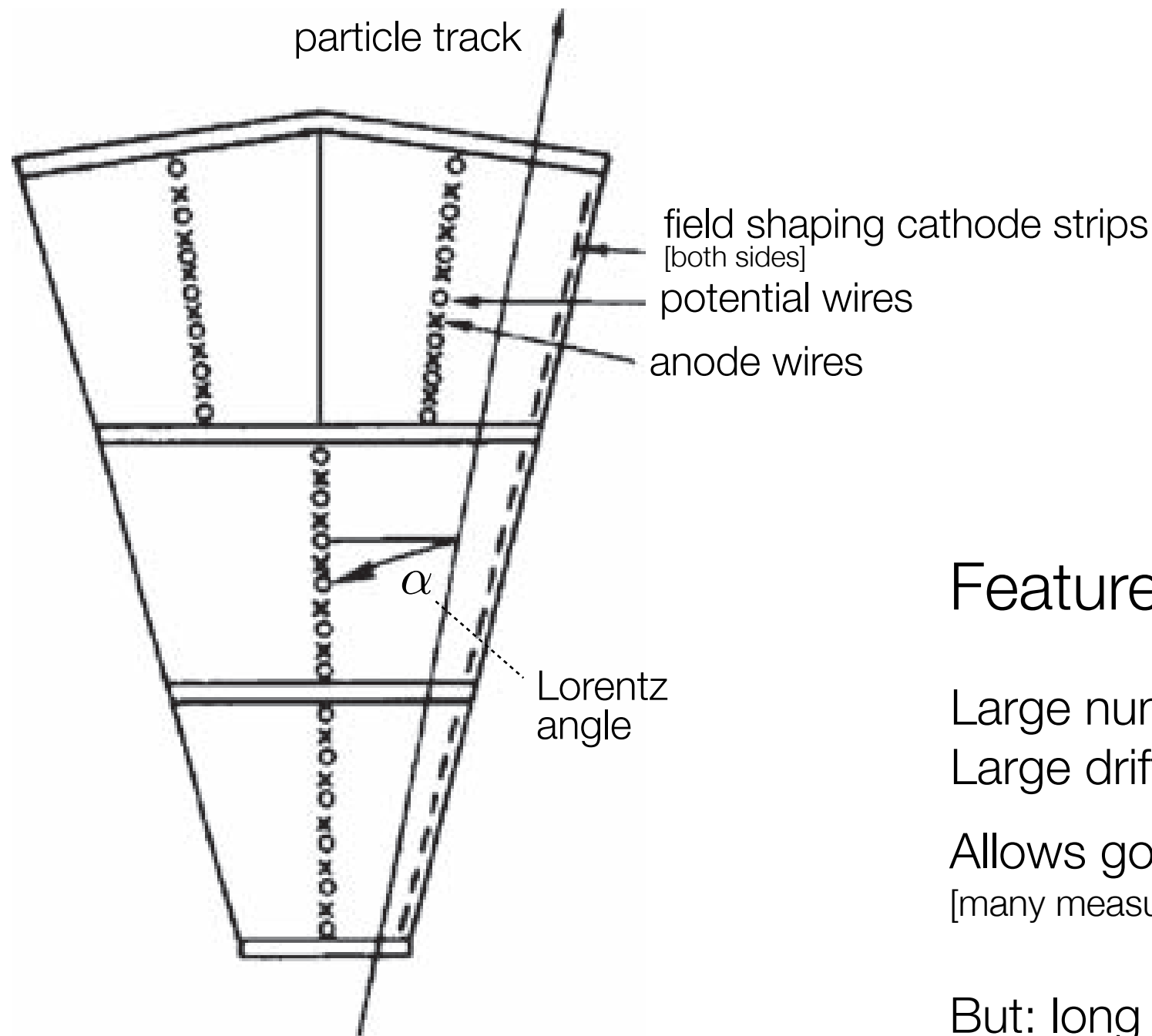
Important:
Avoid unnecessary contamination ...

- Harmful are ...
- Halogen or halogen compounds
- Silicon compounds
- Carbonates, halocarbons
- Polymers
- Oil, fat ...

....



Jet Drift Chambers



Features:

- Large number of sense wires
- Large drift cells

- Allows good dE/dx determination
[many measurements]

But: long drift times ...

Jet Drift Chambers – JADE

MAGNETDETEKTOR MAGNET DETECTOR **JADE**

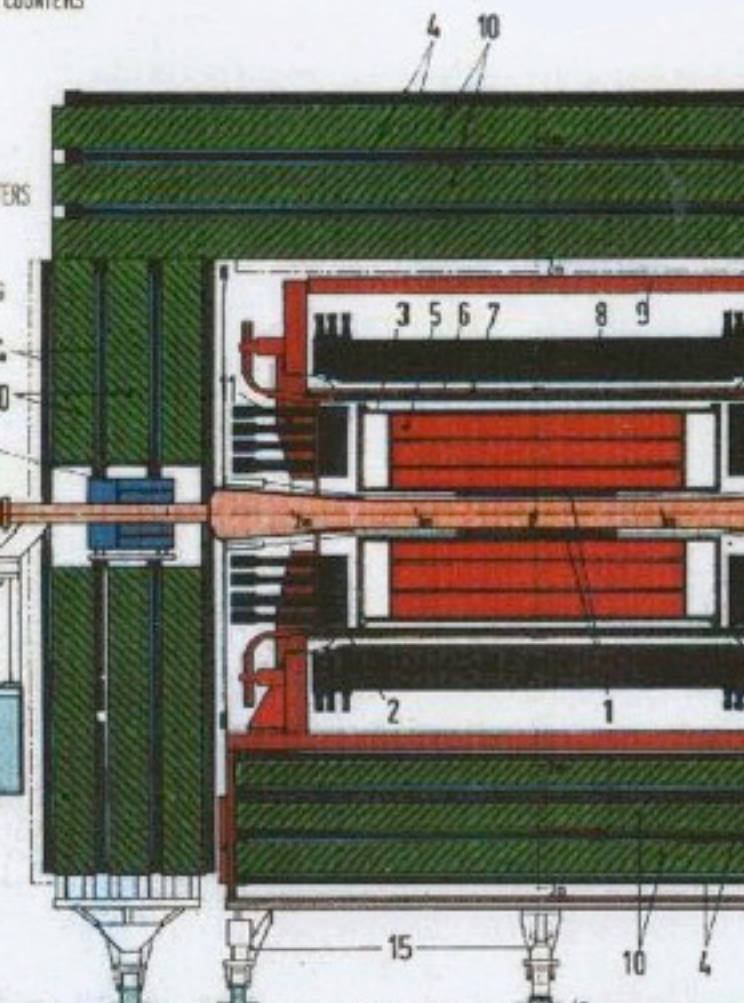
- 1 Strahlrohrzähler BEAM PIPE COUNTERS
- 2 Endseitige Bleiglaszähler END PLUG LEAD GLASS COUNTERS
- 3 Drucktank PRESSURE TANK
- 4 Myon-Kammern MUON CHAMBERS
- 5 Jet-Kammern JET CHAMBERS
- 6 Flugzeit-Zähler TIME OF FLIGHT COUNTERS
- 7 Spule COIL
- 8 Zentrale Bleiglaszähler CENTRAL LEAD GLASS COUNTERS
- 9 Magnetjoch MAGNET YOKE
- 10 Myon-Filter MUON FILTERS
- 11 Beweglicher Endstopfen REMOVABLE END PLUG
- 12 Strahlrohr BEAM PIPE
- 13 Vorwärts-Detektor TAGGING COUNTER
- 14 Mini-Beta Quadrupol MINI BETA QUADRUPOLE
- 15 Fahrwerk MOVING DEVICES

~7000t

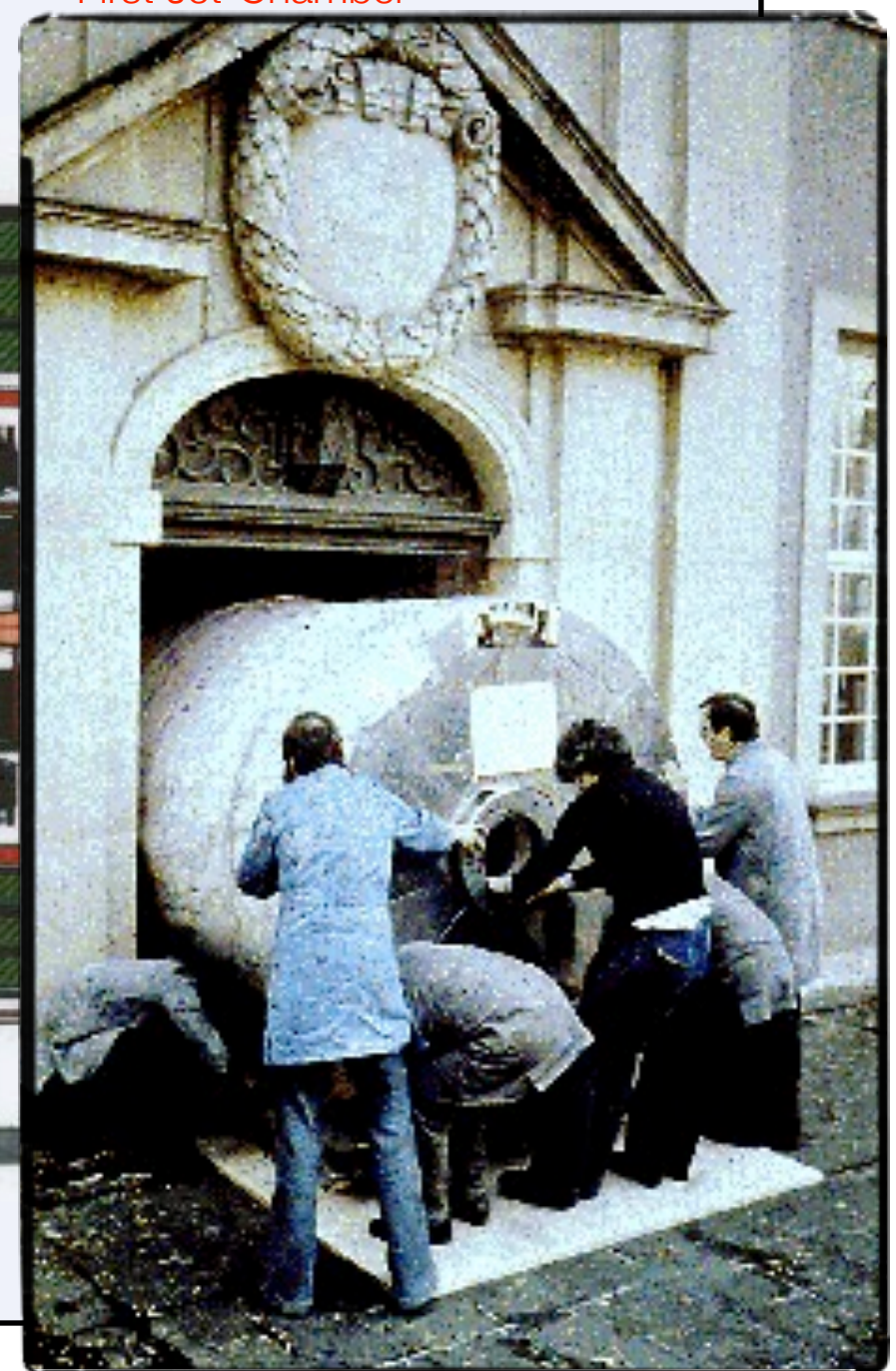
Gesamtgewicht TOTAL WEIGHT: ~1200 t
Magnetfeld MAGNETIC FIELD: 0.5T

Beteiligte Institute PARTICIPANTS

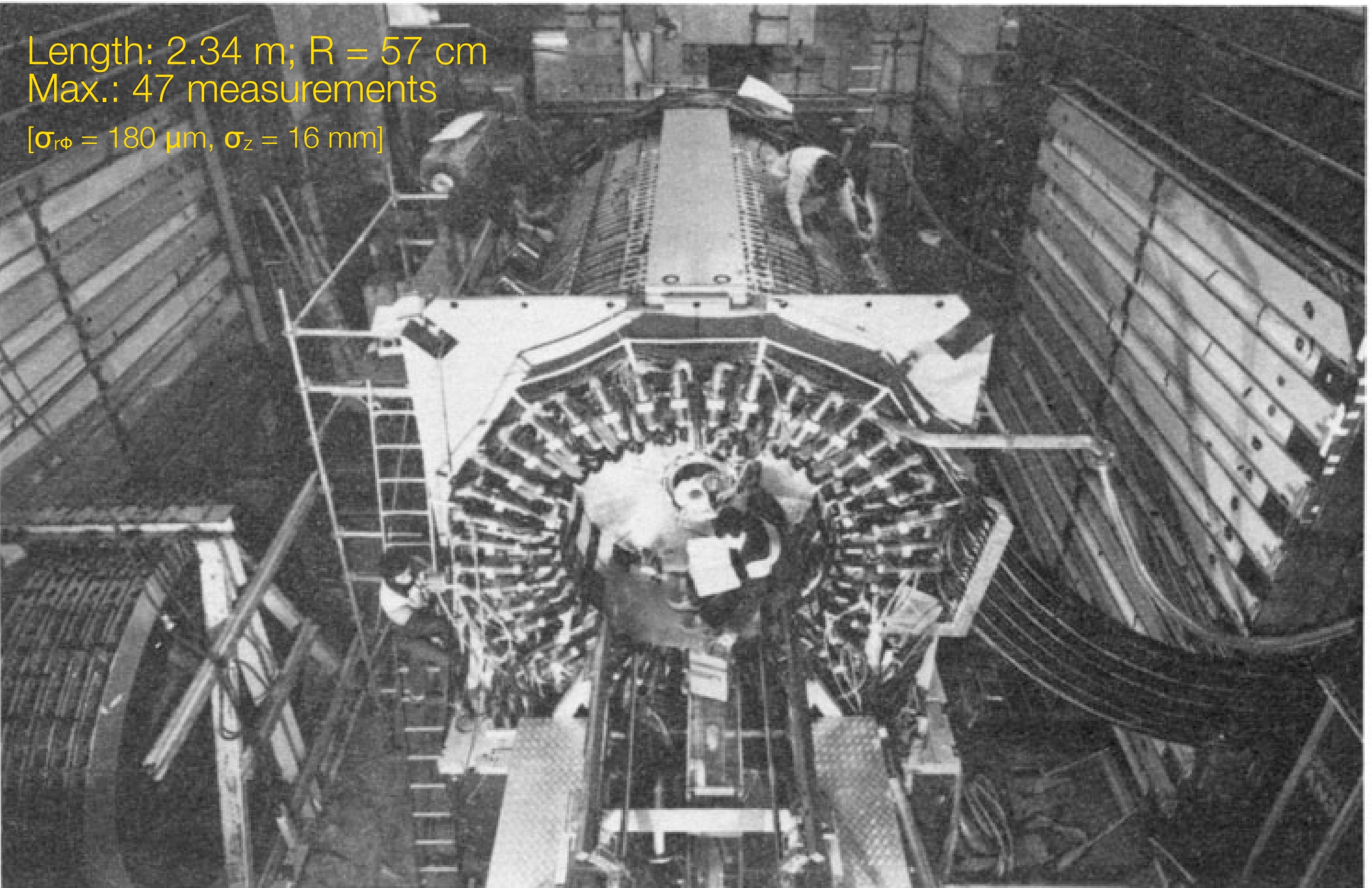
DESY, Hamburg, Heidelberg,
Lancaster, Manchester,
Rutherford Lab., Tokio



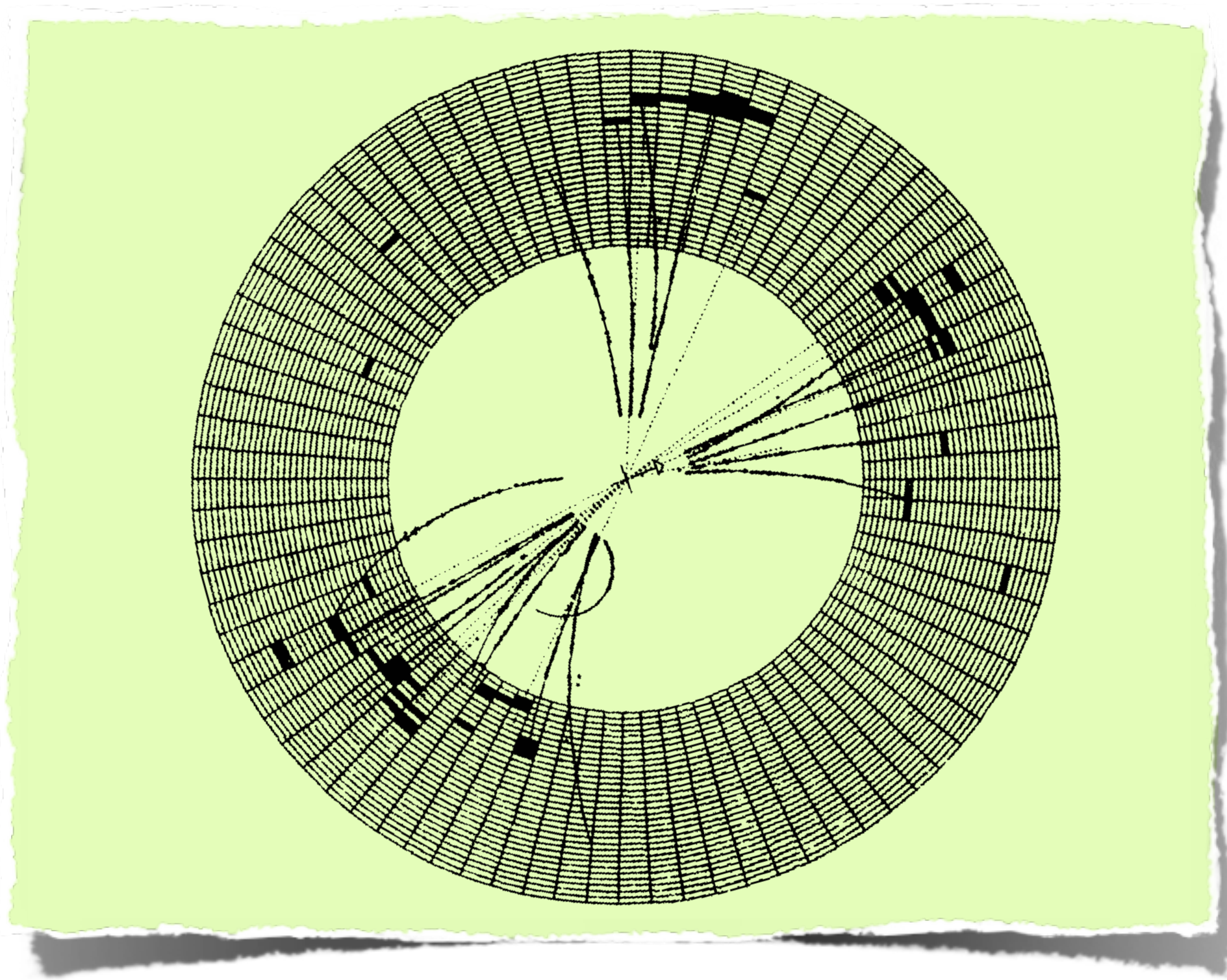
First Jet-Chamber



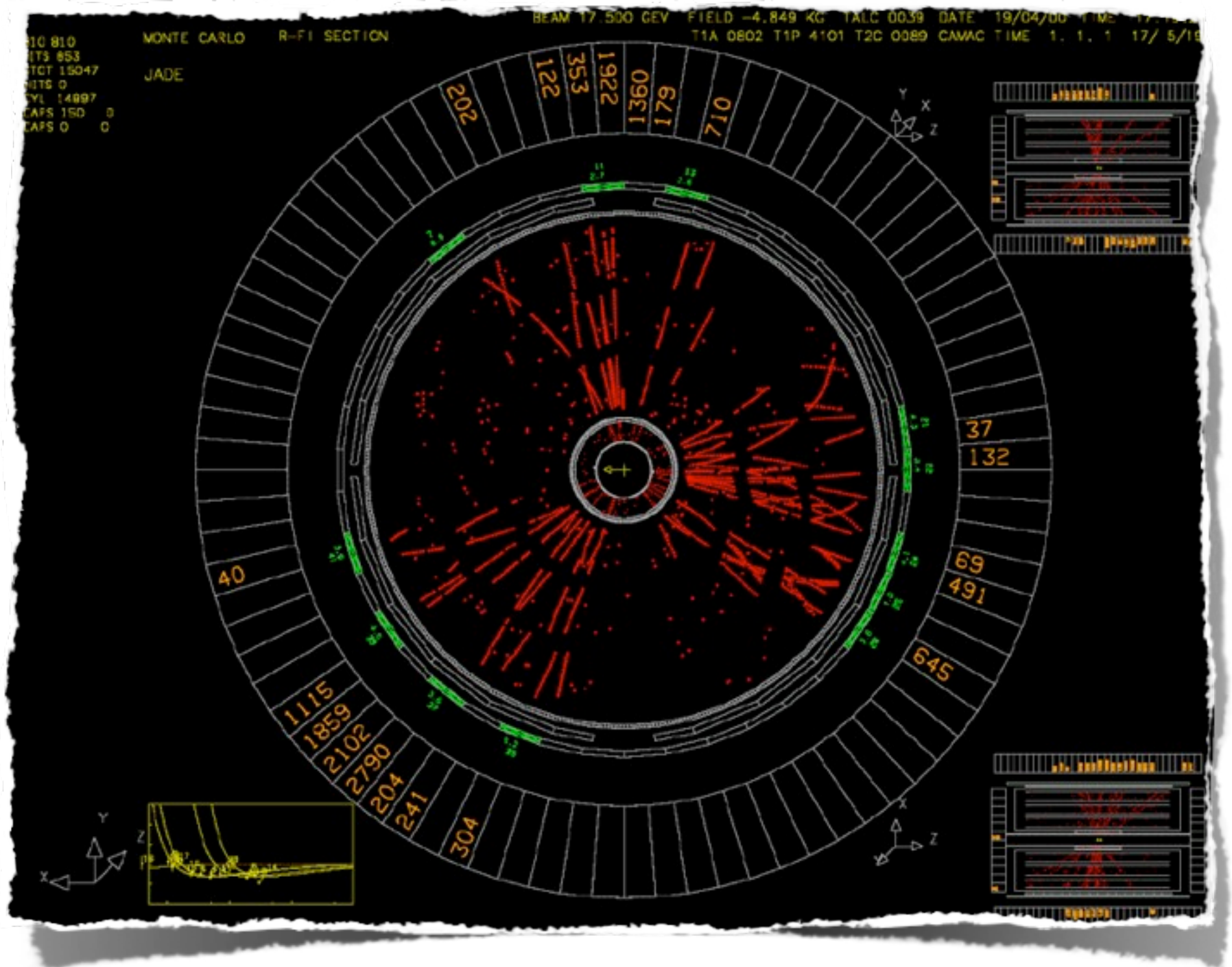
Jet Drift Chambers – JADE



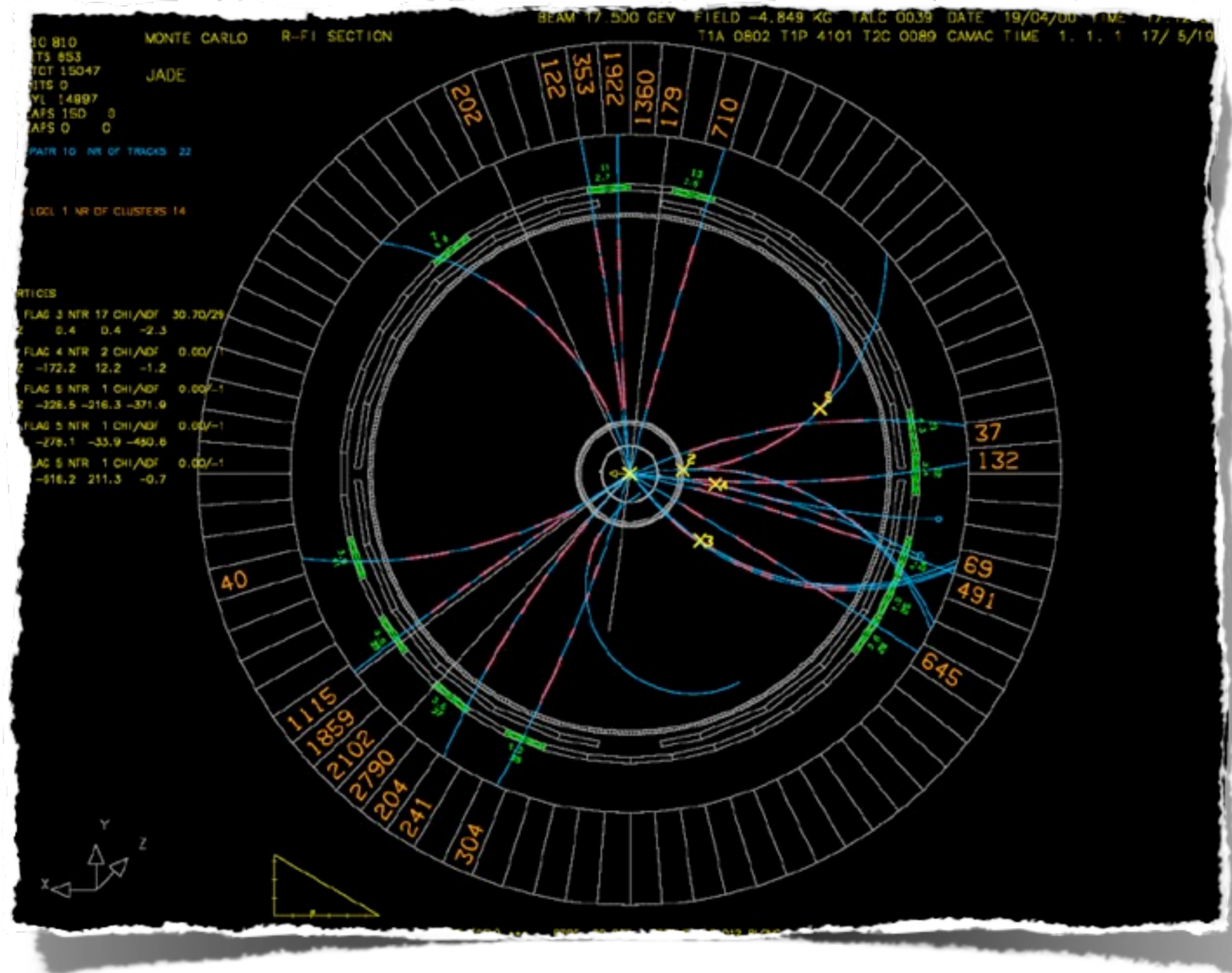
Jet Drift Chambers – JADE



Jet Drift Chambers – JADE



Jet Drift Chambers – JADE



Jet Drift Chambers – OPAL

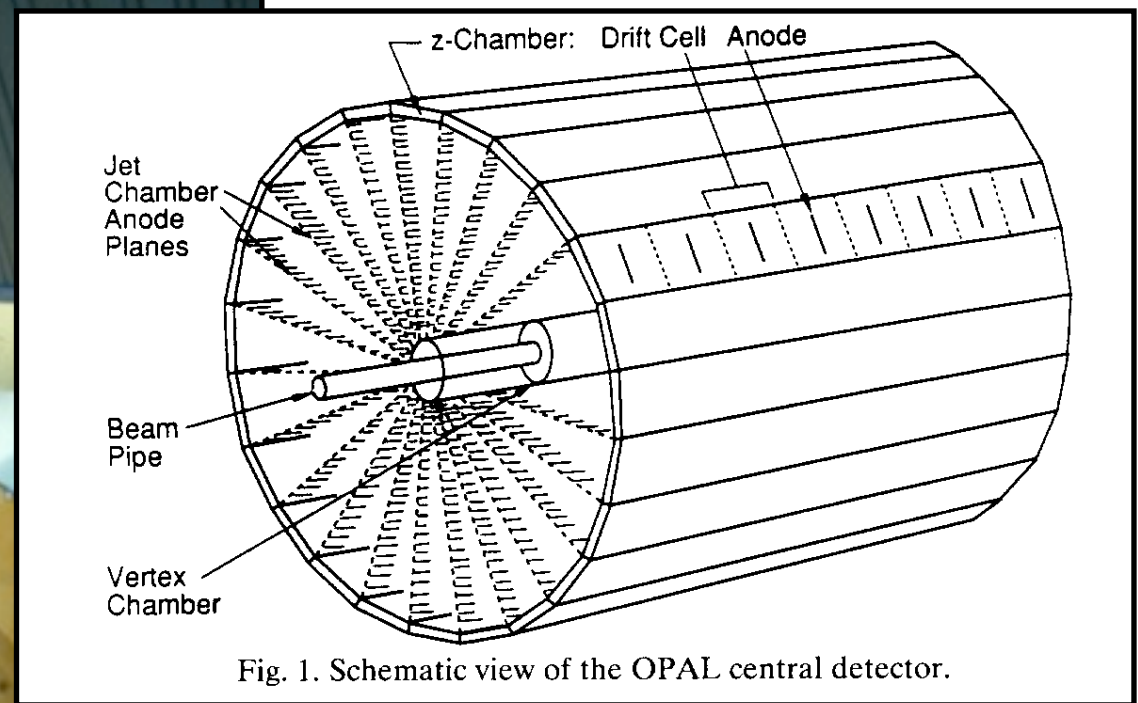
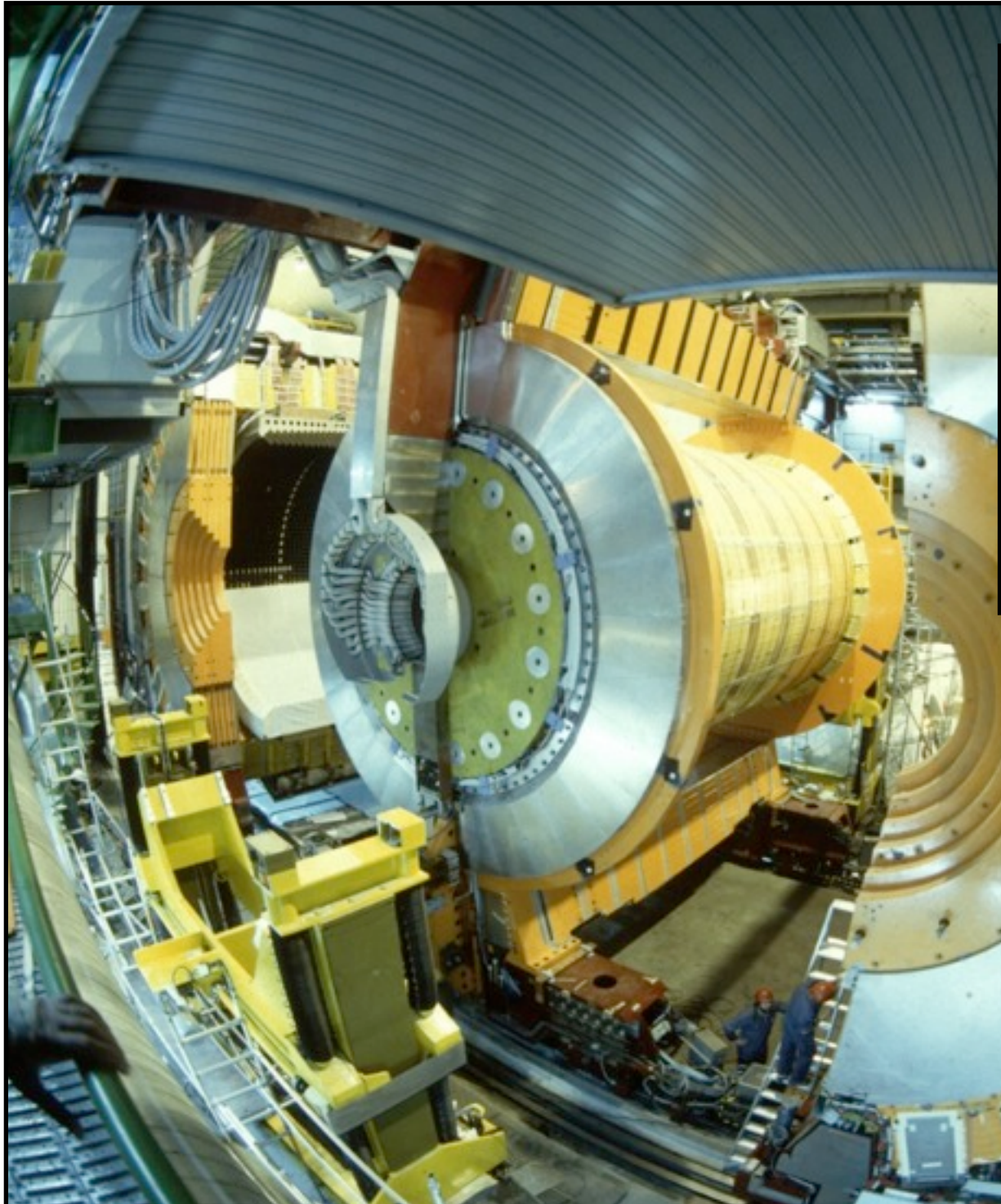
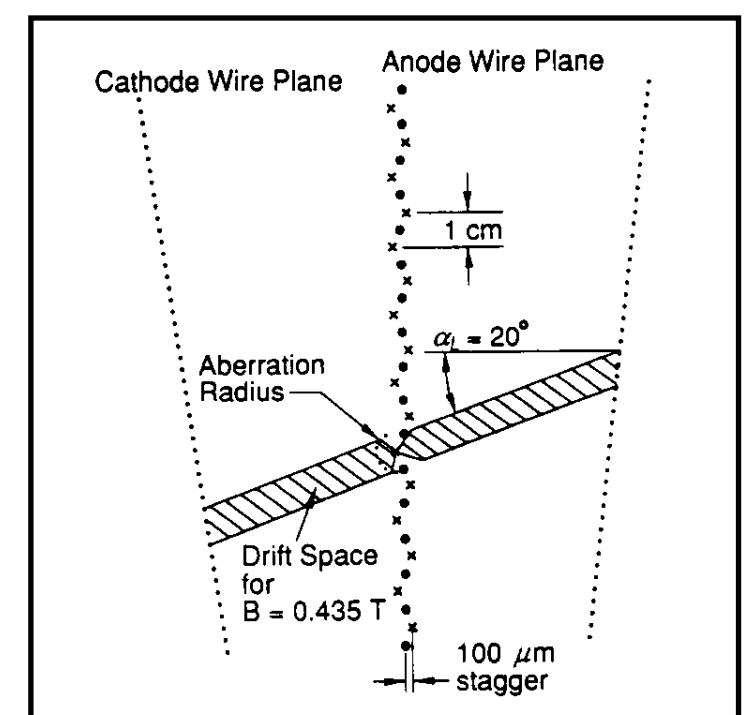


Fig. 1. Schematic view of the OPAL central detector.



Opal Jet Chamber

Jet Drift Chambers – OPAL



Interior of OPAL drift chamber
Length: 4 m; $R = 185$ cm; 159 measurements per track
 $[\sigma_{r\phi} = 135 \mu\text{m}, \sigma_z = 60 \text{ mm}]$

Jet Drift Chambers – OPAL



OPAL Jet Chamber installation

Time Projection Chambers

Electronic 'bubble chamber'
Full 3D reconstruction ...

xy : from wires and pads of MWPC ...
z : from drift time measurement

Momentum measurement ...

space point measurement
plus B field ...

Energy measurement ...
via dE/dx ...

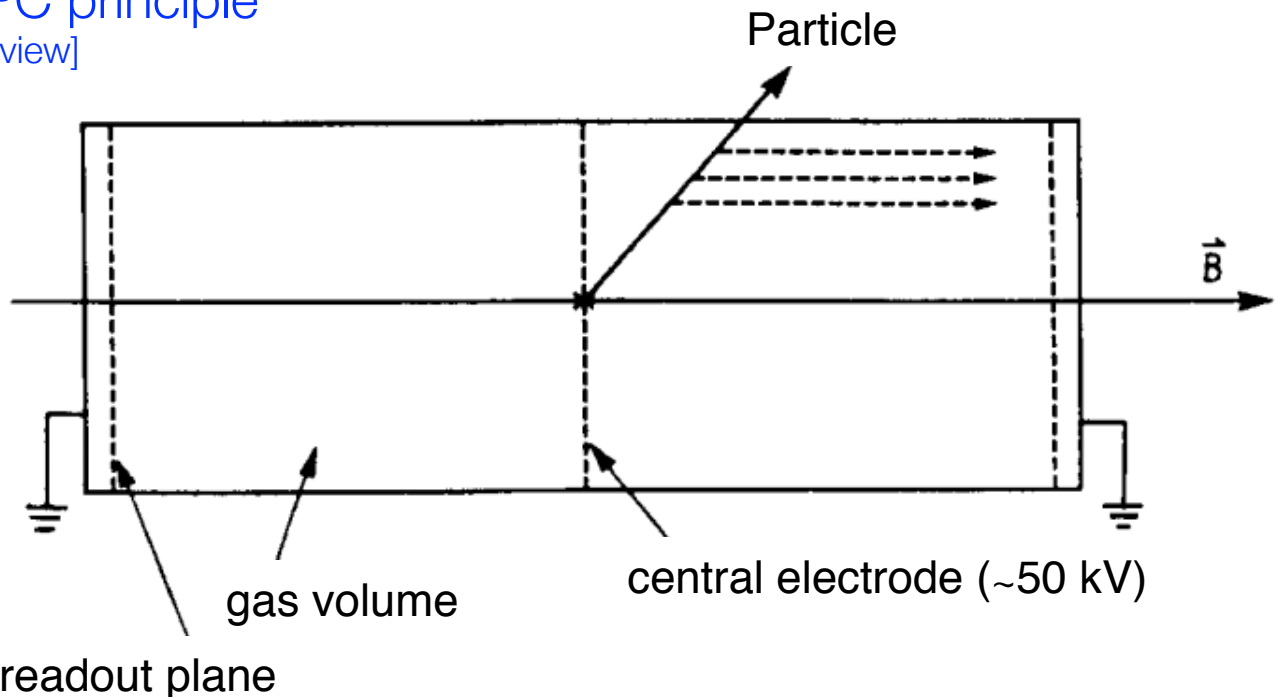
TPC setup:

(mostly) cylindrical detector
central HV cathode
MWPCs at end-caps of cylinder
 $B \parallel E \rightarrow$ Lorentz angle = 0

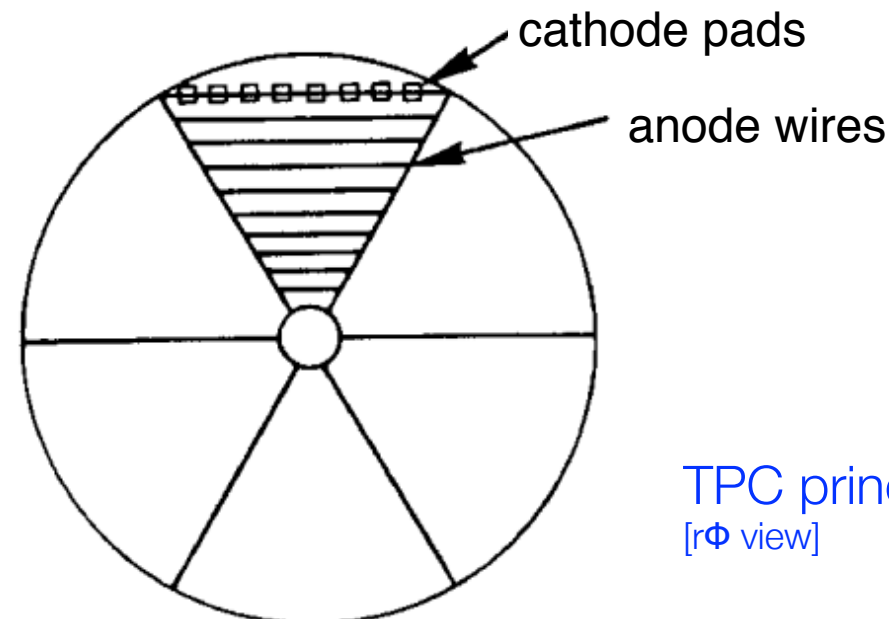
Charge transport :

Electrons drift to end-caps
Drift distance several meters
Continuous sampling of induced
charges in MWPC

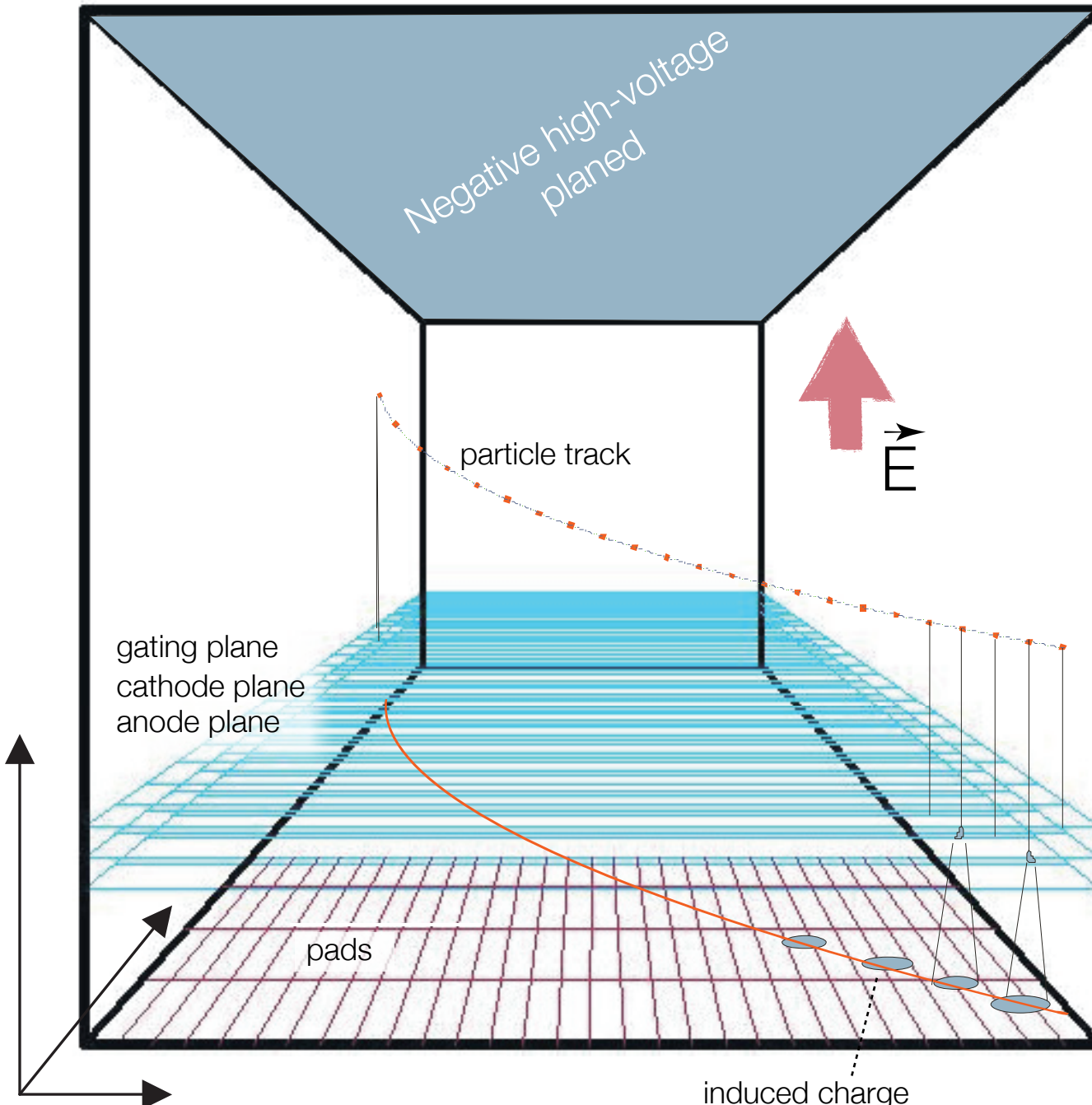
TPC principle
[rz view]



TPC principle
[rΦ view]



Time Projection Chambers



Advantages:

- Complete track within one detector yields good momentum resolution
- Relative few, short wires (MWPC only)
- Good particle ID via dE/dx
- Drift parallel to B suppresses transverse diffusion by factors 10 to 100

Challenges:

- Long drift time; limited rate capability [attachment, diffusion ...]
- Large volume [precision]
- Large voltages [discharges]
- Large data volume ...
- Extreme load at high luminosity; gating grid opened for triggered events only ...

Typical resolution:

z : mm; x : 150 - 300 μm ; y : mm
 dE/dx : 5 - 10%

Time Projection Chambers

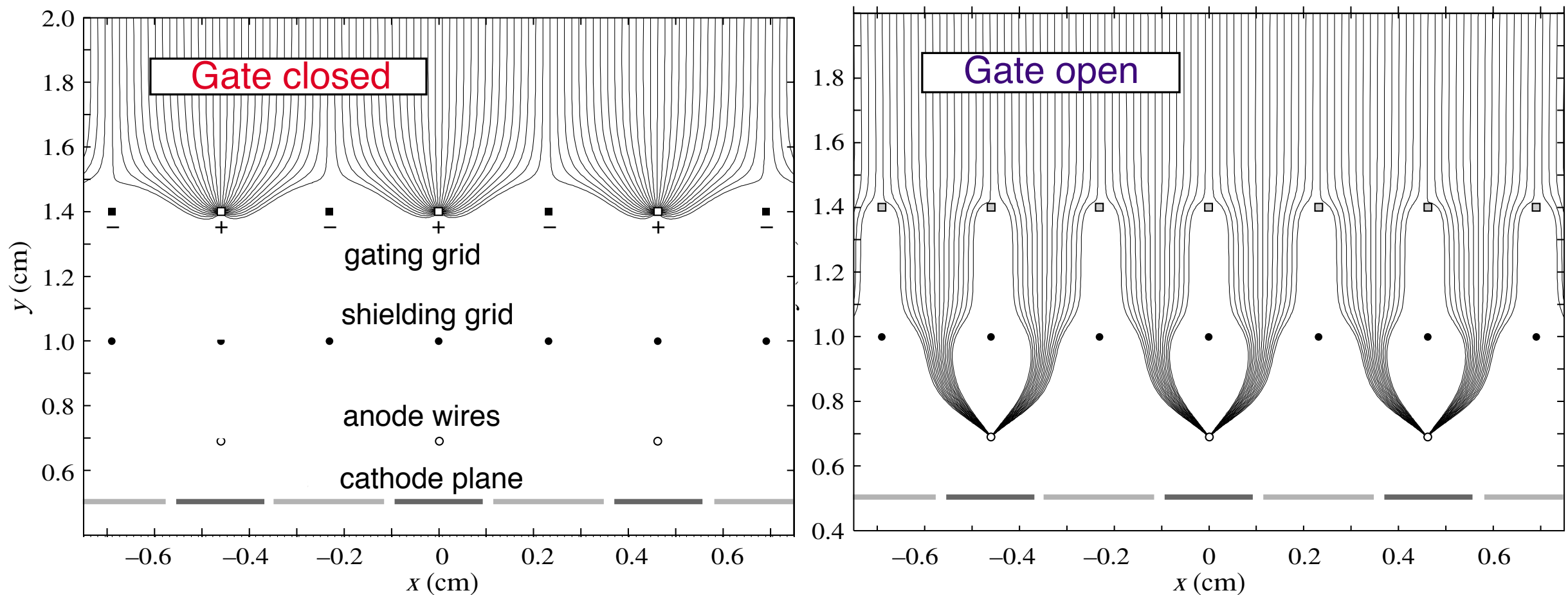
Difficulty: space charge effects due to slow moving ions
change effective E-field in drift region

Important: most ions come from amplification region

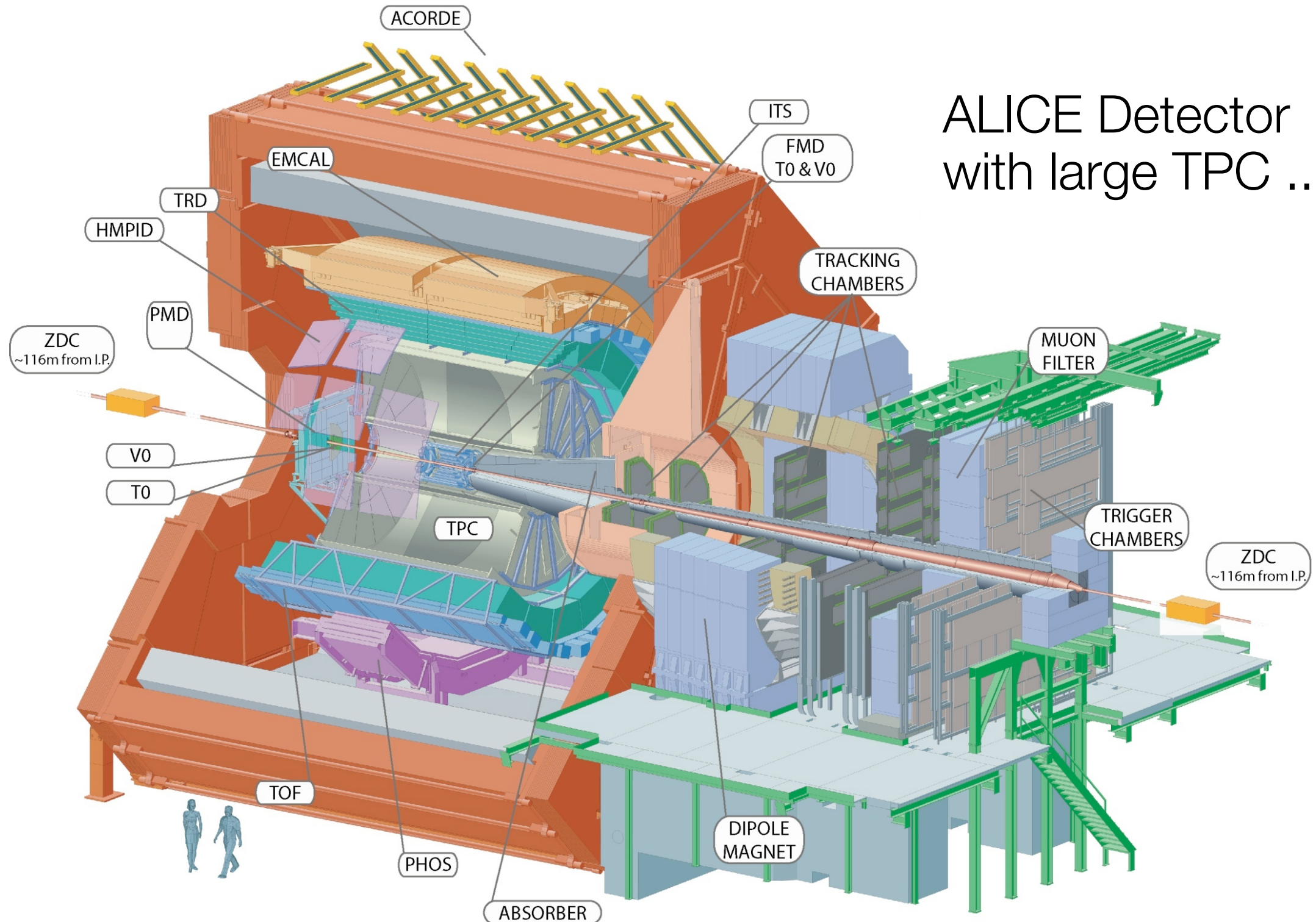
Solution: Invention of gating grid; ions drift towards grid ...

[Also: shielding grid to avoid sense wire disturbance when switching]

Requires external trigger to switch gating grid ...



Time Projection Chambers



Time Projection Chambers

ALICE TPC:

Length: 5 meter

Radius: 2.5 meter

Gas volume: 88 m³

Total drift time: 92 μ s

High voltage: 100 kV

End-caps detectors: 32 m²

Readout pads: 557568

159 samples radially

1000 samples in time

Gas: Ne/CO₂/N₂ (90-10-5)

Low diffusion (cold gas)

Gain: > 10⁴

Diffusion: $\sigma_t = 250 \mu\text{m}$

Resolution: $\sigma \approx 0.2 \text{ mm}$

$\sigma_p/p \sim 1\% p$; $\epsilon \sim 97\%$

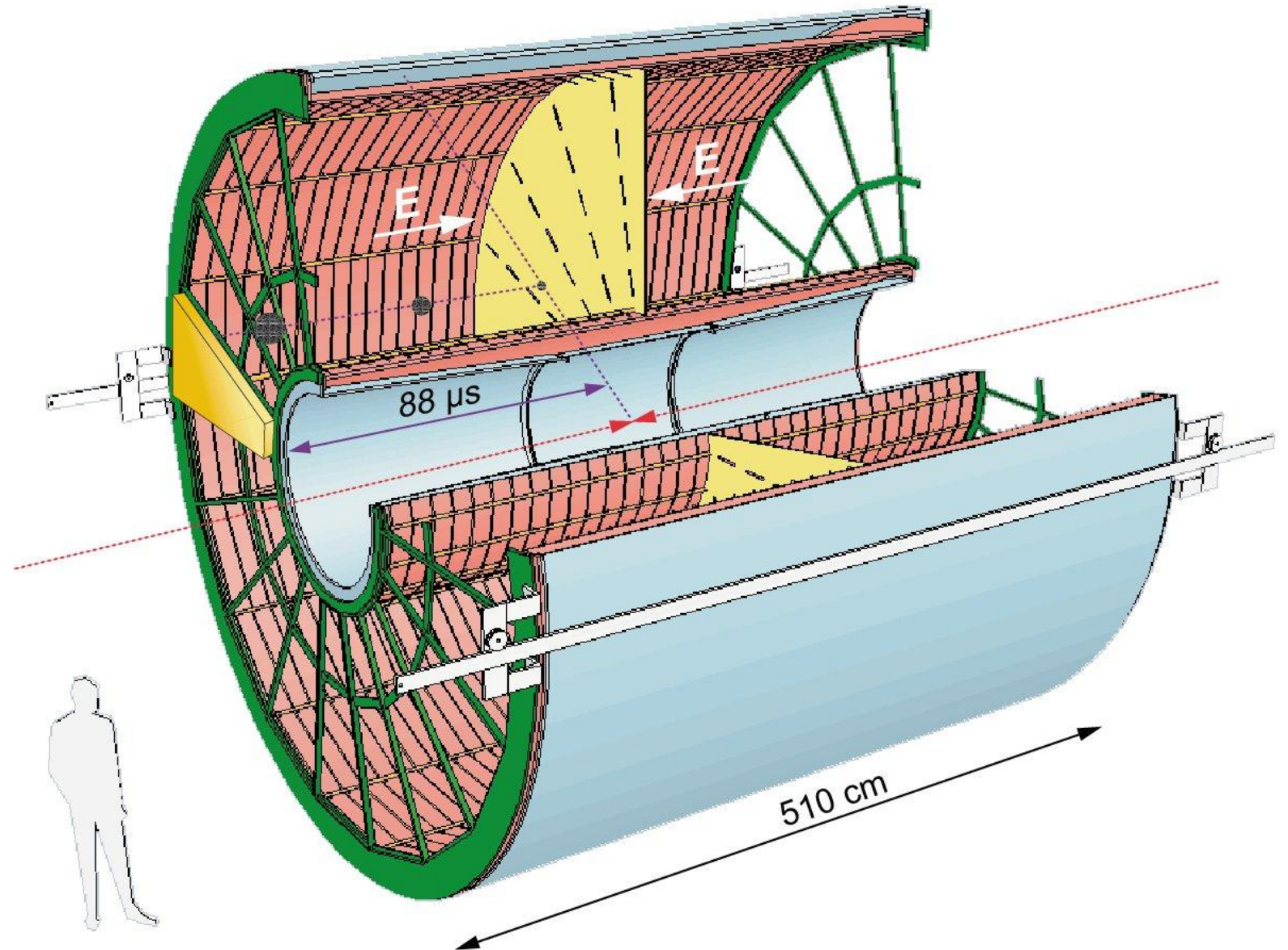
$\sigma_{dE/dx}/(dE/dx) \sim 6\%$

Magnetic field: 0.5 T

Pad size: 5x7.5 mm² (inner)

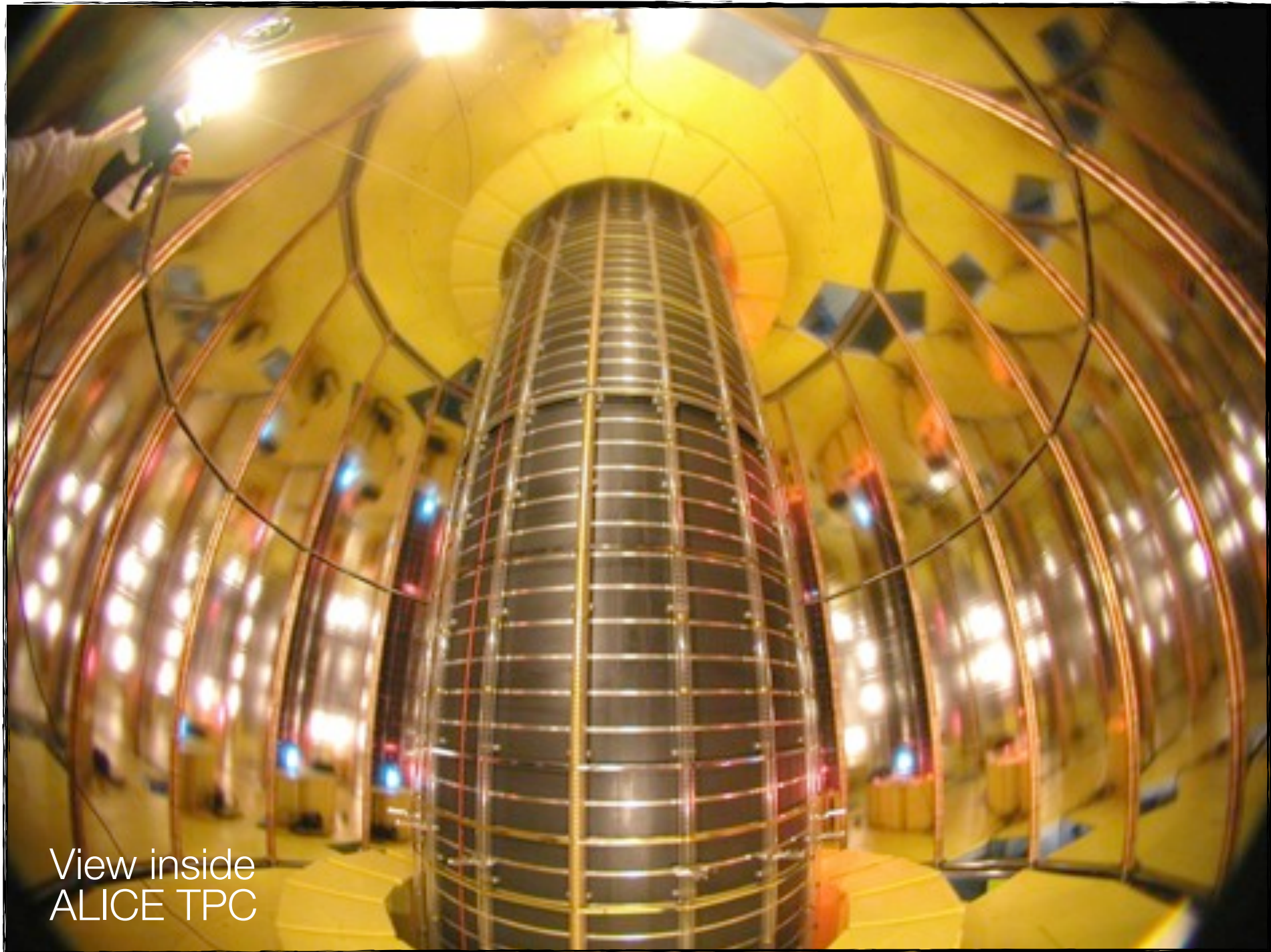
6x15 mm² (outer)

Temperature control: 0.1 K
[also resistors ...]



Material: Cylinder build from composite material of airline industry ($X_0 = \sim 3\%$)

Time Projection Chambers



Time Projection Chambers

